2019

Diuretic, natriuretic, and vasodepressor activity of a lipid fraction enhanced in medium of cultured mouse medullary interstitial cells by a selective FAAH inhibitor

Zdravka P. Daneva
Virginia Commonwealth University

Diuretic, natriuretic, and vasodepressor activity of a lipid fraction enhanced in medium of cultured mouse medullary interstitial cells by a selective FAAH inhibitor

A dissertation submitted in partial fulfillment of the requirements for the degree of Doctor of Philosophy at Virginia Commonwealth University.

by

Zdravka Plamenova Daneva

Bachelor of Psychology and Management, University of Glasgow, 2013

Director, Joseph K. Ritter, Ph.D.,

Professor, Department of Pharmacology and Toxicology

Virginia Commonwealth University

Richmond, VA

January, 2019

Acknowledgements

January, 2019

"I can do all things through Christ who strengthens me."

~ Philippians 4:13, NKJV ~

As I look back at my journey to completing my Ph.D. degree, I find it impossible to express my gratitude to all the people who have supported me and kept me going. I would like to start by thanking my advisor, Dr. Joseph Ritter. He accepted me as his student and mentee at a difficult time during my degree progress, when my continuation in the program was at risk. The trust and confidence in my potential that he has shown me are truly inspirational. Dr. Ritter has always encouraged me to think creatively about scientific problems and find meaning and purpose to my research goals. I am also very grateful for the fact that Dr. Ritter has continuously treated my colleagues and me as equal to himself, asking for our opinions, advice and expertise. It was crucial for my personal development as a scientist to feel free to express my ideas and valued for doing so. His example of treating others with upmost respect and care is one I will pass on to my students one day.

I would like to thank my committee members: Dr. Pin-Lan Li, Dr. Ningjun Li, Dr. Vijay Lyall, Dr. Aron Lichtman and Dr. Siddhartha Ghosh for their continuous support, guidance and advice. Special thanks to Dr. Dewey, Dr. De Felice and Dr. Bigbee. I would not have been able to stay in this program without your compassionate encouragement and belief in me. I will never forget your help!

Needless to say are my eternal gratitude to and love for my mother, father, aunt, uncle and cousin! Mom, thank you for your unconditional love and belief in me. You gave me strength and wisdom when I felt like giving up. Dad, thank you for supporting me, helping me in time of need, and setting an example for becoming a true scientist. I would like to give special thanks to my aunt and uncle in Richmond, who opened their home for me throughout my education here. For all our adventures, family time, holidays, parties and thorough care, I thank you! I also want to thank another very important family member – my cousin, Mark! You are like a brother to me. I learn so much from you and enjoy our cousin-time together. My days are always happier when you are around!

It will be unthinkable to continue without expressing my gratitude to my lab mates, Sara Dempsey and Ashfaq Ahmad! Thank you for sharing your knowledge and experience with me. You made my days at work enjoyable and wonderful! I am looking forward to finding out where we will cross our paths again

Table of Contents

Clarification of Contribution……..…...……vi
List of Tables…….....vii
List of Figures……...….ix
List of Abbreviations…….…….x
Abstract……1
Chapter 1 - Long-term regulation of blood pressure through the kidneys…….....….. 3
1.1 Renomedullary long-term regulation of blood pressure…….....…3
1.2 Pressure natriuresis and renal interstitial hydrostatic pressure……..4
1.3 The renal pressor system……9
1.4 A proposed renal depressor system - historical account and perspectives.....12
1.5 Renomedullary interstitial cells and the antihypertensive renal medulla...…….15
1.6 Tubular mechanisms of diuresis and natriuresis……..17
1.7 Mechanisms of diuretics……..31
Chapter 2 – The renal endocannabinoid system……37
2.1 History of the endocannabinoid system……...37
2.2 The endocannabinoid system……...41
2.3 The renal endocannabinoid system……..48
2.4 Endocannabinoids and regulation of renal function.....51
Rationale and hypothesis...……56
Chapter 3 - Diuretic, natriuretic, and vasodepressor activity of a lipid fraction enhanced in medium of cultured mouse medullary interstitial cells by a selective FAAH inhibitor……59
3.1 Abstract……59
3.2 Introduction……..60
3.3 Methods and materials ……62
3.4 Results……..71
3.5 Discussion……94
Chapter 4 – Diuretic and natriuretic effects of PIP are mediated via a CB1-dependent mechanism…..99
4.1 Introduction……..……99
4.2 Methods and materials……...101
4.3 Results……107
4.4 Discussion……..116
Chapter 5 – Evidence that PIP mediates its diuretic activity via the proximal convoluted tubules of the kidney…….....122
5.1 Introduction…….....122
5.2 Methods and materials……...125
5.3 Results……129
5.4 Discussion……..138
Conclusion……...145

List of References……………………………………………………………………………148
CV………………………………………………………………………………………………166

Clarification of Contribution

Without the technical and scientific contributions of those listed below, the data presented herein would not have been possible. All data included within this dissertation, aside from that described below, is exclusively my own.

Chapter 3

All samples prepared for HPLC/MS/MS analysis were run in the Pharmacology/Toxicology Mass Spectrometry Core at Virginia Commonwealth University (VCU) by Sara Dempsey and Justin Poklis.

List of Tables

Chapter 2

Table I – Localization of cannabinoid receptors in the kidney……..49

List of Figures

Chapter 1

Figure 1 – Schematic of the renin-angiotensin-aldosterone system (RAAS) ……...11

Figure 2 – Na+ transport processes in the first and second halves of the proximal tubule……...20

Figure 3 – Na+/K+ -ATPase as an ion transporter or a signal receptor……22

Figure 4 – Transport mechanisms for NaCl reabsorption in the thick ascending limb of the loop of Henle……..27

Figure 5 – Transport pathways in distal convoluted tubules and collecting duct principal cells..30

Figure 6 – Schematic of nephron segments where diuretics act……32

Chapter 2

Figure 7 – Schematic representation of pathways leading to synthesis and degradation of the two major endocannabinoids……43

Chapter 3

Figure 8 – Immunohistochemical and histological analysis of cultured MMICs and kidney tissue sections……...73

Figure 9 – The effect of PF-3845 in the presence or absence of COX-2 inhibitor on lipid staining in cultured MMICs……75

Figure 10 – Transmission electron micrographs of vehicle- and PF-3845-treated MMICs……..77

Figure 11 – Identification of a lipophilic product in the culture medium of MMICs that shows responsiveness to treatment with PF-3845……79

Figure 12 – The effects of intravenous (i.v.) (A) and intramedullary (i.med.) (B) infusion of the PIP fraction on mean arterial pressure (MAP), urine excretion (UV), sodium excretion (U_{Na}) and potassium excretion (U_K)……...……83

Figure 13 – The effects of a single intravenous (i.v.) infusion of the PIP fraction on the mean arterial pressure (MAP), urine excretion rate (UV), glomerular filtration rate (GFR) and relative medullary blood flow (MBF)……86

Figure 14 – The effects of intravenous (i.v.) and intraperitoneal (i.p.) bolus administrations of the PIP fraction on mean arterial pressure (MAP), urine excretion (UV) and medullary blood flow (MBF)……....89

Figure 15 – Comparison of the effects of intravenous (i.v.) infusion of the PIP fraction on blood pressure and urinary excretion endpoints in FAAH wildtype and FAAH knockout mice……92

Chapter 4

Figure 16 – The effects of an intramedullary (i.m.) infusion of PIP (1AU / 10 min) on the mean arterial pressure (MAP), urine excretion rate (UV) and medullary blood flow (MBF) in C57BL6J mice, treated with SR141716A……109

Figure 17 – The effects of an intramedullary (i.m.) infusion of PIP (1AU / 10 min) on the mean arterial pressure (MAP) and urine excretion rate (UV) in CB1 WT and CB1 KO mice…….111

Figure 18 – The effects of an intraperitoneal (i.p.) injection of PIP (5AU) on the mean arterial pressure (MAP) and urine excretion rate (UV) in CB1 WT and CB1 KO mice…….113

Figure 19 – Inhibition of [^{3}H] SR141716 binding to human CB1-CHO cells by (A) CP 55,940 and (B) PIP……..115

Chapter 5

Figure 20 – Effect of intramedullary infusion of PIP in the presence of amiloride in an acute renal functional model using C57BL6J mice……...131

Figure 21 – Effect of an intramedullary co-infusion of PIP in the presence of furosemide in an acute renal functional model using C57BL6J mice…….133

Figure 22 – Effect of an intramedullary co-infusion of PIP in the presence of HCT in an acute renal functional model using C57BL6J mice……...135

Figure 23 – Effect of an intramedullary co-infusion of PIP in the presence of HCT in an acute renal functional model using C57BL6J mice……...137

List of Abbreviations

2-AG	2-arachidonoyl glycerol
20-HETE	20 – hydroxyeicosatetraenoic acid
AA	Arachidonic acid
AE2	Anion exchanger 2
AEA	Anandamide, *N*-arachidonoylethanolamine
ABHD6/ABHD12	Serine α/β- hydrolases 6 and 12
Ang I	Angiotensin I
Ang II	Angiotensin II
ANK	Ankyrin
ATP	Adenosine triphosphate
AQP1	Aquaporin 1
AVP	Arginine vasopressin
BP	Blood pressure
cAMP	Cyclic adenosine monophosphate
CB1R, CB1	Cannabinoid receptor 1
CB2R, CB2	Cannabinoid receptor 2
CD	Collecting duct
CNS	Central nervous system
COX-2	Cyclooxygenase 2
DAGL	Diacyl glycerol lipase
DCT	Distal convoluted tubule
eCB	Endocannabinoid system
ECF	Extracellular fluid
EDTA	Ethylenediaminetetraacetic acid
ENaC	Epithelial sodium channel
FAA	Fatty acid amides

FAAH	Fatty acid acyl hydrolase
FITC-sinistrin	Fluorescein isothiocyanate - sinistrin
FXYD	Hydrophobic type I polypeptides
GFR	Glomerular filtration rate
$HCO3^-$	Bicarbonate
HCT	Hydrochlorothiazide
HPLC	High pressure liquid chromatography
HRP	Horseradish peroxidase
IDFP	Isopropyl dodecylfluorophosphate
iNOS	Nitric oxide synthase
IP3R	Inositol triphosphate receptor
LIPE	Hormone sensitive lipase
L-Name	N^G-nitro-L-arginine methyl ester
LPS	Lippopolysaccharide
MAGL	Monoacylglycerol lipase
MAP	mean arterial pressure
MAPK	Mitogen-activated protein kinase
MBF	Medullary blood flow
MMIC	Mouse medullary interstitial cells
MO	Medium only
MTAL	Medullary thick ascending loop of Henle
NAPE	N-arachidonoyl-phosphatidylethanolamine
NaPi2	Na^+/phosphate cotransporter
NCC	Na^+/Cl^- symporter
NHE3	Na^+/H^+ exchanger
NKA	Na^+/K^+ ATPase
NKCC2	$Na^+/K^+/2Cl^-$ - cotransporter
nNOS	Neuronal nitric oxide synthase
NO	Nitric oxide

P2Y1	Purinergic receptor 1
PA	Phosphatic acid
PBS	Phosphate-buffered saline
PC	Phosphatidylcholine
PC, PCT	Proximal convoluted tubule
PF-3845	*N*-3-Pyridinyl-4-[[3-[[5-(trifluoromethyl)-2-pyridinyl]oxy]phenyl]methyl]-1-piperidinecarboxamide
PG	prostaglandin
PGE A2	Prostaglandin A_2
PGE E2	Prostaglandin E_2
PGE F2	Prostaglandin F_2
PI-3K	Phosphoinositide 3-kinase
PKA	Protein kinase A
PKC	Protein kinase C
PLC	Phospholipase C
PLD	Phospholipase D
PT	Proximal convoluted tubule
RAAS	Renin-angiotensin-aldosterone system
RIHP	Renal interstitial hydrostatic pressure
ROS	Reactive oxygen species
RPP	Renal perfusion pressure
SR141716A	Rimonabant
SRC	Proto-oncogene tyrosine-protein kinase Src
TDL	Thin descending loop of Henle
TRPV1	Transient receptor potential vanilloid 1
UV	Urine excretion
V_2	Arginine vasopressin receptor 2
WIN 55,212-2	(*R*)-(+)-[2,3-Dihydro-5-methyl-3-(4-morpholinylmethyl)pyrrolo[1,2,3-*de*]-1,4-benzoxazin-6-yl]-1-naphthalenylmethanone mesylate

ABSTRACT

Diuretic, natriuretic, and vasodepressor activity of a lipid fraction enhanced in medium of cultured mouse medullary interstitial cells by a selective FAAH inhibitor

By Zdravka Plamenova Daneva

A dissertation submitted in partial fulfillment of the requirements for the degree of Doctor of Philosophy at Virginia Commonwealth University.

Virginia Commonwealth University, 2018.

Director, Joseph K. Ritter, Ph.D.,

Professor, Department of Pharmacology and Toxicology

The relationship between the endocannabinoid system in the renal medulla and the long-term regulation of blood pressure is not well understood. To investigate the possible role of the endocannabinoid system in renomedullary interstitial cells, mouse medullary interstitial cells (MMICs) were obtained, cultured and characterized for their responses to treatment with a selective inhibitor of fatty acid amide hydrolase (FAAH), PF-3845. Treatment of MMICs with PF-3845 increased cytoplasmic lipid granules detected by Sudan Black B staining and multilamellar bodies identified by transmission electron microscopy. HPLC analyses of lipid extracts of MMIC culture medium revealed a 205nm-absorbing peak that showed responsiveness

to PF-3845 treatment. The biologic activities of the PF-3845-induced product (PIP) isolated by HPLC were investigated in anesthetized, normotensive surgically-instrumented mice. Intramedullary and intravenous infusion of PIP at low dose rates (0.5-1 AU/10 min) stimulated diuresis and natriuresis, whereas at higher doses, these parameters returned toward baseline but mean arterial pressure (MAP) was lowered. Whereas intravenous bolus doses of PIP stimulated diuresis, GFR and medullary blood flow (MBF) and reduced or had no effect on MAP, an intraperitoneal bolus injection of PIP reduced MAP, increased MBF, and had no effect on urinary parameters. Genetic or pharmacological ablation of the cannabinoid type 1 receptors in mice completely abolished the diuretic and vasodepressor properties of intramedullary infused PIP, suggesting that the PF-3845-induced product requires the presence of CB1 receptors in order to elicit its renal effects. In a radioactive competition binding assay, using Chinese hamster ovary cells expressing CB1 receptors, PIP successfully displaced the CB1 selective inverse agonist [3H] SR141716A, revealing that the lipid extract was able to compete for binding to CB1 receptors. Finally, we investigated the tubular location of diuretic activity that the PF-3845-induced lipid fraction exhibits. In a renal function in vivo experiment, we pre-treated anesthetized mice with an intramedullary infusion of one of four well-known diuretics. This procedure was followed by an intramedullary infusion of PIP (1AU). Only inhibition of the proximal tubule sodium reabsorption diminished the diuretic activity of the PF-3845-induced product, suggesting that the lipid fraction requires a physiologically intact proximal tubular reabsorption mechanism for it to produce diuresis. These data support a model whereby PF-3845 treatment of MMICs results in increased secretion of a neutral lipid which acts directly to promote diuresis and natriuresis and indirectly through metabolites to produce vasodepression.

Efforts to identify the structure of the PF-3845-induced lipid and its relationship to the previously proposed renomedullary antihypertensive lipids are ongoing.

Chapter 1 - Long-term regulation of blood pressure through the kidneys

1.1 Renomedullary long-term regulation of blood pressure

Maintenance of blood pressure in a normal range is essential to life and health. Too low and organ perfusion and oxygenation will be inadequate leading to death of tissues and organ failure. Too high and it results in physical damage to organs such as the heart, kidneys and eyes. An important attribute to the feedback system responsible for the long-term regulation of blood pressure (BP) is the kidney. It depends on cardiac output (heart rate x stroke volume) and total peripheral vascular resistance, with the latter being strongly influenced by sympathetically-mediated vasoconstriction (Cervenka et al., 2000; Raven and Chapleau, 2014). Total peripheral resistance (TPR) depends on blood vessel diameter, blood viscosity and total vessel length. Thus, it is also tightly connected to changes in extracellular fluid volume (ECFV) (Granger et al., 2002). Thus, when the volume of fluid increases, BP increases concurrently, and when the total fluid volume decreases in the body, so does pressure. In this line of facts, it has also been known that extracellular fluid volume strongly depends on the total amount of sodium in the organism due to a tight regulation of osmolality. Therefore, the sodium balance in the body is maintained by the ratio of sodium input versus sodium output. The sodium excretion, or natriuresis, is determined by glomerular filtration and by tubular reabsorption. Under non-pathological conditions, the elevated sodium intake is followed by an increased sodium excretion via a

mechanism called ‘pressure natriuresis’ (Granger et al., 2002). Briefly, it is the effect of arterial pressure on the renal excretion of sodium (Hall et al., 1986; Hall, 2003). Thus, increases in renal perfusion pressure lead to decreases in renal sodium reabsorption and, thus, increases in renal sodium excretion. Pressure-natriuresis is considered to be closely related and dependent on changes in the renal medullary hemodynamics (Ritter et al., 2012). The specific intrarenal mechanism responsible for this cascade of actions has not been yet elucidated. However, several physiological findings have been suggested to shed some light on possible mechanisms of pressure natriuresis: the renal pressor system (renin-angiotensin-aldosterone-system) and the renal depressor system (Medullipin system).

1.2 Pressure natriuresis and renal interstitial hydrostatic pressure

Changes in sodium output in response to altered renal perfusion pressure are believed to be due to changes in tubular reabsorption of sodium since GFR and filtered load of sodium are well auto-regulated (Selkurt et al., 1949; Shipley and Study, 1951). Thus, elevated RPP inhibits renal tubular reabsorption of sodium and stimulates its secretion from the kidneys. Despite historical arguments for and against the involvement of RIHP in pressure natriuresis, there is significant amount of evidence in support for its connection to renal perfusion pressure activity that surpasses the autoregulation through whole kidney blood flow and perfusion glomerular filtration rate (Granger and Scott, 1988; Roman et al., 1988). Research by Ott et al. showed that increases in RPP produced a significant rise in RIHP (Ott et al., 1971). Later, Granger and Scott demonstrated that a small increase (from 3 to 4 mm Hg) in RIHP occurred when renal perfusion pressure was elevated from 80 to 130 mm H in anesthetized dogs (Granger and Scott, 1988). Similar changes in RIHP, in response to elevated RPP, have been shown to be present in rat

models (Roman et al., 1988; Garcia-Estan and Roman, 1989). Studies also report that this interrelated regulation of RIHP and RPP can be enhanced by renal vasodilation. Granger et al. compared the effect of RPP or interstitial pressure in the presence and absence of acetylcholine-induced renal vasodilation (Granger and Scott, 1988). The team showed that for any given increase in RPP in vasodilated kidneys, sodium output was significantly higher than that in control kidneys, even though the blood flow regulation remained efficient. Furthermore, Garcia-Estan and Roman demonstrated that the volume status of experimental animals played an enhancing role in the relationship between RPP and RIHP, where the elevation of renal perfusion pressure in volume-expanded rats caused a much higher rise in RIHP than in dehydrated rats (Garcia-Estan and Roman, 1989).

Additionally, research suggests that the regulation of renal interstitial hydrostatic pressure is closely linked to medullary hemodynamics (Roman, 1988; Roman et al., 1988; Roman and Kaldunski, 1988). Roman's team suggested that elevation in RPP increases the flow in vasa recta and thus increases vasa recta's hydrostatic pressure. This hydrostatic pressure elevation limits the fluid intake from tubular reabsorption by vasa recta and causes a heightened level of medullary interstitial fluid and pressure (Granger et al., 2002). Ultimately, the increase in medullary interstitial hydrostatic pressure is thought to be transmitted throughout the kidney (Granger et al., 2002). To test this hypothesis Roman *et al*. demonstrated that papillary (innermost area of the renal medulla) blood flow was not an object of autoregulation between the ranges of 100 to 150 mmH. In comparison the whole kidney and cortical blood flow remained to be efficiently autoregulated (Roman and Kaldunski, 1988). The research team observed that the lack of papillary blood flow autoregulation was probably due to alterations in the number of perfused vessels, as well as alterations in blood flow in individual ascending and descending vasa recta

(Roman and Kaldunski, 1988). In congruence with these findings, the team found that when renal perfusion pressure was elevated from 100 to 150 mm Hg (Roman and Cowley, 1985), the hydrostatic pressure of vasa recta capillaries rose significantly. Why papillary blood flow is not regulated as well as cortical blood flow in response to increased renal perfusion pressure remains unknown. Studies show that single nephron glomerular filtration rate in deep and superficial nephrons is also autoregulated (Haas et al., 1986). This last piece of data suggests that the lack of autoregulation in papillary blood flow is possibly due to changes in postglomerular vascular resistance in deep nephrons (Dehmel et al., 1998; Granger et al., 2002). Another explanation for this phenomenon would be that the inner medulla (including the papilla) may be releasing intrarenal factors that play an important role in regulating RIHP during pressure natriuresis (Dehmel et al., 1998; Nakamura et al., 1998). Several factors with an autocoid (hormon-like) nature have been proposed to be released in response to increased renal perfusion pressure. Examples for these are nitric oxide, kinins, prostaglandin E2, and cytochrome P450 metabolites (Dehmel et al., 1998; Nakamura et al., 1998; Majid et al., 1999; Granger and Alexander, 2000; Hoagland et al., 2001; Majid and Navar, 2001). The evidence for their involvement draws from studies where elevation in renal perfusion pressure was prevented by their inhibition. Additionally, there is evidence revealing that increases in renal perfusion pressure also stimulates renal production of nitric oxide (Majid et al., 1999; Hoagland et al., 2001). Nitric oxide has further been shown to directly inhibit sodium transport and to alter medullary blood flow and RIHP (Granger and Alexander, 2000).

In order for scientists to advance in determining if the renal interstitial pressure is important for pressure-natriuresis to take place, two main approaches have been utilized: [1] to mimic increases in RIHP observed during increases in renal perfusion pressure and [2] to prevent

RIHP to occur by decapsulating the kidneys (Haas et al., 1984; Wilcox et al., 1984; Haas et al., 1986; Granger et al., 1988; Garcia-Estan and Roman, 1989). RIHP stimulation by increasing the renal interstitial volume by injecting iso-oncotic saline directly in the renal interstitium through a catheter. This infusion caused RIHP to rise from 4 to 5 mm Hg, a comparable effect to previously observed responses to elevation in RPP (Granger et al., 1988). These changes occurred without any accompanying shifts in glomerular filtration rate or renal blood flow. Another study by Wilcox et al. showed that cutting the renal lymphatic ducts in normal anesthetized rats increased RIHP and excretion of sodium (Wilcox et al., 1984). These results were magnified in a volume-expanded rat model, supporting earlier findings that volume-expansion plays a role in pressure-natriuresis (Wilcox et al., 1984). Furthermore, renal decapsulation significantly attenuated increases in RIHP in response to various physiological manipulations (Marchand et al., 1977; Hartupee et al., 1982). Garcia-Estan and Roman showed that decapsulation of kidneys in volume-expanded rats markedly blunted the increased RIHP in response to increases in renal perfusion pressure (Garcia-Estan and Roman, 1989). More intriguingly, the blunting of RIHP was accompanied by an attenuation of the pressure-natriuretic activity (up to 40 %) (Garcia-Estan and Roman, 1989). Comparable evidence was provided by Khraibi and Knox who used spontaneously hypertensive rat and Wistar-Kyoto rat models (Khraibi and Knox, 1988). The last two pieces of evidence suggest that pressure natriuresis is only partially due to elevated RIHP in response to elevated renal perfusion pressure. It is possible and has been argued that the rest of the pressure-natriuresis stimulating factors are molecules produced and excreted from the medulla of the kidney in response to elevated renal perfusion pressure (Muirhead, 1991).

The discovery of RIHP's ability to transduce pressure in different areas of the encapsulated kidney triggered a series of studies aiming to determine which tubular mechanisms are involved in the pressure natriuresis cascade. This search for mechanisms was based on the hypothesis that natriuresis does not fully depend on glomerular filtration rate shifts (Haas et al., 1986; Roman and Kaldunski, 1988). Consequently, a decrease in RPP results in an increase in renal tubular reabsorption of sodium and a decrease in sodium output. To clarify the picture, they demonstrated that the proximal convoluted tubular reabsorption of sodium is inhibited directly by paracrine signaling originating from the renal medulla (Haas et al., 1986). Evidence from physiological manipulations shows that medullary blood flow in the renal medulla is poorly autoregulated, which results in its rise in the presence of increased renal arterial pressure (RAP) (Roman et al., 1988). This action causes an elevation in the renal hydrostatic pressure and this increased pressure is transduced throughout the kidney due to renal encapsulation (Roman and Kaldunski, 1988; Garcia-Estan and Roman, 1989; O'Connor and Cowley, 2010). According to Schafer et al. the cascade of events described above inhibits the sodium reabsorption in the proximal convoluted tubule because of a change in the Starling forces across the epithelium (Schafer, 1990). The sodium reabsorption is further inhibited due to an internalization of Na^+/H^+ exchanger isoform 3 (NHE3) (McDonough, 2010). It is unknown why the latter occurs, but it has been suggested that it could be an aftermath of paracrine signaling (Bailey et al., 2004). For instance, ATP is released by the proximal convoluted tubular cells after mechanical stretch and inhibits NHE3 by activation of purinergic P2Y1 receptors (Bailey et al., 2004).

As discussed above, PN may be, at least in part, affected by paracrine signaling in response to elevated RIHP within the renal medulla. One such paracrine mediator has been posed to be the loop of Henle, due to its anatomical proximity to vasa recta (Ivy and Bailey, 2014).

Several compounds, including adenosine triphosphate (ATP), 20-hydroxyeicosatetraenoic acid (20-HETE), reactive oxygen species and endothelin-1, are regarded as important modulators of PN (O'Connor and Cowley, 2010; Garvin et al., 2011; Burnstock et al., 2014). For example, when vasa recta blood flow increases, nitric oxide (NO) also rises significantly (O'Connor and Cowley, 2010). It has been demonstrated that NO enhances the PN response by blunting the myogenic component of autoregulation (Dautzenberg et al., 2011) and inhibiting the $Na^+/K^+/Cl^-$ co-transporter (NKCC2) in the loop of Henle (Ivy and Bailey, 2014). The paracrine communication environ of the kidney elicits a powerful influence on pressure natriuresis. Elucidating the physiological systems underlying its regulation will be an essential tool for the prevention and treatment of hypertension.

1.3 The renal pressor system

The concept that the kidneys produce and release hormones in response to changes in renal perfusion pressure and blood pressure has inspired many to delve into this renal research niche. In 1898, Tigerstedt and his student Bergman reported the seminal discovery that rabbit kidney extracts injected into the renal cortex of rabbits, but not into the medulla, caused a prolonged blood pressure elevation (Paul et al., 2006; Folkow, 2007). The team named this extracted substance, renin, and it became a cornerstone of a century-long research that shaped what eventually became known as the renin-angiotensin-aldosterone-system (RAAS) (see Fig. 1). The legacy of Tigerstedt was continued by Harry Goldblatt's classical experiments on hypertension in the 1930s (Laragh and Brenner, 1990), which advanced our understanding of renin. The next big step came in the early 1940s, when Page and Braun-Menendez' groups

independently showed that renin is an enzyme that is released into the blood stream, where it forms a pressor polypeptide from a plasma globulin (Laragh and Brenner, 1990; Folkow, 2007). The latter was named angiotensin (Ang) after a creative amalgamation of two terms - Page's 'angiotonin' and Braun-Menendez' hypertension (Folkow, 2007). In a nutshell, renin, a protease, cleaves the globulin precursor, angiotensinogen, into the decapeptide, angiotensin I (Ang I), which during passage through the lungs is further transformed to the octapeptide, Ang II (as shown in Fig. 1) (Folkow, 2007). It has been characterized as the organism's most powerful constrictor of pre-capillary smooth muscle. Additionally, in low concentrations, Ang II exerts various properties: it releases aldosterone from the adrenal cortex, accentuates tonic sympathetic activity, stimulates thirst, and has even been suggested to cause mental arousal (Laragh and Brenner, 1990). Moreover, the renal juxtaglomerular cells that produce renin are innervated by efferent fibers of the renal sympathetic nerve. Activation of these fibers releases noradrenaline which acts on β1-adrenergic receptors on the juxtaglomerular cells to stimulate renin secretion. Thus, the kidney receives signals from the brain in order to maintain homeostasis under normal physiological conditions (Laragh and Brenner, 1990). Apart from its medicinally useful properties, the second most prominent contribution of the RAAS to the scientific world was that it served as a trigger for an avalanche of ideas and research hypotheses about other additive as well as counteracting incretory substances produced and released by the renal medulla.

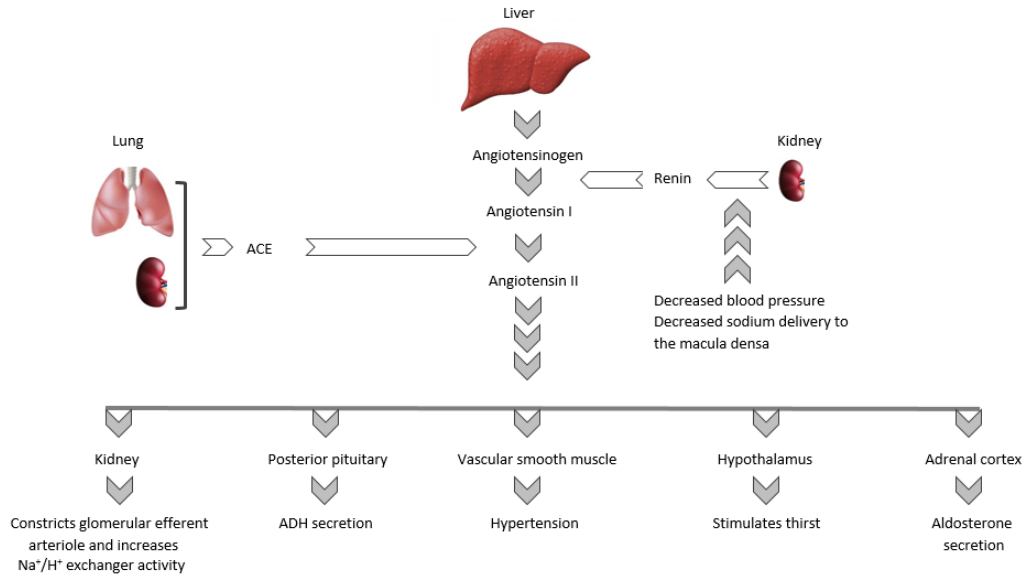

Fig. 1 Schematic of the renin-angiotensin-aldosterone system (RAAS). The juxtaglomerular cells of the kidney release the enzyme, renin, in response to decreased blood pressure or sodium delivery to the macula densa mediated by activation of the sympathetic nervous system. The renin acts on angiotensinogen produced and secreted into the blood from the liver to form angiotensin I. Angiotensin I is then converted to the decapeptide, Angiotensin II, in the pulmonary circulation. Among its multiple prohypertensive properties, a major one is its action on the adrenal cortex to produce and secrete the sodium-conserving mineral corticoid, aldosterone. *Adapted from Koeppen 2013*

1.4 A proposed renal depressor system - historical account and perspectives

With the invaluable finding and contribution that renin presented in the 1940s, it is of little surprise that the scientific community had focused on exploring RAAS and not so much attention was paid to entertaining other renal incretory and regulatory hypotheses. The initial observation that another incretory, possibly a depressor, system might be controlled by the kidney was made by Tigerstedt and Goldblatt while they were studying RAAS (Muirhead et al., 1990). In fact, Goldblatt's realization that the kidneys seemed to host a depressor system did not deter him from his renin-related passion that encouragingly happened to be rather 'fashionable' at the time. The first real attempts to elucidate the kidneys' role in producing and secreting an antihypertensive or RAAS-counteracting agent or agents started in the 1940s and were performed by Arthur Grollman and his pupil, Eric Muirhead. They reported that in bilaterally nephrectomized animals, pressure rose to a hypertensive level and autopsy revealed physiological signs of malignant hypertension (Grollman et al., 1949). Interestingly, he reported that other researchers had previously observed the onset of hypertension following nephrectomy but "failed to be impressed" by this finding (Grollman et al., 1949). Further on, he discovered that under experimental conditions of bilateral ureteral ligation, blood pressure rose, but only temporarily, returning to baseline. When Grollman ligated only one ureter while leaving the contralateral kidney intact, there was no postsurgical change in pressure. Similarly, if one ureter was implanted in the small intestine or vena cava, and the contralateral kidney removed, no hypertension was detectable (Grollman et al., 1949). These results posed that nephrectomy causes hypertension and that the presence on renal tissue in the body protects against the development of hypertension. He went further to propose that hypertension of renal origin did

not appear to be due to liberation of a pressor agent, but results from a failure of the activity of the kidney (Grollman et al., 1949).

Grollman's work on the importance of the renal medulla for the regulation of blood pressure was continued by Muirhead, who later on demonstrated that the hypertension-inducing saline or saline-protein loading in an animal were interjected with the same experimental conditions described above (unilateral ureteral ligation, ureteral implantation in small intestine or vena cava) (Muirhead et al., 1974). A similar level of hypertension occurred after unilateral or bilateral ureteral ligation and bilateral nephrectomy, but ureterovenous anastomosis blunted the hypertensive state significantly (Muirhead et al., 1974). However, Muirhead also considered the fact that when ureteral ligation is performed, this procedure results in damage of the renal medulla, specifically the renal papilla, and that this damage is avoided under the condition of anastomosed ureters. This relationship pinpointed that the renal medulla may be involved in the antihypertensive function of the kidney.

This connection was then refined by autotransplant experiments in which animals, subjected to sodium-volume loading and bilateral nephrectomy, were implanted with either whole kidney, kidney cortex, kidney medulla, spleen or liver tissue (Muirhead et al., 1960; Muirhead et al., 1972a). The subjects implanted with whole kidney or medullary tissue alone did not develop hypertension, while renal cortical, spleen and liver transplants did not protect from hypertension (Muirhead et al., 1960; Muirhead et al., 1972a). In another experiment, Muirhead induced hypertension by treating two groups of animals with angiotensine plus 1% saline. One group underwent a binephrectomy, while the second group had a uninephrectomy and renomedullary autotransplant, followed by a second nephrectomy 7-10 days later (Muirhead et al., 1973). The transplanted group showed protection against the development of hypertension.

These series of experiments demonstrated that the renoprival hypertension is not solely due to hemodynamic changes ascribed to sodium overload. Instead, the hypertensive states were induced by sodium overload and the ablation of renomedullary tissue in the body. Renal medullary transplants also proved to reverse a hypertensive state induced in a Goldblatt-type one-kidney, one-clip model (Muirhead et al., 1970). Later removal of the renal transplant from the Goldblatt animals resulted in a return to the hypertensive state. Other tests by the group also confirmed that viability of the medullary tissue was required for its protective effect against hypertension (Muirhead et al., 1970).

At the time of Muirhead's work, few scientists were focusing on the same scientific niche of the renomedullary regulation of pressure. However, there were some groups who supported Muirhead's notions about the renal medulla by showing that in post-salt hypertension (a retained hypertensive state after a high-salt diet has ended), implanted renomedullary fragments were able to significantly drop pressure (Tobian and Azar, 1971). Notably, in the latter work, Tobian and colleagues observed that renomedullary fragments from a hypertensive rodent were more effective in lowering blood pressure than fragments from a normotensive animal (Tobian and Azar, 1971). An elegantly designed assay by Muirhead further elucidated the effects of transplanted renal medullary tissue in an Ang I- or Ang II- induced hypertensive state, in the presence of 1% NaCl as drinking fluid (Muirhead et al., 1973). Wistar rats were injected subcutaneously daily with Ang I or Ang II and were given drinking water containing 1% NaCl. After 20 days of treatment, the animals had developed hypertension, and transplantation of renomedullary tissue dropped pressure to approximately baseline levels within 24 hours of the surgery. Controlled pressure was maintained for over two weeks, after which the transplant was surgically removed and the hypertensive state resumed (Muirhead et al., 1973). This was the first

evidence that later led Muirhead's team to consider that his beloved and overwhelmingly elusive renomedullary antihypertensive lipid was directly opposing RAAS. The antihypertensive effects of renomedullary tissue transplants were supported by observations in several other laboratories (Tobian and Azar, 1971; Manthorpe, 1973; Manger et al., 1976; Solez et al., 1976; Susic et al., 1976).

1.5 Renomedullary interstitial cells and the antihypertensive renal medulla

An important non-tubular cell type of the renal medulla is the lipid-laden (Type I) interstitial cell i.e., the renomedullary interstitial cell (RIC) (Lemley and Kriz, 1991). Characteristics of this type of interstitial cell include its stellate-like cellular morphology with cytoplasmic projections and increasing cell density toward the tip of the renal papilla. They are noticeable in stained sections of the renal medulla based on their long axes perpendicular to loop of Henle tubules and vasa recta cells, producing a characteristic ladder rung-like appearance. Although cytoplasmic projections from these cells do not make physical contact with loop of Henle or vasa recta, they contact the basement membranes of these structures, and thereby have been suggested to play a role in signaling to these cell types in response to changing conditions (Lemley and Kriz, 1991). Another hallmark is the display of a "conspicuous" perinuclear and cytoplasmic cisternal system (Osvaldo and Latta, 1966). It is characterized by the presence of osmiophilic lipid granules which are rich in arachidonic acid, the precursor of eicosanoid metabolites such as prostaglandin E_2. However, Anggard *et al*. (Larsson and Anggard, 1973) reported that the prostaglandin synthase system was associated with the rough endoplasmic reticulum of and that PGs were not found in RIC lipid droplets. The synthesis of prostaglandin E_2 by interstitial cells was stimulated by angiotensin II and other vasoactive peptides and certain

physiologic conditions (Zusman and Keiser, 1977b). Negative changes in the number of these lipid droplets in experimental models of hypertension (Bohman and Jensen, 1976) suggested a role of these lipid droplets in the secretion of medullipin in response to elevated renal perfusion pressure (Muirhead, 1993; Folkow, 2007).

In search of the renomedullary antihypertensive culprit, Muirhead performed extensive morphological studies of the renomedullary transplants which had prevented or reversed hypertension in his various hypertensive animal models (Muirhead et al., 1970; Muirhead et al., 1972a; Muirhead et al., 1972b). He demonstrated that tubules of the loop of Henle and the vasa recta resorbed upon transplantation of the inner medullary explant in a donor. In the instances where the above-mentioned medullary components were not resorbed, they remained as degenerated vestiges. Collapsed basement membrane material was also present but did not appear to be functionally important. Light microscopic and electron microscopic analysis provided clear evidence that renal interstitial cells and accompanying capillaries were present. The most important observation in this experiment was that the RIC were proliferating and were in close proximity to the developing capillaries (Muirhead et al., 1972a; Muirhead et al., 1972b). The viability of the renal interstitial cells under surgical transplantation conditions made them the best candidate for producing and secreting the medullary hormonal antihypertensive molecule that Muirhead devoted his career to identifying.

To continue his heroic effort to understand the antihypertensive renal medullary substance, Muirhead cultured the renal interstitial cells. The cultured primary cells exhibited similar morphological characteristics as their native cohorts and cells within a proliferating transplant (Muirhead et al., 1972c; Muirhead et al., 1974). The cultured renomedullary interstitial cells displayed the ability to produce the prostaglandins (PGE2, PGA2 and PGF2) that were

characteristic of these cells. Soon after the isolation of the renomedullary interstitial cells, Muirhead's team went on to test if they elicited similar antihypertensive effects as the original transplanted renomedullary fragments. They found that, in hypertensive animals, the cells produced a significant drop in blood pressure to approximately the baseline level within 24 hours of implantation. The transplanted cells were allowed to grow in the animals for 9 days, during which pressure remained low. Afterwards, they were removed from the body, which coincided with a return in pressure to the original hypertensive level. Since the morphology of the implanted cultured RICs was identical to that previously observed with the transplanted medullary fragments, surrounded by capillaries, Muirhead confirmed that the renomedullary interstitial cells were crucial for the reduction of blood pressure under hypertensive conditions. His data were backed by results obtained in other research laboratories, increasing the case for renomedullary interstitial cells being a source of a depressor system (Dunn et al., 1976).

1.6 Tubular mechanisms of diuresis and natriuresis

In order for our understanding of pressure natriuresis to advance, it is necessary for scientists to make progress in pinpointing the exact locations within the kidney, where mediators of pressure natriuresis work. One suggested way to test what areas of the kidney affect pressure natriuresis is to analyze what areas are affected by renal perfusion pressure. RPP has been implicated to affect several segments of the nephron, including the proximal convoluted tubule (PCT), loop of Henle and collecting ducts (CD) (Leyssac, 1964; Dresser et al., 1971; DiBona et al., 1973; Boulpaep and Sackin, 1979; Haas et al., 1986; Roman and Kaldunski, 1988; Kinoshita and Knox, 1990). As previously mentioned, GFR stimulation is not required for the biological induction of natriuresis (Haas et al., 1986; Roman, 1988). More importantly, there is evidence

suggesting that the renal sodium reabsorption is inhibited directly by a cascade of paracrine and biophysical events originating in the renal medulla (Ivy and Bailey, 2014). In previous sections we touched upon that medullary blood flow is poorly regulated and rises when arterial pressure increases. This response is accompanied by increases in renal interstitial pressure. Ultimately, pressure gets transduced from medullary areas to other areas in the kidney, directed and entrapped by the renal encapsulation (Garcia-Estan and Roman, 1989).

One consequence of this mechanical pressure is that sodium reabsorption in the proximal convoluted tubules gets inhibited due to a change in Starling forces across the epithelium (Schafer, 1990). The proximal convoluted tubule reabsorbs approximately 67% of filtered water, Na^+, Cl^-, and other solutes (Koeppen and Stanton, 2013). In addition, it reabsorbs virtually all the glucose and amino acids filtered by the glomerulus. It has been appointed to represent the key element for the reabsorption on the basolateral membrane in this tubule. If it gets over- or under-stimulated, that affects the functioning of all other transporters in the PT (Koeppen and Stanton, 2013). In the first half of the tubule, Na^+ is reabsorbed primarily with $HCO3^-$ and a number of other solutes (P_i, glucose, amino acids, etc.) (see Fig. 2). In contrast, in the second half of the proximal tubule, it is reabsorbed mainly with Cl^-. Interestingly, this effect of mechanical pressure in response to elevated RPP and renal encapsulation has been suggested to be specifically mediated by an internalization of a sodium transporter in the PTs, namely the Na^+/H^+ exchanger (NHE3) (McDonough, 2010). This last phenomenon has not been clearly defined, but it is highly possible that paracrine signaling stimulated by mechanical stretch, following heightened medullary interstitial pressure or RPP, may be responsible for the cascade (Bailey et al., 2004; McDonough, 2010). For example, Bailey demonstrated that ATP can be released by the proximal tubules in response to stretch, and inhibits NHE3 by purinergic P2Y1 receptors (Bailey et al.,

2004). McDonough also showed that when blood pressure or renal perfusion pressure are increased, the lipid raft-associated NHE3 remains at the base of the tubular microvilli, while a Na^+/phosphate cotransporter (NaPi2) gets endocytosed, culminating in decreased Na^+ transport and increased PT flow rate (McDonough, 2010). Furthermore, McDonough observed that a dissociation existed between regulation of apical and basolateral sodium transporters, the change of apical transporters appeared to be rate-limiting for the reabsorption of sodium and that a significant inhibition of the Na^+/K^+-ATPase activity alone was not sufficient to inhibit PT sodium transport (Fig. 2). The intratubular relationship between different transporters is essential to elucidate if we are to advance in our understanding of the renal system and its regulation of blood pressure.

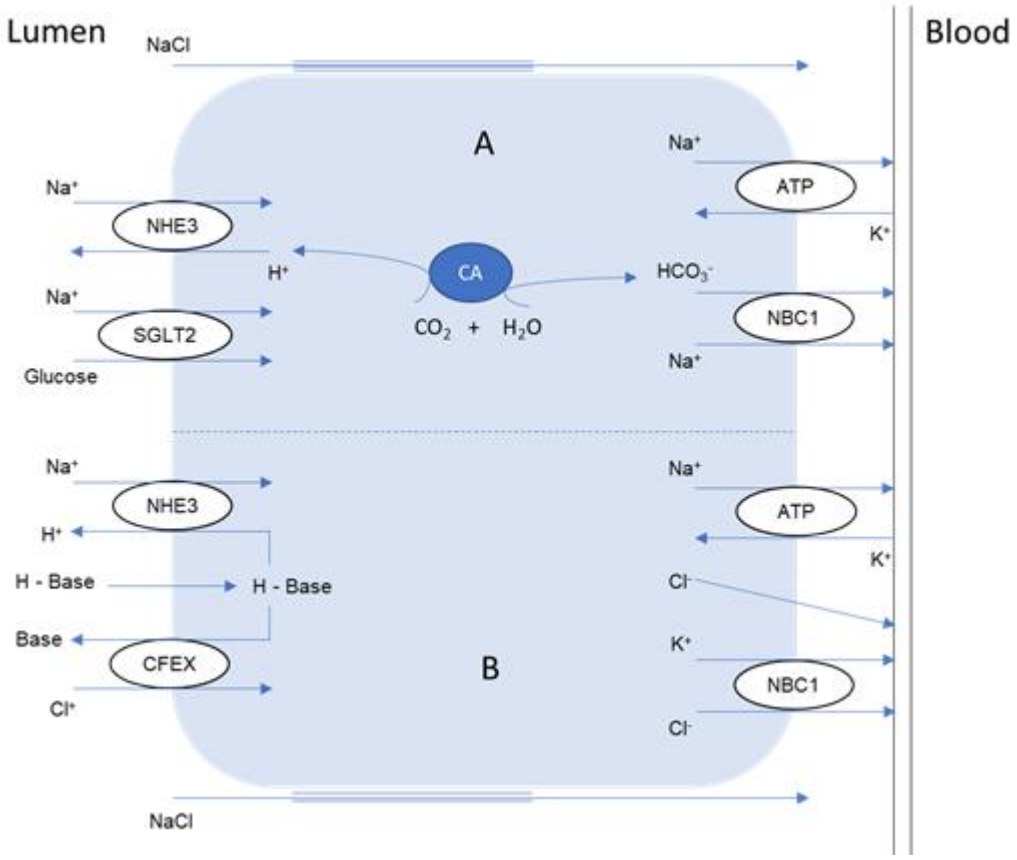

Fig. 2 Na^+ transport processes in the first and second halves of the proximal tubule. **A,** Operation of the Na^+ –H^+ antiporter (*NHE3*) in the apical membrane and the Na^+/K^+-ATPase and bicarbonate transporters, including the Na^+ -$HCO3^-$ cotransporter (*NBC1*) in the basolateral membrane in the first half of the proximal tubules. Carbon dioxide (CO_2) and water combine inside the cells to form H^+ and HCO_3^- in a reaction facilitated by the enzyme carbonic anhydrase (*CA*). Also shown in A is the operation of the Na+ - glucose transporter (*SGLT2*) in the apical membrane, in conjunction with the Na^+ -K^+ -ATPase and glucose transporter (*GLUT2*) in the basolateral membrane that mediate Na^+ - glucose reabsorption. **B,** Na^+ transport in the second half of the proximal tubule. Na^+ and Cl^- enter the cell across the apical membrane through the operation of parallel Na^+ -H and Cl^- -base (e.g., formate, oxalate, and bicarbonate) antiporters (*CFEX*). The secreted H^+ and base combine in the tubular fluid to form an H^+ -base complex that can recycle across the plasma membrane. Inside the cell, H^+ and the base dissociate and recycle back across the apical plasma membrane. The net result is NaCl uptake across the apical membrane. Higher Cl^- concentration in the tubular fluid provides the driving force for Cl^- diffusion. Some glucose is also reabsorbed in the second half of the proximal tubule through a similar to the above-mentioned mechanism, except that the Na^+ -glucose symporter (*SGLT1* gene) transports $2Na^+$ with one glucose. *Modified from Koeppen 2013*

In recent decades focus has been given to an endogenous cardiotonic steroid that acts by inhibiting the Na^+/K^+ ATPases (NKA) and is of essence for the Na^+ signaling regulation in the proximal tubules (Hamlyn and Manunta, 2011). This enzyme is an integral membrane protein that catalyzes ATP-dependent transport of three Na^+ out and 2 K^+ into the cell (see Fig. 2) (Silva and Soares-da-Silva, 2012). The Na^+/K^+ ATPase consists of two main subunits, α- and β-subunit (Feraille and Doucet, 2001). The α-subunit is the catalytic unit of the protein and contains binding sites for Na^+, K^+, ATP, steroid hormones and phosphorylation sites for protein kinase A (PKA) and protein kinase C (PKC) (Bertorello et al., 1991; Ewart and Klip, 1995; Aizman et al., 2001). The β-subunit is involved in enzyme maturation, localization of plasma membrane, and stabilization of the K^+-occluded intermediate (Geering, 2008). A third, non-integral part of Na^+/K^+ ATPase has been identified. It belongs to the FXYD proteins, known as hydrophobic type I polypeptides expressed in tissue-specific manner (Cornelius and Mahmmoud, 2003; Geering et al., 2003; Geering, 2006; Geering, 2008). Reports state that it is involved in the modulation of kinetic properties by molecular interactions with specific Na^+/K^+ ATPase domains.

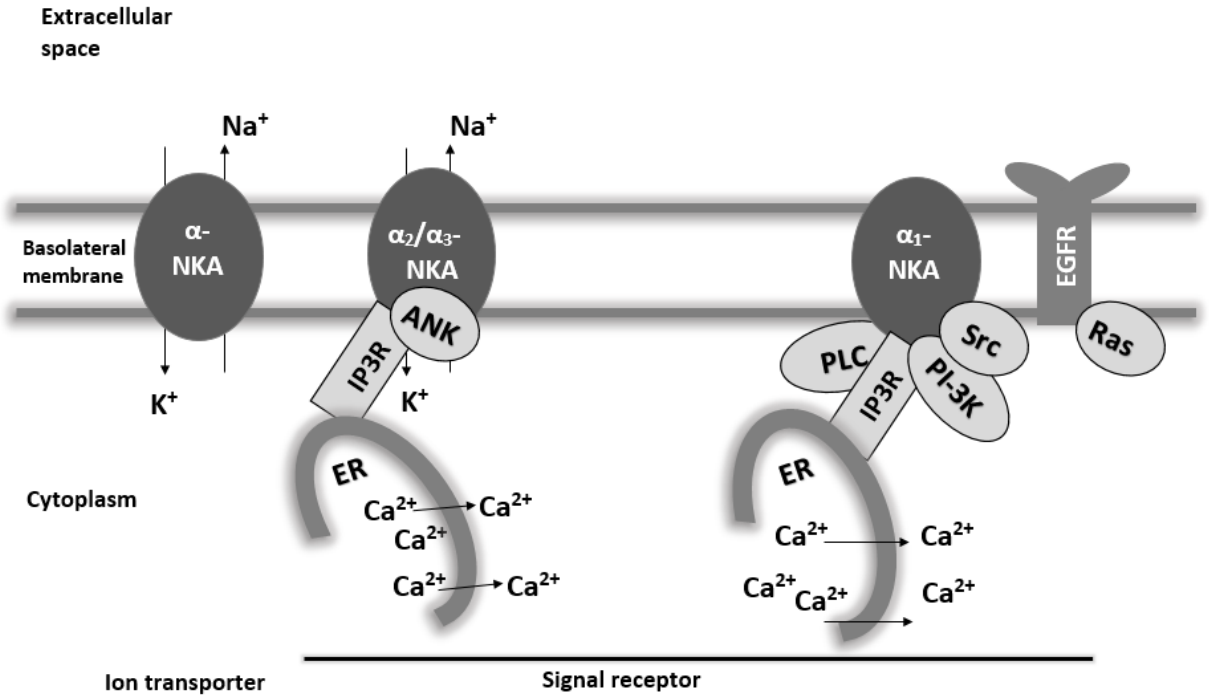

Fig. 3 Na^+/K^+ -ATPase as ion transporter or a signal receptor. From left to right. Na^+/K^+ -ATPase inserted in the basolateral membrane and transporting Na^+ and K^+ against their concentration gradient. Na^+/K^+ -ATPase α_2/α_3-subunits inserted in the basolateral plasma membrane signaling through Ca^{++} oscillations due to interactions with ankyrins (ANK) and inositol triphosphate receptor (IP3R). Na^+/K^+ -ATPase α_1-subunits inserted in caveolae signaling through Src-dependent phosphorylation and/or activation of phospholipase C (PLC), IP3R, and phosphoinositide 3-kinase (PI-3K). *Adapted from Silva and Soares-da-Silva, 2012*

There are four known α- (α 1-4) and three known β- (β 1-3) isoforms of NKA subunits, which allow for the enzyme to be expressed in diverse combinations and tissue localization (Blanco and Mercer, 1998; Vagin et al., 2007). For example, while the α1 isoform is ubiquitous in the body, it is the main isoform found in the kidney (Kaplan, 2002). A2 isoforms are predominantly expressed in the brain, heart, vasculature, skeletal muscles and adipocytes; α3 is mostly present in neuronal tissues; and α4 – in testes (Urayama et al., 1989; Zahler et al., 1992; Woo et al., 2000; Zhang et al., 2005). Among the three β- subunits, β1 is found in most tissues (including the kidney), β2 is found in neuronal tissues, and β3 – in the lungs and testes (Shyjan et al., 1990; Arystarkhova and Sweadner, 1997; Avila et al., 1998; Vagin et al., 2007). The third subunit type, FXYD, comes in 5 isoforms, which provides even more opportunity for diversification of NKA, based on function and concentration in specific body tissues. Studies show that each combination of the isoform subunits demonstrates unique cellular functions and appears to be under cell-specific control (Silva and Soares-da-Silva, 2012). Thus, depending on the Na+/K+- ATPase isoforms (especially due to α1) different cellular signaling events can be generated. As Fig. 3 is showing, A1-NKA is known to interact with several proteins to form an active receptor complex: caveolin-1, Src, phosphoinositide 3-kinase (PI-3K), Ankyrin and inositol triphosphate receptor (IP3R) (see Fig. 3) (Liang et al., 2006; Liang et al., 2007; Quintas et al., 2010). Activation of Src transactivates other tyrosine kinases and, together, they recruit and phosphorylate more proteins. This chain of events results in the generation of second messengers such as phospholipase C (PLC), Ca2+ and reactive oxygen species (ROS) (Silva and Soares-da-Silva, 2012). The α1-NKA is also strongly dependent on the normal functioning of NHE3. If the NHE3 is overexpressed or overstimulated, more Na+ enters the cell, which stimulates a response by the Na+/K+ ATPase to reestablish a physiological Na+ concentration

within the cytoplasm (Cantley, 2002). Furthermore, there is a growing evidence that regulation of NKA is done through a cyclic adenosine monophosphate (cAMP)-dependent protein kinase (Cantiello, 1995a; Cantiello, 1995b; Cantiello, 1997; Sampaio et al., 2014).

Some endogenous catecholamines, peptide hormones and cardiotonic steroids also play a role in the regulation of NKA (Aizman et al., 2001; Feraille and Doucet, 2001; Xie, 2003). Research shows that catecholamines peptides bind to receptors and activate cell signaling cascades that modulate the activity of the ion channel (Efendiev et al., 2000; Gomes and Soares-da-Silva, 2002; Efendiev et al., 2003). Studies also indicate that adenylyl cyclase – cAMP – PKA signaling pathways, often regulated by the endocannabinoid system in the kidney, and PLC – diacylglycerol (DAG) – PKC pathways are responsible for the regulation of Na^+/K^+ ATPase in the kidney. Based on the tissue concentration of PKC, NKA can be up- or down-regulated within different tissues. Binding of PKC and PI-3K and adaptor protein 2 (AP2) to the α1 isoform of NKA has been demonstrated to be a particularly important regulatory mechanism in the proximal convoluted tubules.

Another area of the renal nephron, embedded in the medulla and possibly affected by changes in the medullary blood flow is the loop of Henle (also known as Henle's loop and nephron loop) (see Fig. 4). It is the portion of the nephron connecting the proximal convoluted tubule and the distal convoluted tubule. It has been agreed upon that its main function is to establish a concentration gradient in the medulla of the kidney (Dunn et al., 2011). Henle's loop reabsorbs approximately 25% of the filtered NaCl and 15% of the filtered water. The loop of Henle consists of four differentially acting regions: [1] thin descending limb, [2] thin ascending limb, [3] thick ascending limb, and [4] cortical thick ascending limb, draining urine in the distal convoluted tubule. The thin descending limb of Henle expresses a low permeability to ions and

urea, but remains permeable to water (exclusively through AQP1 water channels). Reaching the depth of the renal medulla, the thin descending limb converts to the thin ascending limb of Henle's loop. This section of the nephron is impermeable to water but becomes permeable to ions. Shortly after, the tubule changes morphologically to become the thick ascending loop of Henle, the most important sodium regulating function unit in the loop of Henle. The key element in solute reabsorption by medullary thick ascending limb of Henle in the Na^+/K^+ -ATPase pump in the basolateral membrane (see Fig. 4). As with reabsorption in the proximal convoluted tubule, reabsorption of every solute by the thick ascending limb is linked to the Na^+/K^+ -ATPase (Koeppen and Stanton, 2013). This transporter maintains a low intracellular concentration of Na^+, which provides a favorable chemical gradient for the movement of Na^+ from the lumen into the cell. The movement of Na+ across the apical membrane into the cell is mediated by the $Na^+/K^+/2Cl^-$ - cotransporter (NKCC2), which couples the movements of Na^+ with K^+ and $2Cl^-$. A K^+ channel on the apical membrane plays an important role in the reabsorption of NaCl by the MTALs by allowing K^+ that has been transported into the cell by NKCC2 to be recycled back to the lumen of the tubule. Because the K^+ concentration in the lumen is relatively low, its recycling is crucial for the functioning on NKCC2 (see Fig. 4). A Na^+/H^+ antiporter in the apical cell membrane also facilitates Na^+ reabsorption, as well as H^+. Then, Na^+ leaves the cell through the basolateral membrane via the Na^+/K^+ -ATPase pump, while K^+, Cl^- and $HCO3^-$ leave the cell across the basolateral membrane by separate pathways (Koeppen and Stanton, 2013). Increased NaCl transport by the thick ascending loop of Henle increases the magnitude of the positive voltage across the lumen and this voltage drives the paracellular transportation of Na^+, K^+, Mg^{++} and Ca^{++} from the lumen. Thus, reabsorption across the thick ascending loop of Henle occurs both by transcellular and paracellular pathways. Around 50% of the transport is transcellular, and

around 50% - paracellular. The thick ascending loop of Henle does not reabsorb water, due to its lack of aquaporins (water channels) (Koeppen and Stanton, 2013).

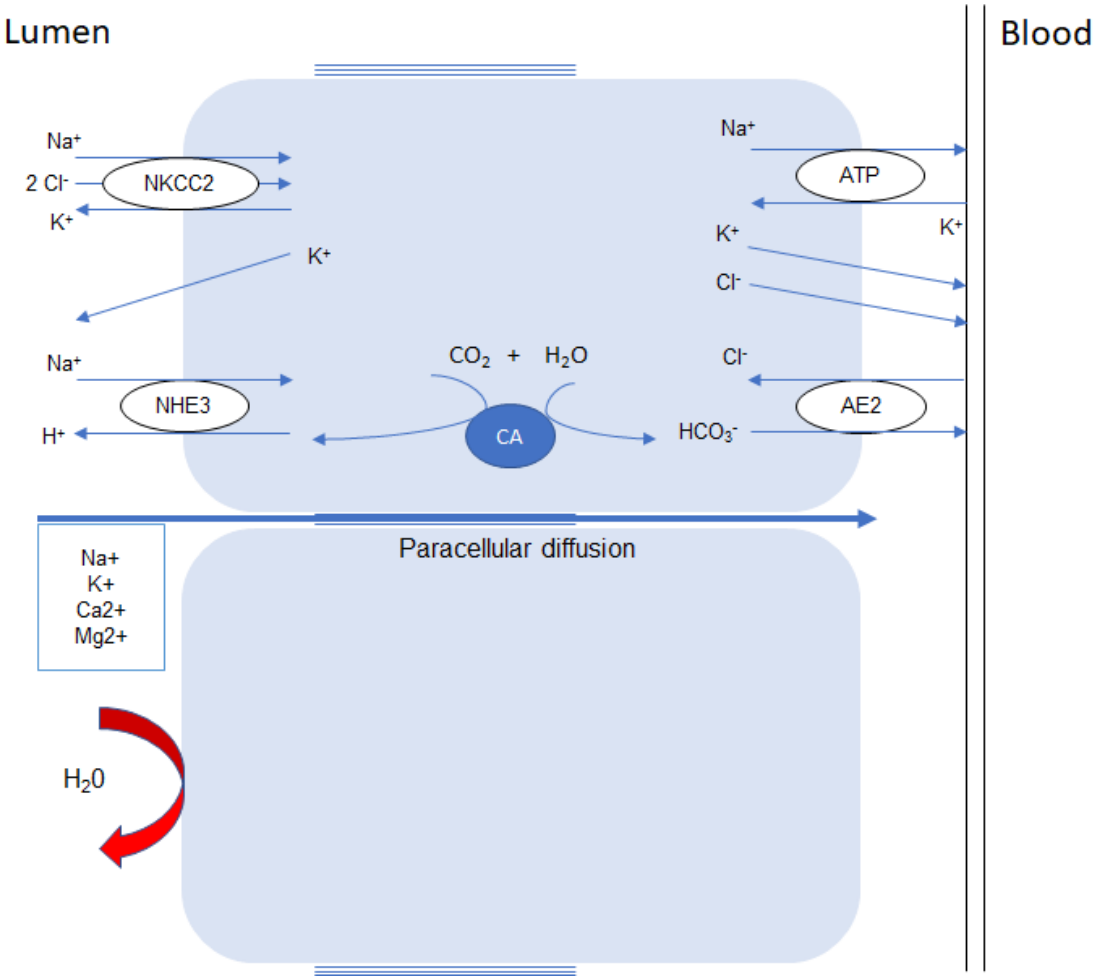

Fig. 4 Transport mechanisms for NaCl reabsorption in the thick ascending limb of the loop of Henle. The positive voltage in the lumen plays an important role in driving the passive paracellular reabsorption of cations. Because the apical membrane is conductive primarily to K^+, the apical membrane voltage is more negative than the basolateral membrane voltage, which is conductive to K^+ and Cl^-, thereby resulting in a lumen-positive transepithelial potential. Genetic mutations of the apical membrane K^+ channel, $Na^+/K^+/2Cl^-$ cotransporter, or the basolateral Cl^- channel can cause serious pathological conditions. AE2, anion exchanger 2. *Adapted from Koeppen, 2013*.

The distal convoluted tubule and collecting duct reabsorb approximately 8% of the filtered NaCl, secrete a variable amount of K^+ and H^+ and reabsorb a variable amount of water (around 8% to 17%). The initial portion of the distal tubule is impermeable to water, but is involved in the reabsorption of Na^+, Cl^- and Ca^{++} (Koeppen and Stanton, 2013). Luminal NaCl enters the cell across the apical membrane through a Na+ - Cl- symporter (NCC) (Tamargo et al., 2014). Na^+ leaves the cell from the Na^+/K^+ -ATPase and Cl^- leaves the cell by diffusion through Cl^- channels (see Fig. 5A). Sodium chloride reabsorption is reduced by thiazide and thiazide-like diuretics which inhibit NCC. Thus, the urine dilution that has begun in the thick ascending limb continues through the distal tubule. The last segment of the distal convoluted tubule and the collecting duct comprise of two types of cells - principal and intercalated cells (see Fig. 5B) (Koeppen and Stanton, 2013). The principal cells are responsible for the reabsorption of Na^+ and water, and the secretion of K^+. The ability of this cell to regulate the reabsorption and secretion of sodium and potassium depends on the activity of Na^+/K^+ -ATPase in the basolateral membrane. As Figure 5B depicts, the apical membrane contains a heterotrimer sodium channel called the epithelial sodium channel (ENaC) (Hanukoglu and Hanukoglu, 2016). In vertebrates, these channels control the reabsorption of sodium in kidneys, colon, lung and sweat glands; they have also been determined to play a role in taste perception (Garty and Palmer, 1997; Mummalaneni et al., 2014). The CD intercalated cells are divided into three types: α-, β- and non-α/non-β- intercalated cells (Roy et al., 2015). The α-intercalated cells secrete H^+ and reabsorb $HCO3^-$ and K^+, thus, regulating the acid-base balance. β-intercalated cells have pendrin transporters that secrete HCO3- and reabsorb Cl^- in the apical membrane and H^+ -ATPase that reabsorbs H^+ in the basolateral membrane. The non-α/non-β- intercalated cells are located in the connecting segment or the connecting tubule. Similarly, to β- intercalated cells, they possess

pendrin and H^+ -ATPases, but they are both located in the apical membrane (Madsen et al., 1988; Kim et al., 1999).

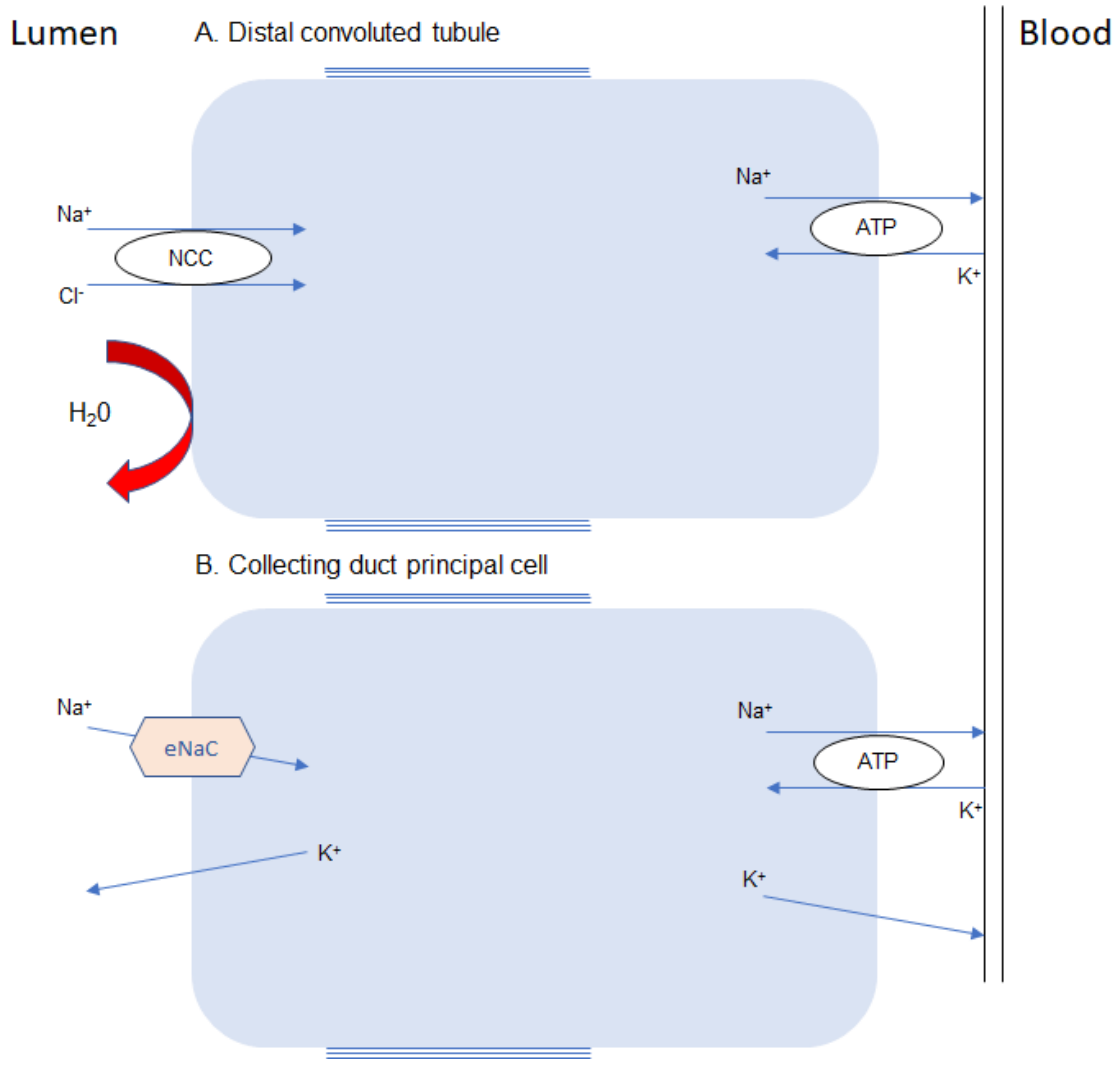

Fig. 5 Transport pathways in distal convoluted tubules and collecting duct principal cells. A, Na^+ and Cl^- reabsorption in the early segment of the distal convoluted tubule is facilitated by the sodium chloride transporter (*NCC*) in the apical membrane. This region is also impermeable to water. B, Principal cells reabsorb sodium through the epithelial sodium channel (*ENaC*) in the apical membrane and the Na^+/K^+ -ATPase in the basolateral membrane. *Adapted from Koeppen 2013*

1.7 Mechanisms of diuretics

It has long been known that the renal system is essential for the maintenance of salt and water homeostasis. By diligently controlling the relationship between renal perfusion pressure (RPP), urinary sodium excretion (U_{Na}), and water excretion (UV), over time the kidney is able to exert this long-term regulation of pressure (Cowley and Roman, 1996). This sensitive balance can easily be disrupted in pathological conditions such as essential hypertension (which is accompanied by the absence of any pathological change in body organs). The primary action of diuretics is to increase the excretion of sodium and water excretion. Changes in Na+ excretion from the kidney result in alterations in the volume of extracellular fluid (ECF) compartment. Therefore, they are commonly given in patients, in whom expanded ECF is causing hypertension.

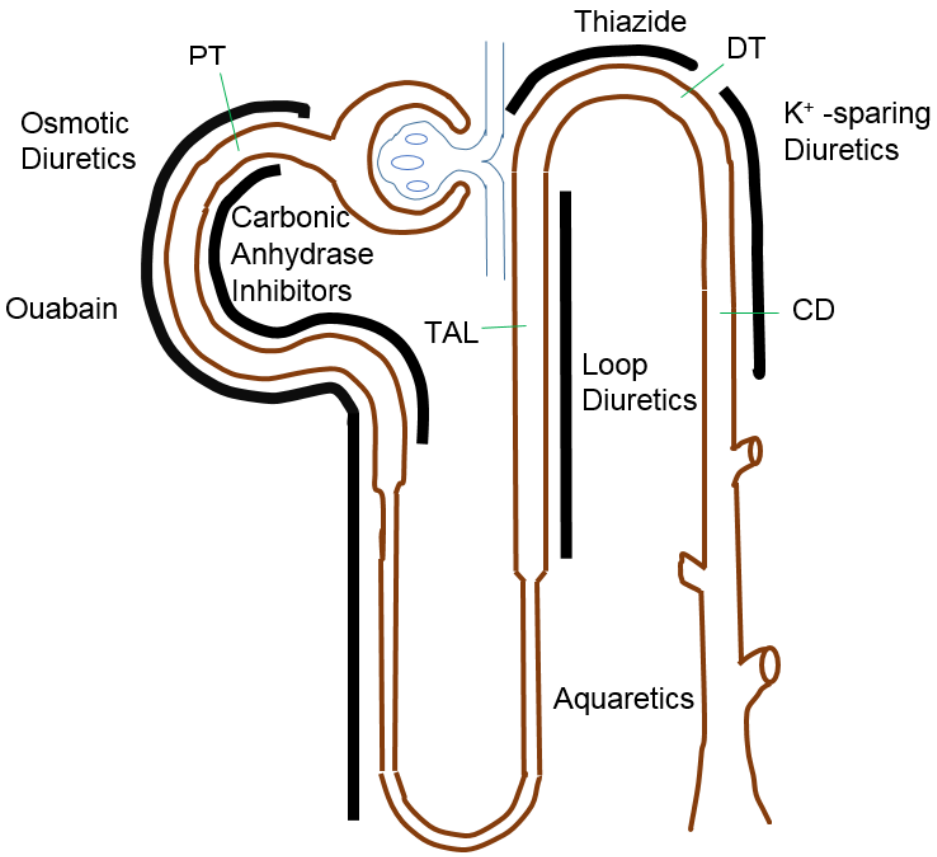

Fig. 6 Schematic of nephron segments where diuretics act. Osmotic diuretics, carbonic anhydrase inhibitors and ouabain act in the proximal convoluted tubules (PT). Loop diuretics act within the thick ascending limb of the loop of the Henle (TAL). Thiazides focus on inhibiting sodium absorption in the distal convoluted tubules (DT). K^+ -sparing diuretics, such as amiloride and benzamil, act in last section of DT and in the collecting duct cells (CD). *Adapted from Koeppen, 2013*.

Figure 6 depicts all nephron sites, at which the different types of diuretics work. Osmotic diuretics act along the proximal tubule and portions of the thin descending loop of Henle. Carbonic anhydrase inhibitors also act predominantly in the proximal tubule. The thick ascending loop of Henle is the tubular target for all loop diuretics. The early part of the distal convoluted tubule is the site of action of thiazide and thiazide-like diuretics. K^+ sparing diuretics can act in the late parts of the distal tubule and the cortical areas of the collecting ducts. Which tubular portions diuretics act in determines the magnitude of natriuresis and diuresis exerted by the kidney. For instance, diuresis stimulated in the loop of Henle is much more potent than this in the distal convoluted tubule, because MTAL reabsorbs a larger amount of Na^+. The effect that diuretics exert on other solutes also depends on their site of action.

Osmotic diuretics, like their name suggests, are compounds that inhibit the reabsorption of solutes and water by affecting the osmotic driving force of reabsorption. Differently from other diuretics, osmotics do not act on membrane transporters to inhibit reabsorption, but generate an osmotic pressure gradient. Osmotic diuretics, such as mannitol, reach the PT through glomerular filtration. Since they are poorly reabsorbed, osmotic diuretics remain in the lumen, where they can exert their actions. They affect portions of the tubules that are very permeable to water, such as the PT and the thin descending loop of Henle. Because of the large amount of fluid reabsorption by the proximal tubules (60 – 70 %), this section of the nephron is the best target for osmotic diuretics. However, it is important to notice that some of the Na^+ that is not taken up by the proximal tubule, is reabsorbed by the downstream tubular segments. Due to that phenomenon, the effect of osmotic diuretics is not as potent as expected. Only about 10% of Na^+ in the filtrate gets excreted.

Carbonic anhydrase inhibitors, such as acetazolamide, work on carbonic anhydrase in proximal tubules (see Fig. 6). They are also present in other tubules of the kidney, but their diuretic activity is almost entirely achieved through the proximal tubules. The reason for it is that around one third of Na^+ reabsorption through the proximal tubule occurs by exchange with H^+ (through the Na^+/H^+ antiporter). Even though one third of proximal tubule Na+ reabsorption is coupled to H+ excretion, the overall natriuresis during carbonic anhydrase is not very large. There ae several reasons why this occurs. Firstly, a complete inhibition of the carbonic anhydrase does not imply a complete blockade of Na^+ reabsorption, some still gets through the proximal tubule via other transporters. Secondly, when the proximal tubule reabsorption is impeded, the downstream tubules compensate for this biological malfunction by reabsorbing more Na^+. Finally, increased concentration of Na^+ in the macula densa causes a decrease in GFR. Clinical reports show that treatment with carbonic anhydrase inhibitors lead to a mild elevation in Na^+ excretion- around 5 to 10%.

Loop diuretics are organic anions that enter the lumen through organic anion secretion of the proximal tubule. Some clinically used representative loop diuretics are furosemide, bumetanide, torsemide and ethacrynic acid). They inhibit Na^+ reabsorption by acting in the $Na^+/K^+/2Cl^-$ symporter on the apical membrane of the Henle loop (refer to Fig. 6). However, inhibition of the NKCC is not their only diuretic mechanism of action. They reduce the level of urine dilution within the loop as Na+ reabsorption decreases. This, then, inhibits the generation of medullary interstitial hyperosmotic gradient. Additionally, with the lower renomedullary interstitial osmolality, the CD provides only a limited water reabsorption, thus enhancing diuresis. Loop diuretics are the most potent among diuretics enabling approximately 25% fluid to be excreted.

Hydrochlorothiazide, chlorthalidone and metolazone are another type of organic anions that act as diuretics. These compounds target the Na^+/Cl^- symporter in the apical site of the distal convoluted tubular cells by blocking it and, therefore, enhancing Na+ excretion (refer to Fig. 6). In this portion of the nephron water cannot be reabsorbed, so under normal conditions, urine gets diluted. However, when Na^+ reabsorption is impeded by thiazides, this filtrate dilution is minimized. Natriuresis with thiazides reaches around 5 - 10% of the filtered Na^+.

Another class of diuretics acts in tubular regions where K^+ secretion happens. This group of compounds is called K^+-sparing diuretics and causes only a small natriuretic effect (3 – 5% of the filtered Na^+) (Pearce et al., 2015). There are two sub-classes of K+/sparing diuretics: aldosterone antagonists in principal collecting duct cells and epithelial Na+ channels (ENaC) in the apical side of the CD cells (see Fig. 6). Members of the former are spironolactone and eprelenone. Aldosterone antagonists prevents the aldosterone-stimulated Na+ reabsorption and K+ excretion. ENaC blockers, such as amiloride and triamterene, block the entry of Na+ in the principal cell by directly inhibiting the Na+ channel (Pearce et al., 2015). This lower Na^+ entry decreases the activity of the Na^+/K^+ ATPase on the basolateral site of the same cells. Inhibition of Na^+ uptake in this tubule also causes a change in the electrical gradient. The altered electrical gradient of Na^+ across the membrane causes a reduction in the electrochemical gradient for K^+ secretion. Thus, K^+ is additionally protected from excretion.

Recently, more diuretic medications have been developed that act as AVP receptor (V2) antagonists. Some examples are tovlaptan and lixivaptan. They target the AVP receptors, located in the late distal tubule and the collecting duct to block the action of arginine vasopressin. Consequently, the filtrate becomes more dilute and gets excreted. These diuretics are preferred in

medical cases when urine is hypoosmotic and the kidneys fail to excrete solute-free water due to AVP dysfunctions.

Last but not least, a group of cardiotonic steroids, such as Ouabain, has been implicated to act as a class of Na+/K+ ATPase inhibitors in cells possessing this enzyme. They achieve their function by binding to the α1 subunit of the NKA and inhibiting the reabsorption of Na+ (see Fig. 6). This activity alters the intracellular concentration of Na+ and inhibits NHE3-mediated inflow of Na+ within the cell. They are believed to have important physiological role in the regulation of blood pressure and other cellular functions, some of which are proliferation and differentiation (Hamlyn et al., 1991; Tian et al., 2009; Jaitovich and Bertorello, 2010; Hamlyn and Manunta, 2011). However, ouabain and other members of this family have not been considered as useful diuretics due to the ubiquitous localization of the Na/K pump (brain, kidney, liver, lungs, adipocytes and others). Nevertheless, it is noteworthy that NKAs come in different isoform combinations, which could be a useful tool to designing a more specific NKA inhibitor that would be tissue specific.

Chapter 2 - The renal endocannabinoid system

2.1 History of the endocannabinoid system

Cannabis, also known as marijuana, is an umbrella term for all plant extracts that come from the genus Cannabis in the plant family cannabaceae and elicits its activities through the mammalian endocannabinoid system (Whiting et al., 2015). The endocannabinoid system has been a target of man's interest and ingenuity for millennia for both its central and peripheral effects (Evans, 1991). References of *Cannabis sativa*, the plant containing the psychoactive substance THC (Δ^9-tetrahydrocannabinol) dates back over 12,000 years (Abel, 1979). Sources indicate that marijuana has been used as a medicinal substance in China, India, the Middle East, South Africa and South America. Some of the ancient civilizations even considered it to be one of the oldest existing drugs in history (Mechoulam and Feigenbaum, 1987). Ancient records from China demonstrate that it was used for the treatment of constipation, malaria, rheumatic pains and "female" disorders. In India, cannabis was used medicinally to reduce fever, induce sleep, stimulate appetite, relieve headaches and even cure some venereal diseases (Mechoulam and Feigenbaum, 1987). It was also the ancient civilizations such as in China, Greece and the Roman Empire that first took advantage of the natural strength that cannabis plants provided to make clothes and ropes. These additional properties of the plant were known and utilized in early settlement towns, such as in Jamestown, VA, in North America around 1611 (Grinspoon and Bakalar, 1997).

As a modern age medicinal compound, cannabis entered the Western world medical field after an extensive study of its safety in patients and experimental animals conducted by W.B.

O'Shaughnessy, a 30-year-old Irish physician, serving in the British army in India (Johnson et al., 1984). He found that cannabis administered in both low and high doses was not harmful to animals. Furthermore, O'Shaughnessy reported the administration of cannabis to human patients suffering from seizures, tetanus, rabies and rheumatism and recorded success, along with side effects such as catalepsy. His findings that the plant elicits anticonvulsant, analgesic, anxiolytic and antiemetic effects first made cannabis usage an acceptable form of medicine in Europe in 19th century. At the time cannabis could be acquired from any pharmacy in the forms of oils, tinctures and creams. However, shortly after the emergence of the hypodermic needle as a drug administration tool, the usage of cannabis in both North America and Europe considerably dwindled. The rate of decline was partially due to lack of solubility and poor stability, but also the variability of its effects among the patient population (Grinspoon and Bakalar, 1997). Therefore, water-soluble drugs like opioids, aspirin and barbiturates prevailed among healthcare practitioners. The case for cannabis was not assisted by the federal prohibition of marijuana in the 1937 via the Marijuana Tax Act, which led to criminalization of the substance. Far from this being the end of the imposed restrictions on marijuana, it was further restrained by a war on drugs and the placement of marijuana in the most restricted drug category. Cannabis had lost its popularity up until 1975, when a series of experiments testing the effect of the psychoactive marijuana ingredient, THC, in patients undergoing cancer chemotherapy took place. The study revealed that THC significantly alleviated the emetic effects of chemotherapy in comparison to control groups (Sallan et al., 1975). Other studies showed that 20 mg of THC was equally efficacious as a 60 to 100 mg codeine (Noyes and Baram, 1974; Noyes et al., 1975) as an analgesic. These and similar findings encouraged scientists to revisit THC as a potential

therapeutic agent. California was the first state to legalize marijuana for some specific diseases in the 1990s (Park et al., 2017).

Interestingly, although marijuana has been used for medicinal and recreational purposes throughout the ages, isolation and structural elucidation of its major cannabinoid constituents – including THC – was achieved as recently as the 1960s and 1970s. This discovery was followed by the identification of two cannabinoid receptors, cannabinoid-1(CB1R) and cannabinoid-2 (CB2R) receptors. CB1 receptors were discovered in 1988 by A.C. Howlett at al. and later cloned in 1990 (Johnson et al., 1988; Matsuda et al., 1990). In 1992 the first endogenous cannabinoid, anandamide (AEA, the most well studied endocannabinoid ligand), was isolated from porcine brain by Raphael Mechoulam and his lab members W. A. Devane and Lumir Hanus after a search for an THC-analogue molecule that binds to CB receptors in the brain (Devane et al., 1992). Shortly after, a second cannabinoid receptor, CB2, was discovered and successfully cloned in 1993 by Munro *et al.* from the promyelocytic leukaemic cell line HL-60 (Munro et al., 1993). The second major known endocannabinoid ligand, 2-arachidonoyl glycerol (2-AG) was discovered in canine intestines also by Raphael Mechoulam (Abrahamov and Mechoulam, 1995; Mechoulam et al., 2014). This boost in scientific findings encouraged the development of pharmacological "tools" to study the endocannabinoid system. More specifically, the observation that the cannabinoid agonist, THC, in its many preparations enhanced appetite led to the logical extension that blocking of the cannabinoid receptors would cause a decrease in appetite Mackie (Mackie, 2006). The first selective CB1 receptor antagonist / inverse agonist was SR141716A, discovered in 1994 (Rinaldi-Carmona et al., 1994). Another cornerstone for the endocannabinoids research was the discovery of the first endocannabinoid degrading enzyme, fatty acid amide hydrolase (FAAH) by Deutsch in 1993 (Deutsch and Chin,

1993) which was followed by its cloning in the Cravatt laboratory (Cravatt et al., 1996; Giang and Cravatt, 1997). This rapid series of discoveries undoubtedly assisted the advances in the endocannabinoid research that are still ongoing and has spread beyond the scope of psychoactivity.

The positive changes in perceptions and the encouraging scientific findings later led to the legalization of marijuana's recreational usage in Colorado and Washington in 2012. Following the American pro-marijuana state of mood, in 2013 Uruguay became the first country in the world to legalize marijuana nationwide. By February 2018, nine states and Washington, D.C. had embraced the legalization of recreational marijuana. State reports vouching evidence in support of the beneficial economic and societal benefits of this act have contributed to an all-time high level of public support (64 %) for the substance's legalization (drugpolicy.org/legalization-status-report, 2018). Allegedly, the majority of Americans - including 51 % of Republican now support the legalization of marijuana. According to the 2015 National Survey on Drug Use and Health, cannabis is the most commonly used illicit drug – over 22.2 million people using it over the last month. More recently, a Yahoo News/Marist survey collaboration calculated that approximately 35 million Americans use marijuana on a monthly basis and more than 78 million questionnaire participants admitted to having tried cannabis at least once in their life (Ingraham 2017 from a Washington post article). In 2017 alone, an estimated number of 55 million residents reported using marijuana within the past year. It is significant to note that this figure amounts to more than the number of current active tobacco smokers (37.8 million) (Phillips et al., 2017).

2.2 The endocannabinoid system

The endocannabinoid system (eCB system) is a complex system that regulates the mammalian biological homeostasis. It is present and active in both the central and the peripheral nervous systems, where it elicits its differential effects to accommodate biological development and functions (Tam, 2016). It is also reported to be present in non-nervous system cell types, for example, macrophages, adipocytes and proximal tubular epithelium of the kidney. It is comprised of two main endocannabinoid ligands (eCBs), anandamide or *N*-arachidonoyl ethanolamide (AEA) and 2-arachidonoyl glycerol (2-AG), their cannabinoid-1 and cannabinoid-2 receptors (CB1R and CB2R, respectively), and enzymes responsible for their metabolism, fatty acid amide hydrolase (FAAH) and monoglyceride lipase (MAGL) (Matsuda et al., 1990; Munro et al., 1993; McKinney and Cravatt, 2005). A complete (receptors, enzymes and endocannabinoids) cannabinoid system appears to be universal for all vertebrate animals (Elphick and Egertova, 2005). Apart from the two known cannabinoid receptors, data suggest that cannabinoid ligands can also bind to the transient receptor potential vanilloid-type I (TRPV1) and the orphan G-protein-coupled receptors (Benito et al., 2012). Other degrading enzymes and certain transporters have also been reported to regulate the cannabinoid levels and properties (Piomelli, 2003). Although the endocannabinoids are considered to be neurotransmitters, they are not actually synthesized and stored in cellular vesicles. Instead, they are produced and released on demand. Anandamide and 2-AG are synthesized by cleavage of membrane lipid precursors N-arachidonoylphosphotidylethanolamine (NAPE) and diacylglycerol (DAG) respectively (Rodriguez de Fonseca et al., 2005). The signaling of endocannabinoids follows a retrograde manner: when an endocannabinoid is released from the postsynaptic ganglion, it binds to a cannabinoid receptor on the presynaptic membrane. Since

they bind to inhibitory signaling molecules, they elicit inhibition of neurotransmitter release in the presynaptic neurons where these receptors are localized. Thus, endocannabinoids are reported to play a role as modulatory regulators of other neurotransmitter systems (Rodriguez de Fonseca et al., 2005).

Anandamide is a polyunsaturated fatty acid neurotransmitter derived from the non-oxidative metabolism of eicosatetraenoic acid (arachidonic acid or AA) and is an essential ω-6 polyunsaturated fatty acid. Its name comes from the Sanskit word *ananda*, which means "joy, bliss delight" and amide (Devane et al., 1992; Mechoulam et al., 1995). There are three known biosynthesis pathways that generate AEA in the body: [1] formation of the N-acyl derivative of phosphatidylethanolamine, N-arachidonoyl-phosphatidylethanolamine (NAPE), followed by cleavage by a NAPE-specific phospholipase D (NAPE-PLD); [2] α/β-hydrolase 4 (ABH4) cleavage to an intermediate lipid that is then hydrolyzed to anandamide by a metallo-dependent phosphodiesterase; and [3] phospholipase C (PLC)-catalyzed cleavage of NAPE to phosphoanandamide, which is subsequently dephosphorylated by a phosphatase (Leung et al., 2006; Simon and Cravatt, 2006). Given the differential distribution of all these biosynthesis-related factors in diverse tissues, it has been hypothesized that their localization and concentrations could partially alter cannabinoid signaling (Liu et al., 2008). Endogenous AEA is found in relatively low concentration within the body, but this concentration can be also affected by dietary supplements of arachidonic acid and other essential fatty acids (Berger et al., 2001; Osei-Hyiaman et al., 2005). Most studies suggest that cannabinoids and other lipids binding to CB receptors, administered orally, get degraded in the intestine and liver, although such lipids could bind and elicit some activities on gut CB receptors (Katayama et al., 1997). Anandamide is one of the endogenous cannabinoids that, apart from CB1 receptors, also binds to the transient

receptor potential cation channel subfamily V member 1 (TRPV1). Activation of this receptor signaling cascade has been determined to cause hypotension, analgesia and increased diuresis in mice (Pacher et al., 2004; Haller et al., 2006; Xie and Wang, 2009). However, most endocannabinoids and all studied phytocannabinoids elicit their effects in the body through CB1 or CB2 receptors (Lam et al., 2005; Li and Wang, 2006). There is a possibility for novel cannabinoid agonists to result in therapeutic actions via TRPV1 receptors along with actions elicited through the cannabinoid receptors 1 and 2.

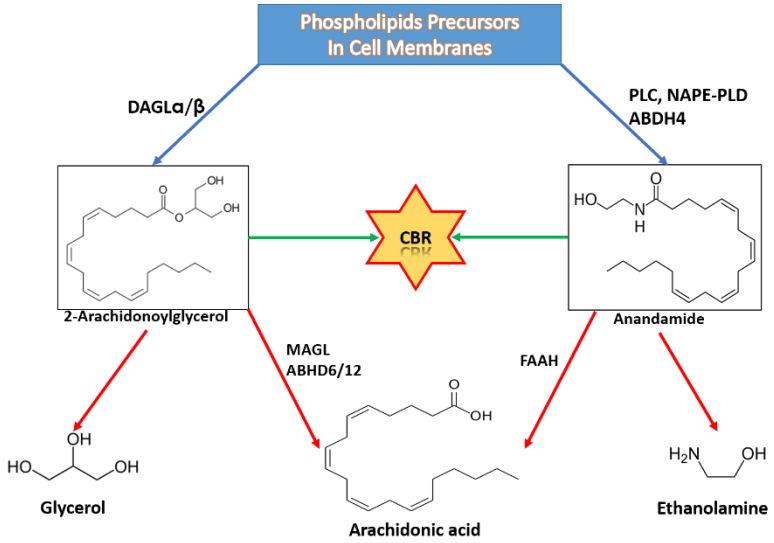

Fig. 7 Schematic representation of pathways leading to synthesis and degradation of the two major endocannabinoids. Precursors for the synthesis of both are phospholipids that are metabolized via several different lipases to produce ligands that bind to cannabinoid receptors (CBR). Degradative enzymes catalyze the ligand to arachidonic acid, which is inactive on the cannabinoid receptors.

2- Arachidonoylglycerol (2-AG) is the primary endogenous cannabinoid that binds to CB2 receptors (Stella et al., 1997). It is an ester that is formed from arachidonic acid and glycerol. 2-AG is synthesized from arachidonic acid-containing diacylglycerol (DAG). It can also be derived from phosphatidylcholine (PC) and phosphatidic acid (PAs) by the action of DAG lipase and the hydrolysis of acid-containing lysophosphatidic acid (Murataeva et al., 2014). 2-AG is considered to be present in relatively high levels in the CNS (~ 5 - 10 nmol / g tissue in mouse brain) (Kondo et al., 1998). Of the two isoforms of DAGL, α and β, DAGL-α predominantly regulates the 2-AG concentration in the brain (see Fig. 1) (Mukhopadhyay et al., 2010; Ludanyi et al., 2011). Recent studies show that degradation of 2-AG involves three different metabolizing enzymes. 85% of 2-AG in the CNS gets metabolized by MAGL, while 4% and 9% is degraded by the relatively novel and uncharacterized serine α/β- hydrolases 6 and 12 (ABHD6/ABHD12) (Blankman et al., 2007). Interestingly, FAAH has also shown a positive metabolic activity toward 2-AG in vitro, but negligible metabolic activity in whole brain (Blankman et al., 2007). The localization of 2-AG's degrading enzymes within the body could potentially play a role in the endocannabinoid's ability to bind its receptors and produce its actions.

FAAH and MAGL are responsible for the metabolism of anandamide to arachidonic acid and 2-AG to ethanolamine/glycerol (Palmer et al., 2002; Piomelli, 2003). FAAH is AEA's primary degrading enzyme. Fatty acid amide hydrolase (an anandamide amidohydrolase) is a member of the serine hydrolase family of enzymes. In humans it is encoded by the gene FAAH (Cravatt et al., 1996). FAAH is an integral membrane hydrolase with a single N-Terminal

transmembrane domain. *In vitro*, it has an esterase and amidase activity (Patricelli and Cravatt, 1999). In vivo, it acts as a catabolic enzyme for a class of bioactive lipids called fatty acid amides (FAAs), such as: anandamide, 2-AG, other *N*-acylethanolamines, oleamide and *N*-acyltaurines (Cravatt et al., 2001). Studies have shown that transgenic FAAH KO mice express an analgesic phenotype with reduced pain sensation in hot plate tests, formalin tests and tail flick tests (Massa et al., 2004). Additionally, because of their altered ability to degrade anandamide, FAAH KO animals appear to be over-sensitive to exogenous anandamide (Cravatt et al., 2001). Abundant research suggests that FAAH could be a useful potential drug target for the treatment of pain, drug abuse and anxiety disorders (Panlilio et al., 2013; Salaga et al., 2014; Ghosh et al., 2015). However, more knowledge about FAAH's regulatory properties is required to fully evaluate the potential of the hydrolyzing enzyme as a drug target, especially in peripheral systems, where it is also abundantly present. The second endocannabinoid-metabolizing enzyme, monoacylglycerol lipase or MAGL is a protein that is encoded in humans by the MGLL gene (Karlsson et al., 1997). It is a membrane-associated member of the serine hydrolase family. MAGL functions together with hormone-sensitive lipase (LIPE) to hydrolyze intracellular triglycerides stored in adipose tissues to fatty acids and glycerol (Karlsson et al., 2001). Monoacylglycerol lipase is the prevalent enzyme that metabolizes 2-arachidonoyl glycerol to free fatty acids and glycerol (Dinh et al., 2002). When the enzyme is inhibited there occurs a >10-fold accumulation of 2-AG in the brain of mice, along with a significant downregulation of CB1 receptors (Savinainen et al., 2012).

Initially, it was hypothesized that, because of their high lipophilicity, cannabinoids exerted their actions in the body through altering membrane fluidity. Later, in 1990, CB1 receptors were cloned from rat, mouse and human tissue. Shortly after this discovery, a second

member of the cannabinoid receptor family, the CB2 receptor, was discovered. CB1 receptors are highly expressed in the brain, but are present in numerous organs (Pertwee, 2012). In the CNS, they are expressed in abundance in the olfactory bulb, the cerebral cortex, the hypothalamus, the hippocampus, the striatum and the cerebellum (Le Boisselier et al., 2017).

When CB1 receptors are stimulated by an agonist, they inhibit adenylyl cyclase, and therefore, it also inhibits the cyclic adenosine monophosphate (cAMP) formation via $G\alpha_{i/o}$ proteins. Consequently, this decreases protein kinase A-dependent phosphorylation processes (Le Boisselier et al., 2017). Moreover, studies reveal that they may also activate Gs, Gq/11, and G-protein independent signaling pathways (Howlett, 2005). CB1 receptors are also associated with the modulation of some ion channels with inhibition of Ca^{2+} and stimulation of several types of K^+ channels (Gyombolai et al., 2012). On binding to CB1 receptors, cannabinoids can also mediate inhibition of N- and P/Q-type calcium channels and stimulation of potassium channels (Berger et al., 2001). In the peripheral tissues, this cannabinoid receptor subtype is found in cardiovascular tissues, the gastrointestinal tract, liver, reproductive system, muscles, bones and skin (Freund et al., 2003; Julien et al., 2005; Osei-Hyiaman et al., 2005; Van Sickle et al., 2005; Ofek et al., 2006; Onaivi et al., 2006; Tam et al., 2006; Pacher and Kunos, 2013). Studies have suggested that CB1 receptors also play an important role in regulating the cardiovascular system through two main actions: [1] downregulation of inotropy in the myocardium, and [2] vasodilation in vascular tissues. Both these effects have been associated with the hypotensive property of cannabinoids (O'Sullivan, 2015).

CB2 receptors are primarily found in immune cells at similar sites as CB1 receptors (non-parenchymal liver cells, endocrine pancreas and bone). They are also reported to regulate the immune system (releasing cytokines) and the hematopoietic system (Maccarrone et al., 2015).

CB2Rs are found in the CNS, more particularly located in neurons and microglia. They primarily couple to $G_{i/o}$ proteins to modulate a plethora of signaling pathways: adenylyl cyclase, MAPK, c-Jun N-terminal kinase, Akt kinase/ protein kinase B, phosphoinositide 3-kinase/Akt nuclear factor k-light-chain-enhancer, nuclear factor of activated T cells, cAMP response element–binding protein/activating transcription factor, Janus kinase/ signal transducer and activator of transcription, sphingomyelinase, and caspase, as well as some potassium and calcium ion channels (Bouaboula et al., 1996; Pertwee, 1997; McAllister et al., 1999; Sugiura and Waku, 2000; Howlett, 2002; Molina-Holgado et al., 2002; Ehrhart et al., 2005; Herrera et al., 2005; Pertwee, 2010; Atwood et al., 2012). Despite the discovered connection between CB1R activation and all these signaling pathways, modulation of adenylyl cyclase and extracellular signal-regulated kinases ½ (ERK1/2) have been the two most well studied directions in the CB2 receptor niche. Due to lack of psychotropic effects, characteristic for CB1R activation, CB2 receptor activation has been observed to produce desirable actions in pre-clinical models (Leleu-Chavain et al., 2012; Han et al., 2013) have been a target of research in both academic and commercial laboratories. For instance, targeting CB2 receptors with synthetic agonists has been associated with alleviation of acute pain, chronic inflammatory pain and neuropathic pain (Ehrhart et al., 2005). Other researchers have found evidence that CB2 receptor targeting may be important for the treatment of neurodegenerative or neuroinflammatory diseases, such as multiple sclerosis (Pertwee, 2007), amyotrophic lateral sclerosis (Kim et al., 2006; Shoemaker et al., 2007), Huntington's disease (Sagredo et al., 2012) and stroke (Pacher and Hasko, 2008). CB2 targeting has also been proposed to represent a great potential therapy for peripheral disorders that comprise inflammation, including atherosclerosis (Mach et al., 2008; Mach and Steffens, 2008), inflammatory bowel diseases (Izzo and Camilleri, 2008; Wright et al., 2008),

ischemia/reperfusion injury (Batkai et al., 2007), renal fibrosis (Barutta et al., 2011) and liver cirrhosis (Izzo and Camilleri, 2008; Mallat and Lotersztajn, 2008). Finally, CB2 agonists have been associated with positive results in several preclinical models of cancer (Guzman, 2003; Wright et al., 2008). However, the preclinical success of CB1 agonists in the treatment of numerous diseases has not fared so well in clinical trials. More studies are continuously being done in attempts to resolve this gap in efficacy between preclinical and clinical trials.

2.3 The renal endocannabinoid system

Uncovering the biological functions of the endocannabinoids in the body has become possible only after the discovery of selective and potent inhibitors of CB1 and CB2 receptors and the generation of transgenic animal strains in these (Rinaldi-Carmona et al., 1994; Rinaldi-Carmona et al., 1998). The presence and functional importance of endocannabinoids in the kidney were initially studied and introduced by Deutsch and Chin, who showed enzymatic activity that catalyzes anandamide in a crude homogenate of a rat kidney (Deutsch and Chin, 1993). Soon after that, transcripts of the CB1 receptors, identified in the human kidney made it possible to find functional CB1 receptors in the entire kidney (Shire et al., 1995; Barutta et al., 2010; Larrinaga et al., 2010). Some of these areas included different parts of the nephron: afferent and efferent arterioles, glomeruli, tubules, loop of Henle and collecting ducts (Koura et al., 2004; Janiak et al., 2007; Barutta et al., 2010; Larrinaga et al., 2010; Nam et al., 2012; Silva et al., 2013; Lecru et al., 2015). It has also been detected in other renal cells, including podocytes, proximal and distal tubular epithelial cells and mesangial cells (see Table 2) (Janiak et al., 2007; Barutta et al., 2010; Jenkin et al., 2010; Larrinaga et al., 2010; Lim et al., 2010; Lim and Park, 2012; Nam et al., 2012; Tam et al., 2012; Jourdan et al., 2014; Sampaio et al., 2014).

Table 2 Localization of cannabinoid receptors in the kidney

Receptor	Localization (general)	Localization (specific)	Species	References
CB_1	Tissue	Whole kidney	Human, rat, mouse	Larrinaga 2010, Shire 1995, Barutta 2010
	Region	Arterioles	Rat	Koura 2004
		Glomerulus	Rat, mouse	Shire 1995, Barutta 2010, Lecru 2015, Janiak 2007
		Tubules	Human, rat, mouse	Larrinaga 2010, Lecru 2015, Lin 2014
		Loop of Henle	Rat	Silva 2013
		Collecting ducts	Human	Larrinaga 2010
		Interstitium	Human, rat	Lecru 2015
	Cell type	Podocytes	Rat, mouse	Barutta 2010, Jourdan 2014, Lin 2014, Nam 2012
		Mesangial cells	Rat	Lin 2014
		Proximal tubular epithelial cells	Human, rat, mouse, pig	Larrinaga 2010, Jenkin 2010; 2015, Lecru 2015
		Distal tubular epithelial cells	Human, mouse,	Larrinaga 2010, Lecru 2015
		Intercalated cells	Human	Larrinaga 2010
CB_2	Tissue	Whole kidney	Rat	Barutta 2011
	Region	Cortex	Rat	Barutta 2011
	Cell type	Podocytes	Rat	Barutta 2011
		Proximal tubular epithelial cells	Human, rat	Jenkin 2010;2013;2014
		Mesangial cells	Rat	Deutsch 1997

Adapted from Tam, 2015

Differently from CB1 receptors, there is no consistent information on expression and functionality of CB2 receptors in the kidney. On the one hand, some research groups have not been able to detect CB2 gene or protein expression in human and rat renal tissue (Larrinaga et al., 2010; Silva et al., 2013). On the other hand, there are reports stating that there are CB2 receptors in human and rat renal cortexes, with elevated expression in podocytes, proximal tubule cells and rat mesangial cells (see Table 2) (Deutsch et al., 1997; Jenkin et al., 2010; Barutta et al., 2011; Jenkin et al., 2013; Simcocks et al., 2014). It is noteworthy that there are two splice variants of CB2, namely CB2A and CB2B, which vary in their kidney distribution (Hryciw and McAinch, 2016). This may contribute to the discrepancy of findings.

The kidneys are enriched in anandamide and its metabolizing enzymes, but there remains a gap in our understanding of the cannabinoid regulation of diuresis and natriuresis in the kidney.

However, little is known about the cellular localization of either of the two endocannabinoid members (Ritter et al., 2016). Studies show that anandamide was detected in isolated cultured renal endothelial cells and mesangial cells (Deutsch et al., 1997). These cells were also found to be able to synthetize AEA from arachidonic acid and to catabolize it by amidase activity (Deutsch et al., 1997). Regional distribution assessment of anandamide concentration in the kidney demonstrated that its concentration is higher in the renal medulla in comparison to the renal cortex (Ritter et al., 2012). High anandamide levels in the medulla could be explained due to low medullary expression of its main metabolizing enzyme, FAAH, which would allow for accumulation of the endocannabinoid in this region (Ritter et al., 2012). Similarly, physiological expression levels of FAAH in glomeruli, proximal and distal tubule cells, and collecting duct cells, attests for the lower presence of AEA in these renal regions. In comparison to the abundant AEA in the renal medulla, three other fatty acids with acylated acidic groups, including 2-AG and the non-CB N-ethanolamides of palmitate and oleate showed approximately even distribution between the renal cortex and medulla (Ritter et al., 2012). These findings were supported by experiments conducted in our lab that showed an elevation in AEA after in vivo intramedullary treatment with a selective FAAH inhibitor, PF-3845 (Ahmad et al., 2017a). The tissue-specific localization and rising levels during treatment with the selective FAAH inhibitor suggest that anandamide may play a specific role within the kidney, and possibly in the renal medulla. Furthermore, cultured renal mesangial and endothelial cells have been reported to contain low levels of AEA and to be able to catabolize it by amidase activity (Deutsch et al., 1997). Additionally, Sampaio observed that the main enzymes responsible for eCB synthesis and degradation are consistently expressed in immortalized epithelial cells from pig kidney proximal tubule, LLC-PK1 cells (Sampaio et al., 2014).

As mentioned above, biochemical analysis of mouse renal distribution of fatty acid acyl hydrolase revealed a higher concentration of the enzyme in the renal cortex then in the medulla (Ritter et al., 2012). By applying an immunohistochemical approach, the same group discovered diffuse, but significant, staining for FAAH in proximal and distal tubules. FAAH enzymes were also detected in individual cells in the glomerulus and renal vasculature. Moreover, in both the renal cortex and medulla, collecting ducts expressed particularly intense staining for the enzyme. Altogether, these findings suggest that AEA has very particular and probably well-regulated roles in the proximal and distal tubular cells, glomeruli and renal collecting ducts.

2.4 Endocannabinoids and regulation of renal function

Among the many roles that the kidneys play, the most important role is their regulation of electrolytes and fluid homeostasis. This property is regarded to be an essential element for the long-term control of blood pressure. Three separate mechanisms, via which the kidneys achieve their pressure lowering function, have been proposed: [1] renal hemodynamics and microcirculation; [2] renal excretory functions; and [3] neuromodulation of the sympathetic nervous system (Ritter et al., 2016). Decades of research of the endocannabinoid system, in relation to the kidneys, provides evidence that endocannabinoids are involved in the normal functioning of all three of these processes.

Anandamide is a well-established vasodilator of arteries and arterioles, and its actions are mediated via CB1 receptors (Randall et al., 2004). *In vitro* studies show that exogenously administered AEA is capable of vasodilating the juxtamedullary afferent arterioles and to enhance the release of nitric oxide (NO) by endothelial cells (Deutsch and Chin, 1993). These

effects could be completely inhibited by pretreatment with a selective CB1 antagonist or a NO synthase inhibitor. Moreover, binding of AEA to CB1 receptors on the afferent and efferent arterioles elevated renal blood flow and reduced the glomerular filtration rate. These effects were abolished by administering the CB1 antagonists AM281 and AM251 and proved to be independent from AEA's effects on blood pressure and sodium excretion (Koura et al., 2004). These results support a physiological model, where CB1 receptors expressed on endothelial cells of afferent arterioles can stimulate the production of NO, which then diffuses to nearby smooth muscles and causes vasodilation. The tissue-dependent localization and rising levels of AEA during treatment with the selective FAAH inhibitor suggest that anandamide may play a specific role within the kidney, and possibly in the renal medulla. Li and Wang demonstrated that an intramedullary infusion of methanandamide, the methylated analog of anandamide that is refractory to FAAH-mediated hydrolysis, in anesthetized rats elevated urine flow without natriuresis, but with accompanying blood pressure drop (Li and Wang, 2006). These data suggest that endocannabinoids regulate, at least partially, fluid homeostasis and blood pressure. Further experiments showed that efferent arterioles are more sensitive to AEA exposure in comparison to afferents (Koura et al., 2004). Overall vasodilation of the efferent arterioles is congruent with a decrease in hydrostatic pressure and GFR (Ritter et al., 2016).

The hemodynamic effects of endocannabinoids also reach the microcirculation of the kidney. Few data are available to evaluate the activity of AEA or cortical and medullary blood flow, however Li et al. showed that intramedullary infusion of methanandamide did not have an effect on cortical or medullary blood flow (Li and Wang, 2006). Similarly, when AEA was administered intramedullary in anesthetized rats, there was no effect on renal blood flow (Ritter et al., 2012). However, studies by our lab also revealed that inhibition of FAAH by a selective

inhibitor, infused intravenously or intramedullary, produced an elevation in medullary blood flow (Ahmad et al., 2017b). Thus, the endocannabinoid system plays differential regulatory roles to control blood flow in order to maintain fluid homeostasis.

As described in an earlier chapter, tubular reabsorption in the kidney begins from the proximal convoluted tubules in the cortex and ends at the collecting duct in the renal medulla. It has been determined for many years that the endocannabinoid system can alter tubular reabsorption. Sofia et al. demonstrated that Δ^{-9} tetrahydrocannabinol, the psychoactive ingredient of marijuana, elicits diuresis that is accompanied by elevated sodium and potassium excretion after oral administration in rats (Sofia et al., 1977). In congruence with this finding, the CB1 receptor agonist, AM2389, demonstrated a stronger diuretic effect than the non-selective THC and AM4054 (Paronis et al., 2013). One of the more recent studies, regarding tubular action localization of endocannabinoids, showed that AEA regulates sodium transport through the medullary thick ascending loop of Henle. The research group, which discovered this interaction, also posed that the natriuretic activity was due to stimulation of NO release in a CB1-dependent manner. NO then blocked the apical Na^+/H^+ pump and the basolateral Na^+/K^+ ATPase (Silva et al., 2013). Interestingly, a non-selective CB1/CB2 agonist, WIN55,212-2, and the CB1 peptide agonist, hemopressin, proved to be able to reliably modulate the activity of the basolateral Na^+/K^+ ATPase in proximal convoluted tubules (Sampaio et al., 2014). The study found that WIN55,212-2 stimulated Na^+/K^+ ATPase via a PKC-dependent pathway, while hemopressin elevated the activity of cAMP and, thus, PKA (Sampaio et al., 2014). These data are consistent with reports of cannabinoids being able to modulate Na^+/K^+ ATPases in the synaptosome (Araya et al., 2007). However, it is interesting that CB1 agonists, such as WIN55,212-2 can stimulate sodium reabsorption through stimulation of Na+/K+ ATPase-mediated activity, while every *in*

vivo study shows that CB1 agonists produce diuresis (Chopda et al., 2013; Ritter et al., 2016; Ahmad et al., 2018). Apart from CB receptors, it has been successfully demonstrated that cannabinoids also cause diuresis via e TRPV1 receptors (Li and Wang, 2006). Thus, it is possible that the endocannabinoid system acts on several different renal tubular targets in order to achieve its effects. Since it has been known that NO is a regulator and inhibitor of Na^+/H^+ transporters and Na^+/K^+ ATPase in the proximal convoluted tubule, it is possible that, similarly to eCB activity in MTALs, CB1 activation in the PTs leads to release of NO, and consequent inhibition of the two transporters (Ortiz and Garvin, 2002). However, to this date, there is no conclusive explanation for the exact location/s of CB1 activity that lead to the commonly observed diuresis, natriuresis and kaliuresis after *in vivo* treatment with endo- or exo-cannabinoids.

The effects of CB1 activation in the proximal tubules, and in other nephronal regions, have been controversial. This paradox could partially be due to a controversial signaling of nitric oxide within the proximal tubules (Ortiz and Garvin, 2002). Certain studies reported that luminal or basolateral administration of the NO donor, nitroprusside, decreased fluid reabsorption (Eitle et al., 1998). Similarly, Wu et al. shared that luminal treatment with NOS inhibitor, N^G-nitro-$_L$-arginine methyl ester ($_L$-NAME) increases proximal tubule fluid reabsorption, suggesting an endogenous tonic inhibitory effect of NO within the proximal tubule cells (Wu et al., 1999). These findings suggest that the endogenously produced NO inhibits transport within the proximal tubules. However, other studies support a stimulatory effect of NO on PT transport. Low concentrations of the NO donor, nitroprusside stimulated PT fluid and bicarbonate reabsorption by 30-50%, while higher concentrations inhibited both types of reabsorption by 50-70% (Wang, 1997). This set of data is supported by another finding, that systemic blockade of NO production by an intravenous $_L$-NAME infusion decreased fluid and bicarbonate

reabsorption (Wang, 1997). Thus, it could be argued that NO produced by nNOS in the proximal tubules stimulates transport. Since the interconnection between CB1 activation and NO production is so strong, it is of little surprise that data regarding CB1-mediated PT transport is controversial.

Apart from the hemodynamic and tubular regulatory properties of endocannabinoids, this system has also been implicated to play a sympathoinhibitory role in sympathetic neurotransmission (Ritter et al., 2016). A study evaluating the release of radiolabeled norepinephrine after treatment of isolated rat atria and vas deferens with THC and AEA revealed that the cannabinoid ligands inhibited the release of 3H-norepinephrine (Ishac et al., 1996). This inhibitory activity occurred on the presynaptic sympathetic nerve terminals and could imply a prolonged depressor response to an intravenous bolus infusion of AEA (Varga et al., 1996). The sympathoinhibitory effect of cannabinoids was also demonstrated to be dependent on basal sympathetic tone, as the negative response was absent in conscious normotensive animals, but present in conscious spontaneously hypertensive rats (Lake et al., 1997a). In congruence with these data, anesthetized rats, treated with anandamide, revealed a decrease in blood pressure that could be reversed with a blockade of α-adrenergic receptor blockers (phentolamine) or CB1 antagonists (Varga et al., 1995). Godlewski et al. demonstrated that inhibition of FAAH with a novel inhibitor AM3506, could return elevated blood pressure and cardiac contractility to their baseline in spontaneously hypertensive rats (G et al., 2010). Finally, AEA elicits a NO-mediated inhibition of KCl-stimulated norepinephrine release from renal sympathetic nerves of isolated renal arterial segments (Deutsch et al., 1997). Hence, there is evidence that endocannabinoid signaling is involved in a possible neuroregulation of kidney functions.

Rationale and Hypothesis

The significance of this project lies in the fact that one of the most important functions of the kidneys is the regulation of salt and water balance, which is considered critical for the long-term control of blood pressure (Ahmad et al., 2017a). Approximately 70-80 % of all Americans who undergo their first heart attack, stroke or chronic (long-lasting) heart failure have high blood pressure (Fryar et al., 2012; Mozaffarian et al., 2015). More than 360,000 deaths in the United States involved high blood pressure as a primary or secondary cause, which accumulates to 1,000 deaths each day (Mozaffarian et al., 2015). Furthermore, hypertension has been defined as the second leading cause for kidney failure (Mozaffarian et al., 2015). According to data collected by Nwankwo, only in the United States approximately 75 million American adults (32%) have high blood pressure and about 1 in every 3 American adults has prehypertension (Nwankwo et al., 2013). Researchers have suggested that a reduction of the population's sodium intake by 32% per day may reduce cases of high blood pressure by 11 million and save 18 billion dollars every year (Palar and Sturm, 2009).

This thesis project aimed to determine whether a novel lipid product, isolated from the medium of cultured mouse medullary interstitial cells after fatty acid amide hydrolase inhibition with the selective PF-3845 inhibitor shares similar physiological activities with the long-sought medullipin system, proposed by Dr. Eric Muirhead (Muirhead, 1991). Thus, it was hypothesized that administration of the novel lipid fraction in a renal function model using anesthetized mice, the lipid would produce diuresis, natriuresis and would drop blood pressure. These responses are

in congruence with the diuretic, natriuretic and vasodepressor properties of medullipin I and II, proposed by Muirhead.

Throughout his research, Dr. Muirhead entertained the hypothesis that medullipin is structurally related to arachidonic acid, a precursor for the formation of one of the two main endocannabinoid ligands- anandamide. Coincidentally, the lipid fraction, discussed in this project, is obtained from mouse medullary interstitial cells treated with a selective FAAH inhibitor (the enzyme responsible for metabolizing AEA). Furthermore, the type 1 cannabinoid receptors are present in renal regions and tubular cells that suggest a modulatory function of these receptors in hemodynamic and tubular activity within the kidney. Based on these facts, we hypothesized that PIP would elicit its diuretic and natriuretic activities via a CB1-mediated pathway. In order to study this question, we applied genetic and pharmacological inhibition of CB1 receptors in mice and administered PIP to test for ablation of its biological activities. If our hypothesis was confirmed, this lipid would be a highly effective vasodepressor and a diuretic/natriuretic therapeutic agent, advancing medical prevention and treatment of hypertension.

Generally, ENaC has been accepted to be the primary site of sodium regulation (Pearce et al., 2015), however preliminary studies in our lab show that the diuretic effect of the unknown lipid is independent of ENaC activity in the renal tubules. The diuretic activity observed post-treatment with our novel product surpass the mild diuretic effect usually observed with ENaC inhibitors. Also, CB1 receptors have been found to regulate Na^+/K^+-ATPase activity in proximal renal tubules (Sampaio et al., 2014). Based on our earlier findings that CB1 receptor antagonism and genetic ablation hinder pressure-lowering and diuretic responses to treatment with the MMIC-induced lipid(s) after FAAH inhibition, we hypothesize that the novel lipid fraction

induces diuresis and natriuresis via a CB1-regulated Na^+/K^+-ATPase activity in cells of the proximal convoluted tubules. The hypothesis was tested in acute renomedullary infusion studies. Some researchers have suggested that large diuretic effects after treatment with specific compounds are achieved by targeting multiple signaling pathways within the kidney (Granger et al., 2002). Thus, a direct diuretic response by renal tubules can be additionally enhanced by a vasodepressor activity that elevates renal perfusion pressure and renal interstitial hydrostatic pressure (Granger and Scott, 1988; Granger et al., 2002). Therefore, an investigation of the diuretic and natriuretic tubular pathway of the novel compound(s) would clarify if there is a connection between the diuretic/natriuretic pathway and a vasodilatory pathway in the kidney.

Chapter 3 - Diuretic, natriuretic, and vasodepressor activity of a lipid fraction enhanced in medium of cultured mouse medullary interstitial cells by a selective FAAH inhibitor

3.1 Abstract

The relationship between the endocannabinoid system in the renal medulla and the long-term regulation of blood pressure is not understood. To investigate the possible role of the endocannabinoid system in renomedullary interstitial cells, mouse medullary interstitial cells (MMICs) were obtained, cultured and characterized for their responses to treatment with a selective inhibitor of fatty acid amide hydrolase (FAAH), PF-3845. Treatment of MMICs with PF-3845 increased cytoplasmic lipid granules detected by Sudan Black B staining and multilamellar bodies identified by transmission electron microscopy. HPLC analyses of lipid extracts of MMIC culture medium revealed a 205nm-absorbing peak that showed responsiveness to PF-3845 treatment. The biologic activities of the PF-3845-induced product (PIP) isolated by HPLC were investigated in anesthetized, normotensive surgically-instrumented mice. Intramedullary and intravenous infusion of PIP at low dose rates (0.5-1 AU/10 min) stimulated diuresis and natriuresis, whereas at higher doses, these parameters returned toward baseline but mean arterial pressure (MAP) was lowered. Whereas intravenous bolus doses of PIP stimulated diuresis, GFR and medullary blood flow (MBF) and reduced or had no effect on MAP, an intraperitoneal bolus injection of PIP reduced MAP, increased MBF, and had no effect on urine parameters. These data support a model whereby PF-3845 treatment of MMICs results in

increased secretion of a neutral lipid which acts directly to promote diuresis and natriuresis and indirectly through metabolites to produce vasodepression. Efforts to identify the structure of the PF-3845-induced lipid and its relationship to the previously proposed renomedullary antihypertensive lipids are ongoing.

3.2 Introduction:

The kidneys are considered critical for the long-term control of blood pressure by regulation of body fluid and blood volume. In support of this concept, the kidneys control the systemic activity of the pro-hypertensive renin-angiotensin-aldosterone system by regulating the production and release of renin from juxtaglomerular cells in response to decreased renal perfusion pressure or reduced sodium load in the distal tubules (Karlstrom et al., 1990). They have also been proposed to contain a parallel antihypertensive hormonal system, the medullipin system (Muirhead, 1993; Folkow, 2007). In this system, a neutral antihypertensive lipid, known as medullipin or renomedullary neutral antihypertensive lipid, is secreted from interstitial cells of the renal medulla in response to increased medullary perfusion pressure (Gothberg et al., 1982). Medullipin was shown to possess several characteristics consistent with its antihypertensive activity, including vasodepressor activity, inhibition of sympathetic tone, and diuretic effects (Karlstrom et al., 1988). However, attempts to isolate and identify this substance from sources in which it was detected, including extracts of renal medulla, renal venous effluents or medullary interstitial cells did not prove successful (Brooks et al., 1994; Glodny and Pauli, 2006).

Our group is investigating the hypothesis that anandamide or metabolite(s) of anandamide may be related to the proposed antihypertensive renomedullary substance.

Anandamide, the N-acyl ethanolamide of arachidonic acid (Devane et al., 1992), is chemically neutral at physiologic pH. Anandamide was first identified as the endogenous cannabinoid receptor agonist (Bermudez-Silva et al., 2010). The kidney, especially the renal medulla, is unique in its high content of anandamide and the primary anandamide-hydrolyzing enzyme, fatty acid amide hydrolase (FAAH) (Ritter et al., 2012) , (Long et al., 2011; DiPatrizio and Piomelli, 2012). Anandamide has actions in the cardiovascular and renal systems which are consistent with an antihypertensive role, including vasodepressor (Lake et al., 1997b), sympatholytic effects (Ishac et al., 1996; Deutsch et al., 1997), and diuretic and natriuretic activities (Li and Wang, 2006). Infusion of exogenous anandamide into the renal medulla stimulated diuresis and natriuresis (Ritter et al., 2012), an effect which was mimicked by intramedullary infusion of known FAAH inhibitors, including isopropyl dodecylfluorophosphate (Ahmad et al., 2017a) or PF-3845 (Ahmad et al., 2018). These studies support a role of endogenous anandamide or other fatty acyl ethanolamides which accumulate upon inhibition of their hydrolysis. However, in the latter studies, the cellular source in the renal medulla of the diuretic and natriuretic lipid ethanolamides remained unknown.

An important non-tubular cell type of the renal medulla is the lipid-laden (Type I) interstitial cell (Lemley and Kriz, 1991). Characteristics of this type of interstitial cell include its stellate-like cellular morphology with cytoplasmic projections and increased cell density toward the tip of the renal papilla. They are noticeable in stained sections of the renal medulla based on their long axes lying perpendicular to loop of Henle tubules and vasa recta cells, producing a characteristic ladder-like appearance. Although cytoplasmic projections from these cells do not make physical contact with loop of Henle or vasa recta, they have been suggested to play a role in signaling to these cell types in response to changing conditions (Lemley and Kriz, 1991).

Another hallmark is the presence of osmiophilic lipid granules which are rich in arachidonic acid, the precursor of eicosanoid metabolites such as prostaglandin E_2. The synthesis of prostaglandin E_2 by interstitial cells was stimulated by angiotensin II and other vasoactive peptides and certain physiologic conditions (Zusman and Keiser, 1977a). Changes in the number of these lipid droplets in experimental models of hypertension (Bohman and Jensen, 1976) suggested a role of these lipid droplets in the secretion of medullipin in response to elevated renal perfusion pressure (Muirhead, 1993; Folkow, 2007).

The putative role of interstitial cells in secreting the renomedullary antihypertensive substance led us to isolate these cells from the renal medulla of mice in order to study their responses to FAAH inhibition. The isolated cells were assessed for histological, immunohistochemical, and ultrastructural markers consistent with their identity as medullary interstitial cells, and also for the presence of FAAH enzyme. The effect of treating the cells with the selective FAAH inhibitor, PF-3845, on the appearance of lipids in the medium of MMICs was investigated. During the investigation, an unknown 205 nm-absorbing product was identified in lipid extracts of the medium of cultured MMIC which showed enhancement by treatment with PF-3845. The 205-absorbing substance was purified by HPLC and was characterized in an acute renal function model using anesthetized mice after different routes of administration.

3.3. Methods and Materials:

Reagents

Trypsin-EDTA (10X, 0.5%), penicillin-streptomycin (100X), and glutamine (100X) were purchased from Gibco-Invitrogen (Gaithersburg, MD). Fetal bovine serum was from Serum

Source International (Charlotte, NC). Dulbecco's modified Eagle's medium with high glucose (DMEM) was from Gibco/Life Technologies (Grand Island, NY). Polyclonal IgG antibodies to tenascin-C (H-300, sc-20932), COX-2 (M19, sc-1747) and FAAH (C-20, sc-26428) were from Santa Cruz Biotechnology (Dallas, TX). Sudan Black B was from Santa Cruz Biotechnology. Horseradish peroxidase (HRP)-conjugated anti-rabbit and anti-goat IgG antibodies were from Jackson ImmunoResearch Laboratories (West Grove, PA). 3,3'-Diaminobenzidine (ImmPACT DAB Peroxidase Substrate) was from Vector Laboratories (Burlingame, CA). Indomethacin was from CalBiochem (La Jolla, CA) and Sigma Chemical (St. Louis, MO), respectively. PF-3845 was purchased from ApexBio (Houston, TX). HPLC grade water and methanol were purchased from Thomas Scientific (Swedesboro, NJ). Medical grade nitrogen was purchased from National Welders Supply Company (Richmond, VA).

Animals

Male C57BL/6J mice (Jackson Laboratory, Bar Harbor, ME) and male and female homozygous $FAAH^{+/+}$ wildtype (FAAH WT) and $FAAH^{-/-}$ (FAAH KO) mice (2-5 months old) (from a colony established at Virginia Commonwealth University by Dr. Cravatt) were used in the present study (Cravatt et al., 2001). The FAAH KO mouse colony has been maintained by backcrossing onto a C57BL/6 background for more than 20 generations (Wise et al., 2008). The mice in this study weighed 20-35 grams and were housed 4-5 per cage in a temperature (20-22°C) and humidity (50-55%)-controlled environment with a 12 hr light/dark cycle with free access to food and water. All experiments involving animals in this study were approved by the Institutional Animal Care and Use Committee of Virginia Commonwealth University in

accordance with the National Institutes of Health Guide for the Care and Use of Laboratory Animals.

Mouse medullary interstitial cells

Mouse renomedullary interstitial cells were established in primary culture from transplants of isolated and fragmented mouse renal inner medulla using the approach of Muirhead (Muirhead et al., 1990) and subsequently applied and adapted by many others (Dunn et al., 1976; Zusman and Keiser, 1977b; Zou et al., 2001; Moeckel et al., 2003) including our laboratories (Li et al., 2007; Wang et al., 2011). Briefly, C57BL/6J mice were anesthetized using thiobutabarbital (Inactin™, Sigma-Aldrich, St. Louis, MO) and ketamine (Ketathesia™, Henry Schein Animal Health, Dublin, OH) and sacrificed, and the kidneys removed aseptically. The kidneys were bisected and the inner medullary regions excised, minced, and suspended in DMEM. The suspended fragments were injected subcutaneously over the left rear flank of an isogenic recipient mouse using an 18-gauge syringe needle. After 7-10 days, the recipient mouse was anesthetized and sacrificed, and the yellowish nodules attached to the serosal surfaces over the injection sites excised. The nodules were minced, trypsinized with 0.05% trypsin-EDTA at 37°C for 15 min (GIBCO-Life Technologies, Grand Island, NY), and centrifuged at 500 x g for 5 min. The pellet was resuspended in DMEM containing 10% fetal calf serum and 100 U/mL penicillin G and 100 µg/mL streptomycin and transferred to a single well of a 12 well tissue culture dish. For the first week after plating, the growth medium also contained amphotericin B (25 µg/mL). At 90% confluence, the cells were trypsinized and passaged successfully to larger dishes. At passage four, the cells were trypsinized, resuspended in frozen storage medium (80% DMEM, 10% fetal bovine serum, and 10% DMSO), and stored in frozen aliquots under liquid

nitrogen. MMICs were maintained by regular feeding in complete growth medium, passaging every 7 days (1:3 split ratio). The experiments described in this work used MMICs between passages 4-15.

Transmission electron microscopic analysis

For ultrastructural imaging, cells were trypsinized, pelleted, resuspended in phosphate-buffered saline, repelleted, and resuspended in 0.1M cacodylate buffer, pH 7, containing 2.5% glutaraldehyde at room temperature. Subsequently, the cells were fixed in osmium tetroxide, dehydrated, and embedded according to standard methods. Sections (600–700Å thick mounted on grids) were prepared using a Leica EM UC6i Ultramicrotome (Leica Microsystems, Buffalo Grove, IL) then stained with 5% uranyl acetate and Reynold's Lead Citrate. Imaging was performed with a JEOL JEM-1230 transmission electron microscope (Jeol U.S.A., Inc., Peabody MA, USA) with a Gatan Orius SC1000 digital camera (Gatan, Pleasanton, CA, USA).

Immunohistochemistry of kidney tissue and cultured MMICs

MMICs were cultured on tissue culture dishes overnight and then fixed in 4% paraformaldehyde in PBS for 15 min. For kidney tissue sections, mouse kidneys were perfused *in situ* with PBS followed by neutral 4% paraformaldehyde. After excision, the kidneys were fixed overnight in 10% neutral-buffered formalin and embedded. Tissue sections (5 µm) cut onto glass slides were processed for immunostaining as described previously (Li et al., 2007). After washing in PBS-0.1% Tween (PBS-T), the samples were incubated with 3% blocking serum for 30 min at room temperature. Primary antibodies and their dilutions (in PBS-0.1% Tween) were: tenascin-C (1:50 dilution), COX-2 M-19 (1:50) and FAAH C-20 (1:50). Secondary antibodies were diluted 1:200. Incubations with primary antibodies were overnight at

4°C and with HRP-conjugated secondary antibodies for 30 min at room temperature with gentle rocking. HRP staining was detected using 3, 3'-diaminobenzidine as a substrate. After counterstaining nuclei with hematoxylin, stained tissues and cells were washed, mounted and observed by phase contrast microscopy.

Sudan Black B lipid staining

MMICs were stained for neutral lipids using Sudan Black B (Schneider et al., 2015). After washing and fixing as described above, the cells were washed with PBS, then with 70% ethanol followed by staining for 10 min at room temperature with Sudan Black B solution (0.7% in 70% ethanol, filtered immediately before use). Cells were washed with PBS and observed by phase contrast light microscopy.

Dose response of PF-3845-inducible MMIC product

MMICs (3×10^6 cells per T-175 sq cm flask) were plated and incubated with either vehicle (ethanol, 0.1%) or PF-3845 at the indicated concentrations (dissolved in ethanol, 0.1% final concentration) for 24 hr in a humidified 37°C incubator with 5% CO_2. In some cases, the effect of indomethacin or celecoxib (10 µM final) was tested either alone or in combination with PF-3845. Complete growth medium was incubated without cells as a control. Lipids were extracted by the Folch method (Folch et al., 1957). Briefly, culture medium (1 mL) was extracted with a 2:1 (v/v) mixture of chloroform/methanol (2 mL) and 0.73% sodium chloride (200 µL). After centrifuging, the organic phase was collected, and the aqueous phase was extracted twice more with chloroform (1 mL). The organic phases were combined and evaporated to dryness under nitrogen. The residue was reconstituted in 500 µL methanol and 50 µL was analyzed by

reverse phase HPLC with ultraviolet detection as described above. The concentration of product was expressed in units of area under the peak (AU) normalized for the volume of culture medium.

HPLC purification of PF-3845-inducible MMIC product

MMICs were dissociated by trypsinization and plated in tissue culture dishes (3 x 10^6 cells/150 mm dish) followed by addition of vehicle (ethanol,0.1%) or vehicle containing PF-3845 (10 μM final concentration). The culture medium was extracted using Clean-Up C18 solid phase extraction columns (500 mg, United Chemical Technologies, Bristol, PA). Briefly, the SPE columns were conditioned with 3 mL of methanol followed by 3 mL of deionized water. The samples of culture medium (25 mL) were then passed through the columns and washed, first using 3 mL of DI water followed by 3 mL of 25% methanol and 3 mL of 60% methanol. The lipids eluting with 100% methanol were collected and evaporated under nitrogen leaving ~500 μL. 50 μL was transferred to auto-sampler vials for reverse phase HPLC-UV analysis. Chromatographic separation was performed on a Grace Alltech C18 column, 100 × 4.6 mm, 5 μm (Grace, Columbia, MD) using an HP1050 quaternary pump system. The mobile phases were A: water with 0.1% TFA and B: 100% methanol at a flow rate of 0.8 mL/min. The following gradient was used: 0.0–0.5 min 50% B, 0.5-5 min linear gradient to 100% B, and 5-15 min holding at 100% B. Detection was by UV absorption at 205 nm using an HP1050 photodiode array detector.

Because the structure or structural class of the PF-3845-induced product has not been determined and the isolated quantities were too low to permit accurate mass measurement, doses or dose rates for testing its biological activities were expressed in area units under the peak (AU,

milliabsorbance units x time in minutes) as determined by the ChemStation software (Agilent, Santa Clara, CA). Multiple batches of the isolated product were used for testing of biological activity. The isolated product was stable after storage at -20C for > 6 months.

Surgical Preparation for acute renal functional mouse model

Mice were anesthetized and prepared surgically for the acute renal function testing procedure as described previously (Zou et al., 2001; Li et al., 2005). Anesthesia was induced with ketamine (Ketathesia™, Harry Schein Animal Health, Dublin, OH) (100 mg/kg, i.p.) and thiobutabarbital (Inactin™, Sigma Chemical Co., St. Louis, MO, 75 mg/kg, i.p.). The abdominal and neck areas were shaved, and the mice were placed on a thermostatically-controlled warming table to maintain body temperature at 37°C. A tracheotomy was performed by inserting a 2 cm length of polyethylene PE-60 tubing to maintain a patent airway during surgery. After tracheotomy, a catheter prepared from heated and pulled plastic PE-10 tubing and filled with heparin sodium dissolved in saline (Fisher BioReagents, 0.005 mg/mL, 50 IU/mL) was inserted into the left carotid artery and attached to a pressure transducer connected to a data acquisition system (Windaq, DATAQ Instruments, Akron, OH). The right jugular vein was catheterized with a catheter prepared from PE-10 tubing for the infusion of 0.9% saline containing 2% BSA. The rate of intravenous infusion was 1 mL/h/100 g body wt to maintain fluid volume and hematocrit concentration throughout the experiment. For the acute renal function experiments, an incision was performed following the midline of the abdominal area. The left ureter was ligated with a surgical suture and cut on the kidney side of the ligation to allow produced urine to exit freely into the abdominal cavity. The urethra was ligated in proximity to the bladder, and the latter was catheterized with a 2.5 cm cut length of PE-50 tubing for the collection of urine at timed

intervals. The right kidney was elevated on a piece of sterilized gauze and a pulled PE-10 catheter was implanted to 2.5 mm in depth vertically from the dorsal surface into the outer medulla. The catheter was immobilized to the kidney capsule using a cyanoacrylate tissue adhesive (Vetbond, 3M Animal Care Products, St. Paul, MN). All mice received a 1 hour equilibration period, during which the animals received continuous vehicle infusions: 1) intravenous infusion of filter-sterilized 0.9% NaCl containing 2% albumin at a rate of 1 mL/hr/ 100 g body weight, 2) intramedullary infusion with PBS containing (in mM) 205 NaCl, 40.5 Na_2HPO_4, and 9.5 NaH_2PO_4 (pH 7.4, 550 mOsm) at a rate of 2 μL/min to maintain the patency of interstitial infusion (Zhu et al., 2011). The urine excretion rate (UV) was measured gravimetrically, and the sodium and potassium concentrations in urine were measured using flame photometry. UV and the urinary sodium and potassium excretion rates (U_{Na} and U_K, respectively) were factored per gram of kidney weight. At the end of each experiment, the animals were euthanized by exsanguination from the carotid artery catheter for collection of plasma. The placements of the intramedullary catheter in the outer medulla was routinely confirmed by post-mortem kidney dissection following the experiments.

Experimental Protocols

After a 1-hour equilibration period and three sequential 10-min pretreatment control sample collection periods, the lipid was infused intravenously or intramedullary over a 10 minute period, followed by one to five post-treatment control sample collections as indicated. The subjects received either an i.v. or i.med. 10-minute infusion of the compound at doses ranging from 0.25 AU to 8 AU. SHAM mice received only vehicle infusions. The average between the 10-min treatment and 10-min washout periods was taken to represent the response to drug treatment.

Some subjects received i.p. and i.v. bolus injections of the compound following the vehicle pretreatment control periods as indicated for each experiment.

Group 1: continuous intravenous infusion of PIP in increasing cumulative doses (0.25, 0.5, 0.75, 1, 2, 4 and 8 AU) in C57BL/6J mice (n=11); Group 2: continuous intramedullary infusion of PIP (0.25, 0.5, 0.75, 1, 2, 4, 8 AU) in C57BL/6J mice (n=7); Group 3: continuous intravenous vehicle infusion in C57BL/6J mice; Group 4 (n=7): continuous intramedullary vehicle infusion in C57BL/6J mice (n=7); Group 5: intravenous infusion of PIP (1 AU / 10min), followed by three 10-min post-treatment recovery periods (n=4); Group 6: intravenous bolus injection of 5 AU in 20µL vehicle, followed by a 50-minute recovery period (n=4); Group 7: intraperitoneal bolus injection of 5 AU in 20µL vehicle, followed by a 50-minute recovery period (n=4); Group 8: intravenous infusion of PIP (0.25, 0.5, 1, 2, 4 and 8 AU) in FAAH WT and FAAH KO mice (n=6, n=7); Group 9: SHAM, intravenous or intraperitoneal bolus injections with 20µL vehicle alone, followed by a 50-minute recovery period (n=8).

Glomerular Filtration Rate

The glomerular filtration rate (GFR) was determined by urinary clearance of FITC-labeled sinistrin (FITC-sinistrin; Fresenius, Kabi, Austria, 3µg/min/kg in 0.9% saline/2% BSA). The compound was infused intravenously at a constant rate starting during the 1-hour acclimation period before the experiment. Arterial blood was sampled at the beginning of the vehicle infusion and at the end of the experiment. The blood samples were centrifuged 2 min at 1000xg in a microcentrifuge. Urine samples were collected from the bladder catheter every 10 min. FITC fluorescence was determined with an automated fluorescence microplate reader (FLx800, Bio-Tek Instruments, Winooski, VT) and Gen5™ data analysis software.

Medullary Blood Flow (MBF)

For the measurement of MBF, a laser Doppler flow probe (OxyFlo Pro; MNP 100XP; Oxford Optronix, Oxford, United Kingdom) was stabilized on the ventromediolateral surface of the right kidney to measure continuously the MBF (as previously reported in (Ahmad et al., 2017a; Ahmad et al., 2018)The recording of the blood flow was measured by using a dual-channel laser-Doppler flowmeter (Transonic Systems Inc., Ithaca, NY).

Statistical Analysis

Data are presented as the mean ± S.E.M. For comparison between multiple groups of data, one- or two-way analysis of variance (ANOVA) was applied using Tukey, Dunnett's or Fisher's LSD (where appropriate) post-hoc test when significant differences were found. A p-value ≤ 0.05 was considered statistically significant.

3.4 Results:

Characterization of cultured mouse medullary interstitial cells

The MMIC cell population established in our study stained positively for tenascin C (Fig. 8A), whereas cells stained only with the HRP-conjugated secondary antibody were negative (Fig. 8B). To confirm the report of He et al. (2013) that tenascin C is a selective marker for medullary interstitial cells, sections of mouse kidney were also tested (He et al., 2013). Positive immunostaining by the tenascin C antibody was restricted to the inner medulla/papilla (Fig. 8C); the outer medullary (Fig. 8D) and cortical region (not shown) were negative. This immunostaining in the inner medulla was associated with the ladder-like structures of the

medullary interstitial cells, which exhibited oblong nuclei on an axis perpendicular to the tubules of the inner medulla. The cultured MMICs also exhibited intense staining for COX-2 (Fig. 8E) and they stained positively for the presence of FAAH (Fig. 8F). In addition, the cultured MMICs also exhibited abundant cytoplasmic granules visible by phase contrast light microscopy. Positive histochemical staining of cytoplasmic vesicles with Oil Red O and Sudan Black B (Fig. 8G-H) is consistent with the presence of neutral lipid-containing granules in the MMICs.

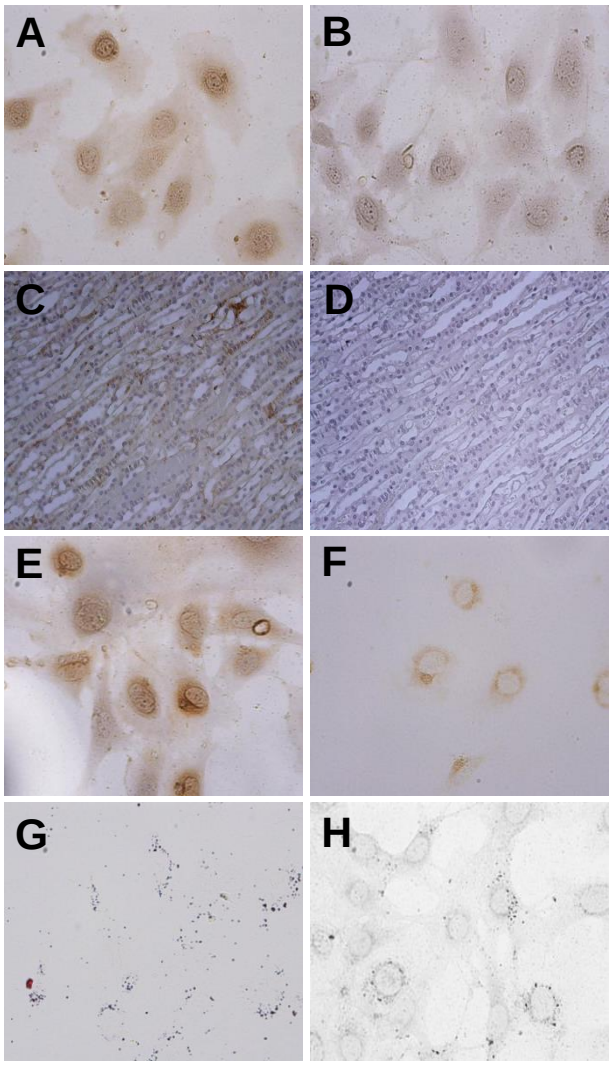

Fig. 8 Immunohistochemical and histochemical analysis of cultured MMICs and kidney tissue sections. Cultured mouse medullary interstitial cells (MMICs) or kidney tissue sections were subjected to immunohistochemical or histochemical analyses as described. Representative images of analyses performed in triplicate are shown (200x magnification). (A) MMICs stained with tenascin-C primary antibody. (B) Negative control MMICs stained only with horseradish peroxidase-conjugated secondary antibody. (C) Section of inner medullary region of mouse kidney stained for tenascin C antibody. (D) Section of outer medullary region stained for tenascin C. (E) COX2-stained MMICs. (F) FAAH-stained MMICs. (G) Oil Red O-stained MMICs. (H) Sudan Black B-stained MMICs.

The apparent size and number of these vesicles varied over time, being most prominently after fresh medium changes. They also showed selective responses to drug treatments. Treatment with the FAAH inhibitor, PF-3845, increased the number and size of these Sudan Black B stained granules, whereas no changes were evident after treatment with the COX inhibitor, celecoxib. Co-treatment with PF-3845 and celecoxib appeared to cause further proliferation of these lipid granules (Fig. 9). The onset of the PF-3845 effect on the Sudan Black B staining pattern was evident within 2-4 hours after the start of treatment and was dose-dependent from 1-20 μM PF-3845 (Fig. 9). These PF-3845-induced lipid granules typically showed greatest accumulation in the perinuclear region.

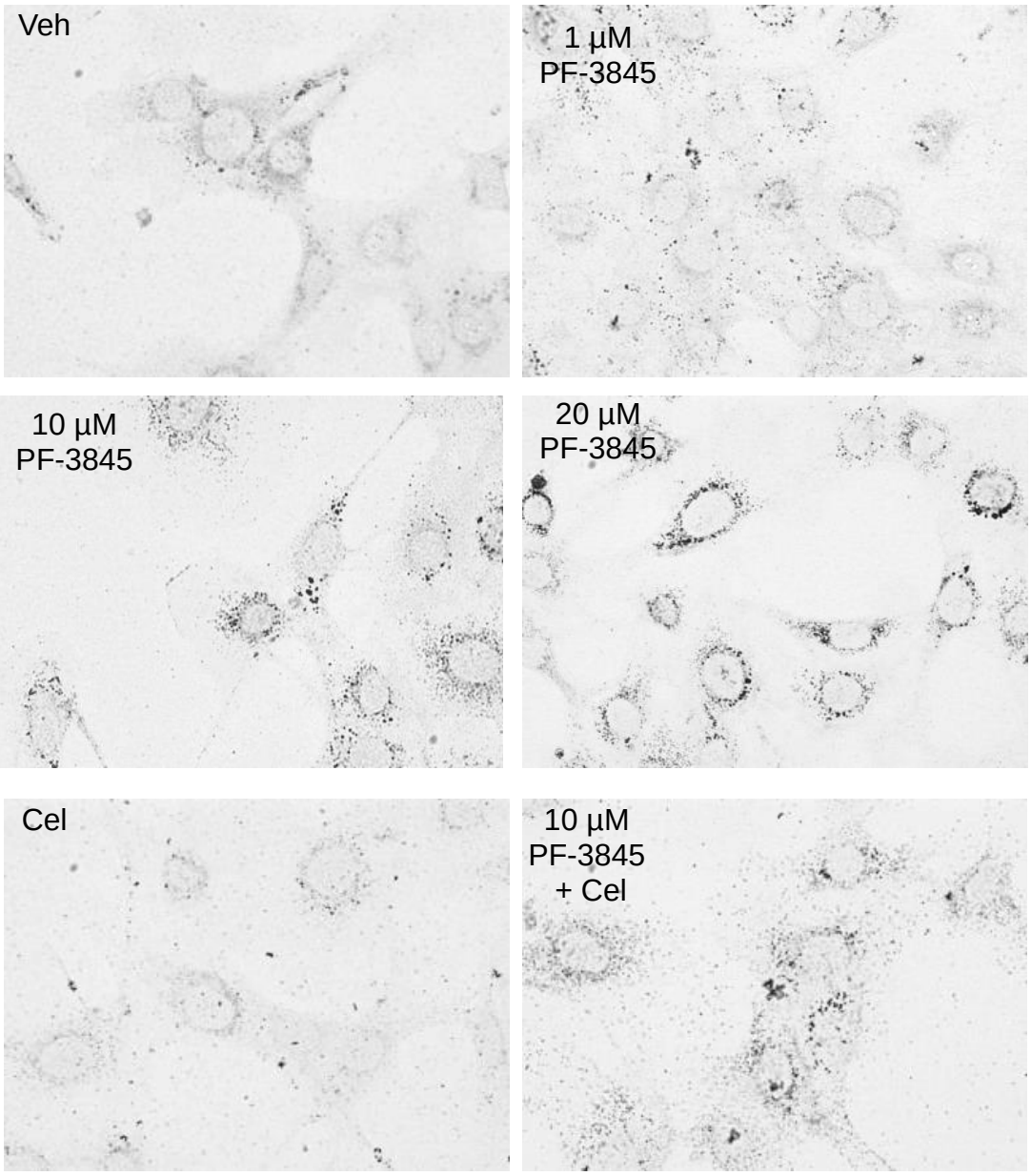

Fig. 9 The effect of PF-3845 in the presence or absence of COX-2 inhibitor on lipid staining in cultured MMICs. MMICs cultured in the presence of vehicle (Veh, 0.1% ethanol), PF-3845 (1, 10 or 20 µM), celecoxib (10 µM), or PF-3845 + celecoxib for 24 hr were stained with Sudan Black B as described under Methods and Materials. Representative images of analyses performed in triplicate are shown (200x magnification).

Analysis of MMICs by transmission electron microscopy

Ultrastructural analysis of the MMICs by transmission electron microscopy revealed large prominent nuclei, abundant mitochondria, and dilated rough endoplasmic reticulum in their cytoplasm (Fig. 10). Stacks of Golgi apparatus could be found. The cytoplasm was rich in granular and vesicular elements, consistent with lipid droplets, vacuoles, lysosomes, and other structures. Multilamellar bodies with their characteristic whorled appearance were visible in some images of control MMICs (Fig. 10B, arrows). Microvilli were apparent on the plasma membrane. Similar analyses of PF-3845-treated MMICs revealed similar general characteristics as described above, with two notable exceptions. The PF-3845-treated MMICs exhibited pronounced nucleoplasmic invaginations (Figs. 10C and 10D) and more numerous and larger multilamellar bodies (Figs. 10C and 10D, arrows).

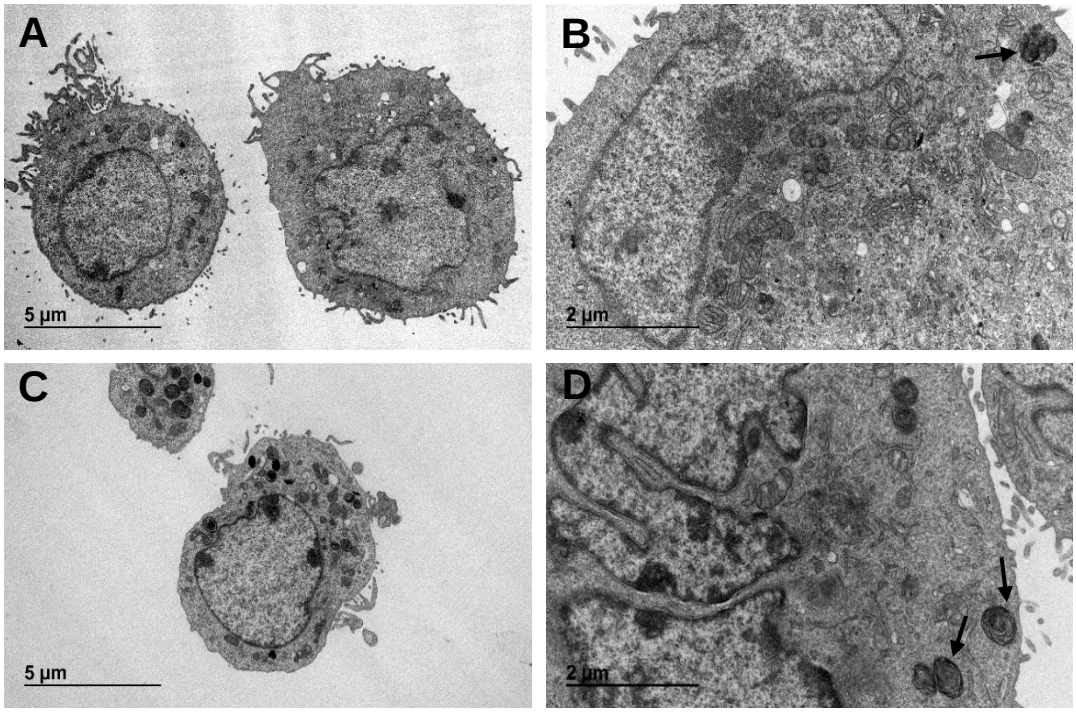

Fig. 10 Transmission electron micrographs of vehicle- and PF-3845-treated MMICs. A and B, MMICs treated with vehicle (Veh, 0.1% ethanol) for 24 hr. C and D, MMICs treated with 10 µM PF-3845 for 24 hr. Low (A, C) and high (B, D) magnification images are shown for each. Osmiophilic lipid granules are seen in the vehicle- and PF-3845-treated MMIC images, including multilamellar bodies (arrows). Cytoplasmic invaginations were also a frequent feature of the PF-3845-treated cells

Identification of an apparent novel PF-3845-induced product of MMICs by reverse phase HPLC

During experiments to assess the effects of PF-3845 treatment on the MMIC secretion of prostaglandin E_2, prostamide E_2, and anandamide, a difference was noted in the chromatographic profile of lipid extracts from medium of PF-3845-treated versus control MMICs (Fig. 11A). A peak at 13.8 min was increased by PF-3845 treatment compared to the control. In contrast, treatment with a COX inhibitor had no effect, whereas co-treatment of cells with PF-3845 and a COX-inhibitor reduced the area of this peak. Quantitation of the effect based on area under the peak is shown in Figure11B. Further analyses showed that the product was present in complete growth medium (DMEM supplemented with fetal calf serum) and that it was increased in the medium from MMIC cultures incubated for 24 hr, suggesting that MMICs can produce and secrete this product. The area of the peak was further increased by treatment with PF-3845. Dose response analysis indicated a maximal 2.6-fold increase at 10 μM and a smaller but significant 0.4-fold increase at 20 μM (Fig. 11C).

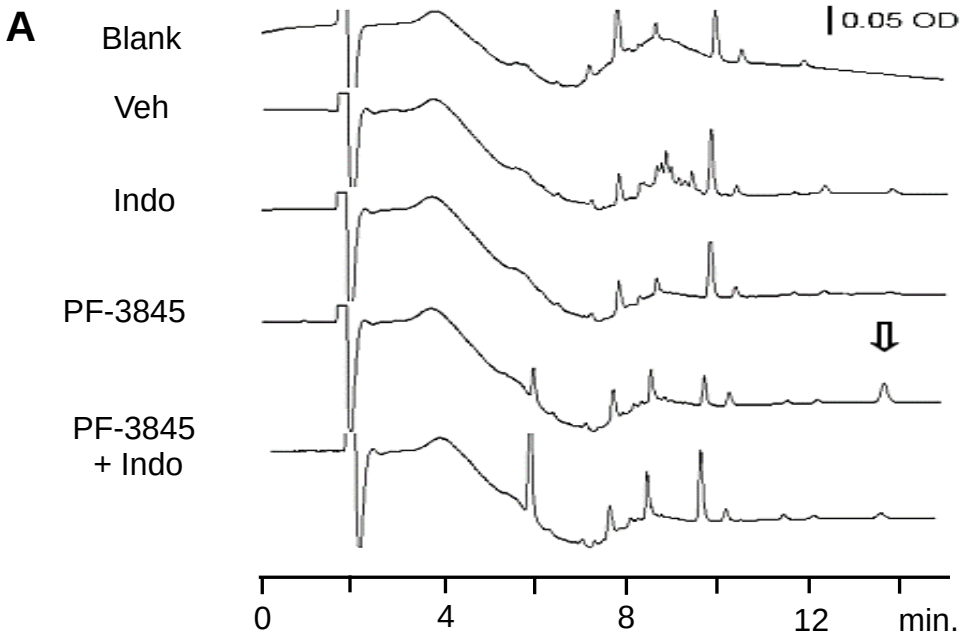
A
Blank
Veh
Indo
PF-3845
PF-3845
+ Indo
0.05 OD
0
4
8
12
min.

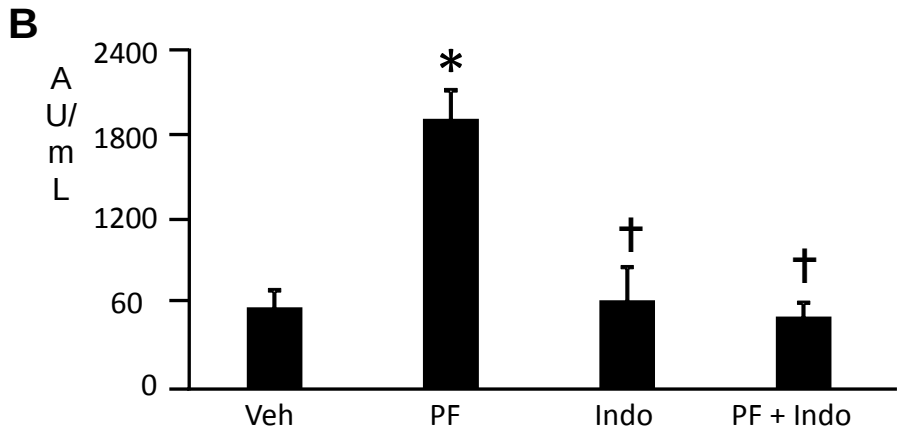
B
AU/mL
2400
1800
1200
60
0
*
†
†
Veh
PF
Indo
PF + Indo

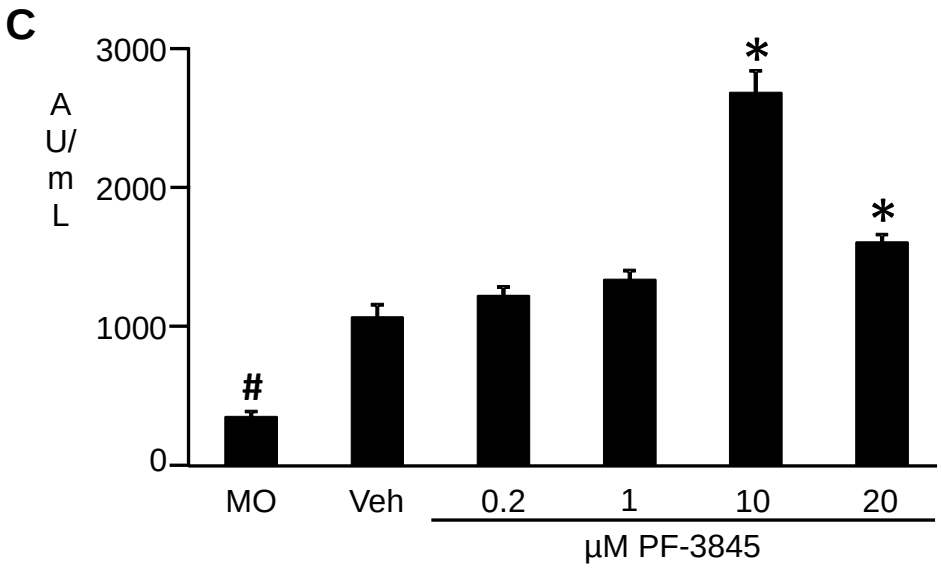
C
AU/mL
3000
2000
1000
0
#
*
*
MO
Veh
0.2
1
10
20
μM PF-3845

Fig. 11 Identification of a lipophilic product in the culture medium of MMICs that shows responsiveness to treatment with PF-3845. (A) Representative chromatograms of negative control (blank methanol) and lipid extracts from MMICs treated with vehicle (Veh), indomethacin (Indo, 10 μM), PF-3845 (10 μM) or combination with the ultraviolet detector set at 205 nm. The arrow indicates a PF-3845-induced product eluting at ~13.8 min (designated PIP). (B) Relative quantitative data of the treatment effects on PIP. Bars represent the mean +/- standard error of the mean of the area under the PIP peak normalized for the volume of culture medium extracted. * indicates a significant difference vs. the Veh group ($p<0.05$, one-way ANOVA with Tukey's post-hoc test. † indicates a significant difference vs the PF-3845 treatment group. n=5 independent samples. (C) Concentration response of the PF-3845 effect on PIP. Treatments at the indicated concentrations were for 24 hr. * indicates a significant difference vs. Veh ($p<0.05$, 1-way ANOVA with Dunnett's post-hoc test) n = 5 per treatment group. # indicates a significant difference ($p<0.05$) between the medium only (MO) and Veh control groups.

Effects of the PIP fraction in an acute renal function model using C57BL/6J mice

To characterize the effects of the PIP fraction on acute renal function, the product was isolated from the culture medium of MMICs exposed to 10 μM PF-3845 for 24 hr and tested for its effects on blood pressure and urinary parameters (Fig. 12). Figure 12A presents the effects of the PIP fraction given by intravenous infusions on MAP, UV, U_{Na} and U_K in C57BL/6J mice. For controls, SHAM-treated mice were included that received only vehicle for the duration of the experimental period but were otherwise identically treated. Neither MAP nor UV were significantly affected over time in the SHAM control mice. The effects of the PIP fraction given intravenously in 10 min infusions at doses ranging from 0.25 to 8 total AU are shown in Fig. 12A. The average MAP for the pretreatment control phases, C1 and C2, were 115 and 112 mmHg, respectively. Although PIP did not significantly change MAP at dose rates of 0.25 to 4 AU per 10 min, there was a decreasing trend in MAP. By the 8 AU dose rate, this decrease was significant (96 mmHg, $p<0.05$), and MAP remained low during the two following post-treatment phases (96 and 91 mm Hg for P1 and P2, respectively, $p< 0.0001$). This drop in blood pressure was also significant compared to the SHAM control group. Intravenous infusion of increasing doses of PIP to the same mice also enhanced the rates of urine formation and sodium excretion, but the changes were not dose-dependent, and the dose response curves exhibited an inverted U-shape. For example, UV increased from 7 μL/min/g kwt in the C1 and C2 control groups to 20, 16, and 18 μL/min/g kwt, respectively, for the 0.25, 0.5 and 0.75 AU dose groups, only to return back toward the control level with the higher PIP doses and during the P1 and P2 post-treatment control phases. A similar absence of dose-dependence and the presence of an inverted U-shaped curve was apparent for the effect of intravenous PIP on sodium excretion. Potassium excretion

was not significantly altered during the time course of the experiment. The same effects were observed using PIP isolates from multiple batches of PF-3845-treated MMIC cell medium on at least five different dates (data not shown).

When the PIP fraction was infused directly into the renal medullary interstitium, MAP was also reduced (Fig. 12B). A similar pattern to the intravenous response was observed with a downward trend in MAP apparent at the low end of the dose range, which reached significance as the dose increased. The mean arterial pressures of the C1 and C2 groups were 119 and 117 mmHg which decreased to 103, 99 and 93 after intramedullary infusion of 2, 4, and 8 AUs per 10 min of the PIP fraction. The average arterial pressures remained low in the P1 and P2 posttreatment groups ($p<0.01$). Urine excretion increased from 15 and 14 μL/min/g kwt for C1 and C2 to 20, 26, and 29 ($p<0.0001$) for the 0.25, 0.5, and 0.75 AU intramedullary doses, respectively. At the 1 AU dose or higher, the magnitude of the effect decreased, returning to the baseline level by 2 AU and remaining at baseline after the two highest doses and in the P1 and P2 post treatment groups. This difference in urine excretion in the PIP fraction-treated mice was also significant vs. the corresponding points for the SHAM control mice ($p<0.0001$). Whereas the sodium excretion rate also showed a similar stimulation at the low but not high doses, the potassium excretion rate was not significantly affected.

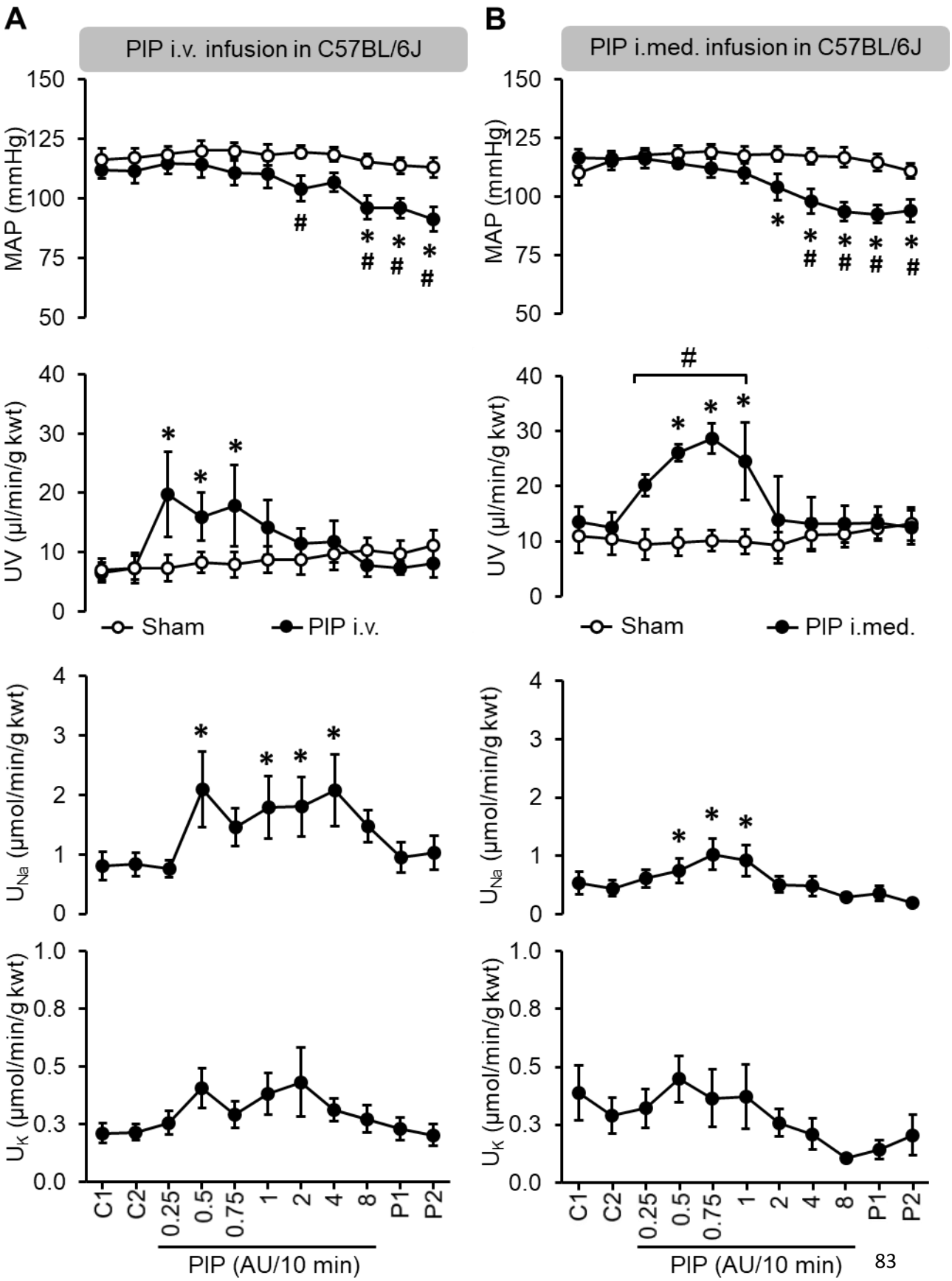
A
PIP i.v. infusion in C57BL/6J
B
PIP i.med. infusion in C57BL/6J
MAP (mmHg)
UV (µl/min/g kwt)
Sham
PIP i.v.
PIP i.med.
U_{Na} (µmol/min/g kwt)
U_K (µmol/min/g kwt)
C1
C2
0.25
0.5
0.75
1
2
4
8
P1
P2
PIP (AU/10 min)

Fig. 12 Effects effects of intravenous (i.v.) (A) and intramedullary (i.med.) (B) infusion of the PIP fraction on mean arterial pressure (MAP), urine excretion (UV), sodium excretion (U_{Na}) and potassium excretion (U_K). C1 and C2 indicate the pre-treatment control phases; P1 and P2 indicate the two 10-min post-treatment control periods. Animals received the PIP fraction at the indicated doses by infusion over a single 10 min period, followed by a 10-minute infusion of vehicle alone. Each data point represents the mean of the 20 min period. SHAM mice received only vehicle the entire experimental period. * indicates a significant difference vs. the C1 group ($p<0.05$, one-way ANOVA with Dunnett's and Fisher's post-hoc tests); # indicates a significant difference between the PIP and SHAM groups ($p < 0.05$' one-way ANOVA with Tukey's post-hoc test); (n = 7 for SHAM, 7 for i.med. infusion, and 11 for i.v. infusion).

Figure 13 presents the results for a single intravenous infusion of the PIP fraction (1 AU per 10 min) on acute renal function including GFR and MBF. Although MAP was not changed during the actual drug infusion period, the MAP decreased significantly on the order of 10 mm Hg during each of the three post-infusion periods (Fig. 13A, $p<0.05$). UV was increased beginning within the first 10 min post-treatment time period and remaining elevated thereafter (Fig. 13B, $p<0.001$). The baseline GFR values for C1, C2 and C3 were 1.8, 1.5 and 1.7 mL/min, respectively, whereas the single 1 AU infusion stimulated GFR to 3.6 mL/min (Fig. 13C), remaining elevated for the immediate term thereafter ($p<0.0014$). GFR began dropping back to baseline levels after 40 min. Treatment with the PIP fraction also significantly elevated MBF (Fig. 13D, $p<0.01$), but this stimulation was brief, returning to control by the P1 post treatment period.

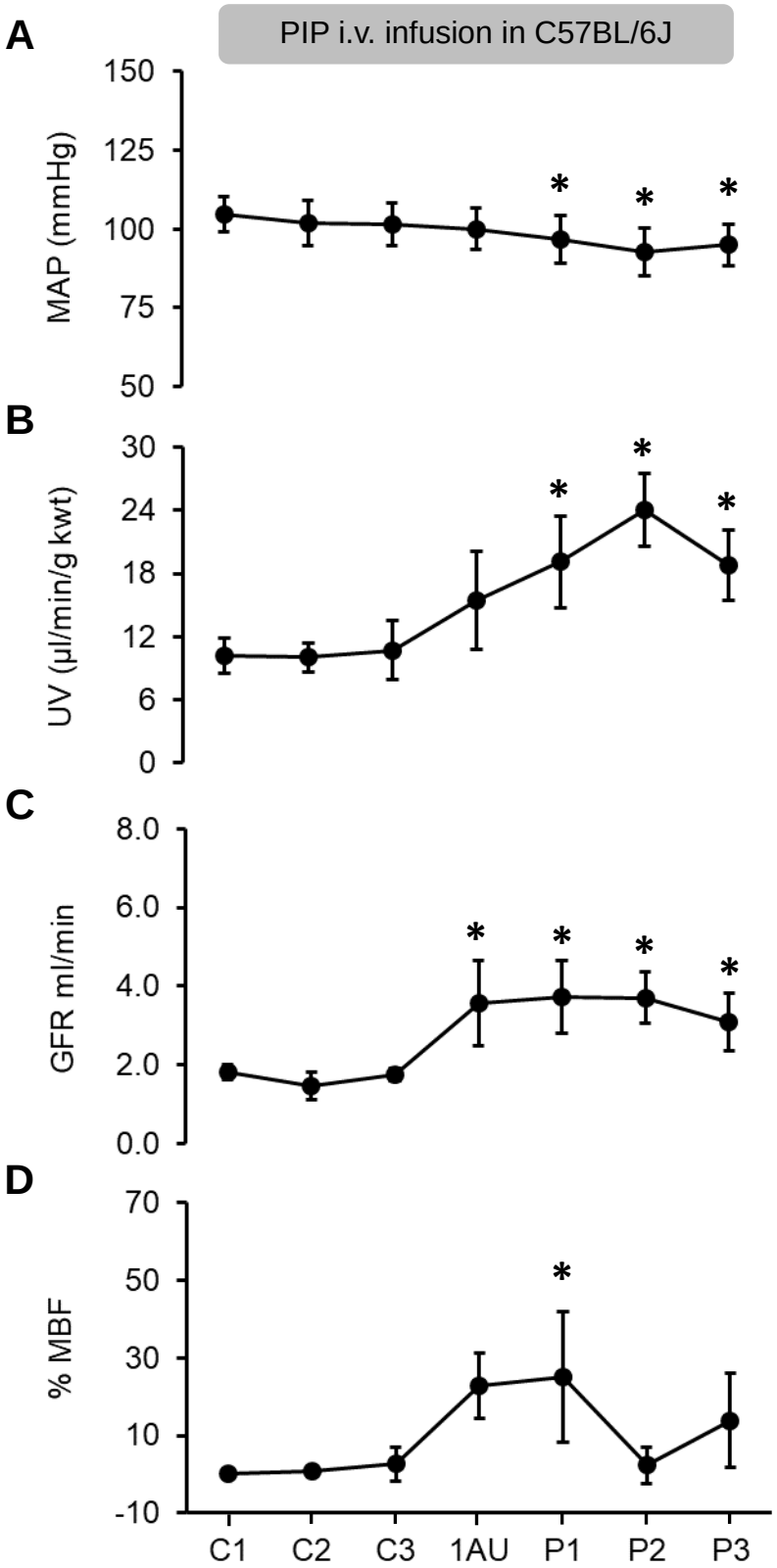
PIP i.v. infusion in C57BL/6J
A
MAP (mmHg)
150
125
100
75
50
B
UV (µl/min/g kwt)
30
24
18
12
6
0
C
GFR ml/min
8.0
6.0
4.0
2.0
0.0
D
% MBF
70
50
30
10
-10
C1
C2
C3
1AU
P1
P2
P3

Fig. 13 The effects of a single intravenous (i.v.) infusion of the PIP fraction on the mean arterial pressure (MAP), urine excretion rate (UV), glomerular filtration rate (GFR) and relative medullary blood flow (MBF). C1-C3 indicate the pre-treatment control phases, during which the animals received intravenous vehicle only (2% BSA in 0.9% saline). Animals then received a single intravenous infusion of 1AU PIP fraction over a 10 min period followed by three 10-min post-treatment control infusion periods (P1-P3) with the vehicle alone. Each data point represents the mean of a 10 min period. *indicates a significant difference vs. the C1 group ($p<0.05$, one-way ANOVA with Dunnett's post-hoc tests); ($n = 4$).

Effects of i.v. or i.p. bolus administrations of the PIP fraction on MAP, UV and MBF

The effects of the PIP fraction were also evaluated after bolus administrations given either i.v. or i.p. (Fig. 14). For the i.v. bolus group, the baseline MAP readings were 110 mmHg for each of the three control groups (Veh, C1 and C2, Fig. 14A) and i.v. bolus administration of 5 AU did not change blood pressure after the dose, even after administering a second 5 AU dose. Whereas MAP showed no response to i.p. injection of vehicle alone (ethanol) remaining at 102 and 102 mmHg for the C1 and C2 periods with respect to the starting MAP of 107 mmHg, the blood pressure was lowered by a 5 AU i.p. bolus injection of the PIP fraction to 90, then to 83 mmHg, remaining there for at least 50 min following the dose. Subsequent administration of a second i.p. 5 AU bolus dropped the pressure initially to 79, then 72 and 71 mmHg.

The UV data for the i.v. vs. i.p. 5 AU bolus dosing showed a striking contrast to MAP results (Fig. 14B). Whereas the baseline UVs for the Veh, C1, and C2 control groups of the i.v. bolus treatment group were 11, 12 and 11 µl/min/g kwt, respectively (Fig. 14B), the urine excretion rate increased to 19 µl/min/g kwt ($p<0.005$) after the i.v. 5 AU bolus and remained elevated during the subsequent post-treatment periods (26-28 µl/min/g kwt, P1-P3). A second bolus of the same i.v. 5 AU dose given 50 min later did not further increase UV, but UV remained elevated. In contrast, UV was unaffected either by a first or second i.p. 5 AU bolus injection. UV in the SHAM group was not significantly affected at any time of the experiment. To test the effects of intravenous and intraperitoneal PIP fraction on medullary hemodynamics, MBF was also measured. MBF was differentially stimulated when the PIP fraction bolus was administered i.p. compared to i.v. (Fig. 14C).

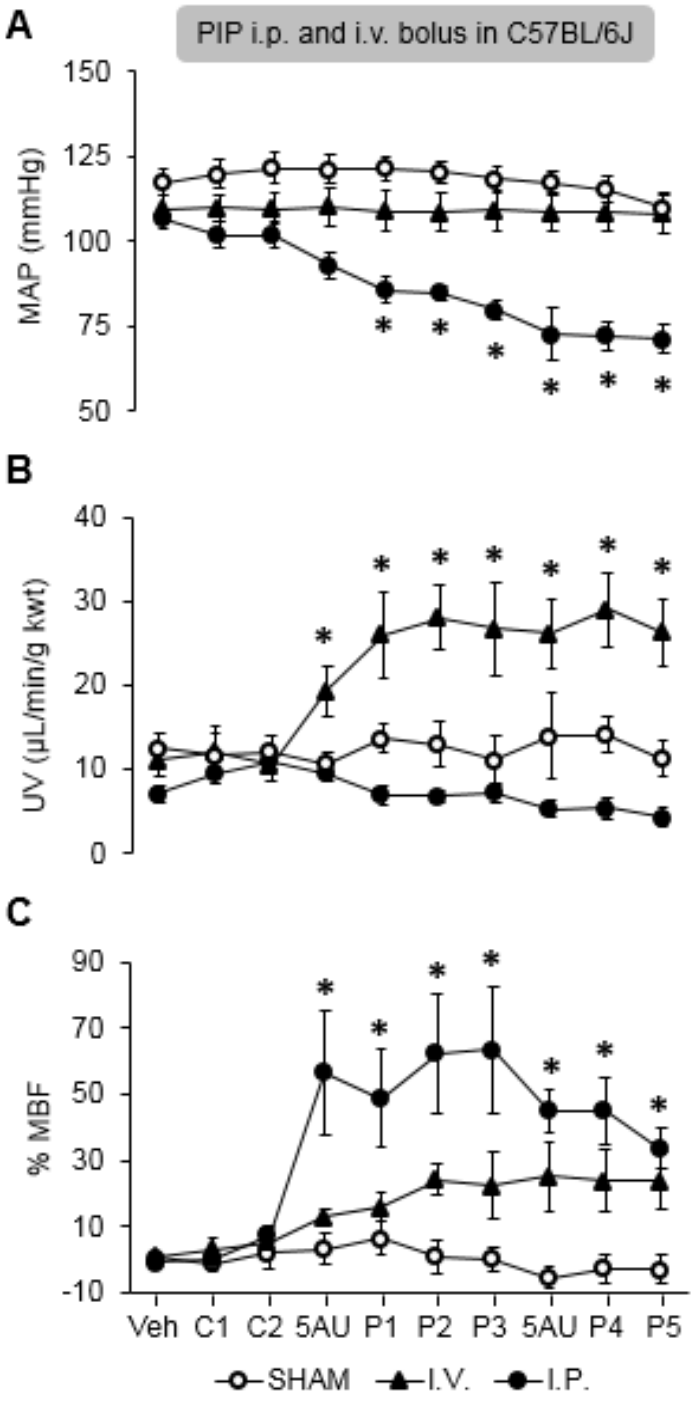
A
PIP i.p. and i.v. bolus in C57BL/6J
MAP (mmHg)
150
125
100
75
50
B
UV (µL/min/g kwt)
40
30
20
10
0
C
% MBF
90
70
50
30
10
-10
Veh C1 C2 5AU P1 P2 P3 5AU P4 P5
SHAM I.V. I.P.

Fig. 14 Effects of intravenous (i.v.) and intraperitoneal (i.p.) bolus administrations of the PIP fraction on mean arterial pressure (MAP), urine excretion (UV) and medullary blood flow (MBF). SHAM animals (open circles) received only continuous infusions of vehicle throughout the entire experimental period. Animals received either an intravenous (closed triangles) or intraperitoneal (closed circles) bolus dose of vehicle (Veh) followed by injections of 5AU PIP fraction. Boluses were delivered over a period of 8 - 15 sec. The vehicles for i.v. and i.p. were 2% bovine serum albumin/0.9% saline and ethanol, respectively. C1 and C2 are post-vehicle control phases, and P1-P5 are 10-min post-treatment control periods. * indicates a significant difference compared to the C1 group

Characterization of the PF-3845-induced MMIC product in an acute renal function animal model in FAAH WT and FAAH KO mice

The responses of MAP and urinary excretion parameters to the PIP fraction were also studied in FAAH KO and their homozygous normal litter mates (FAAH WT) (Fig. 15). The baseline MAP of FAAH KO mice following the 1-hour acclimatization period was 120 and 122 mmHg for the C1 and C2 pretreatment control periods, respectively. MAP was lowered significantly after the 8 AU dose and during the following P1 and P2 post-treatment periods (Fig. 15A). There were no effects of the PIP fraction on UV, U_{Na} or U_K in the FAAH KO mice (Fig. 15B-15D, respectively).

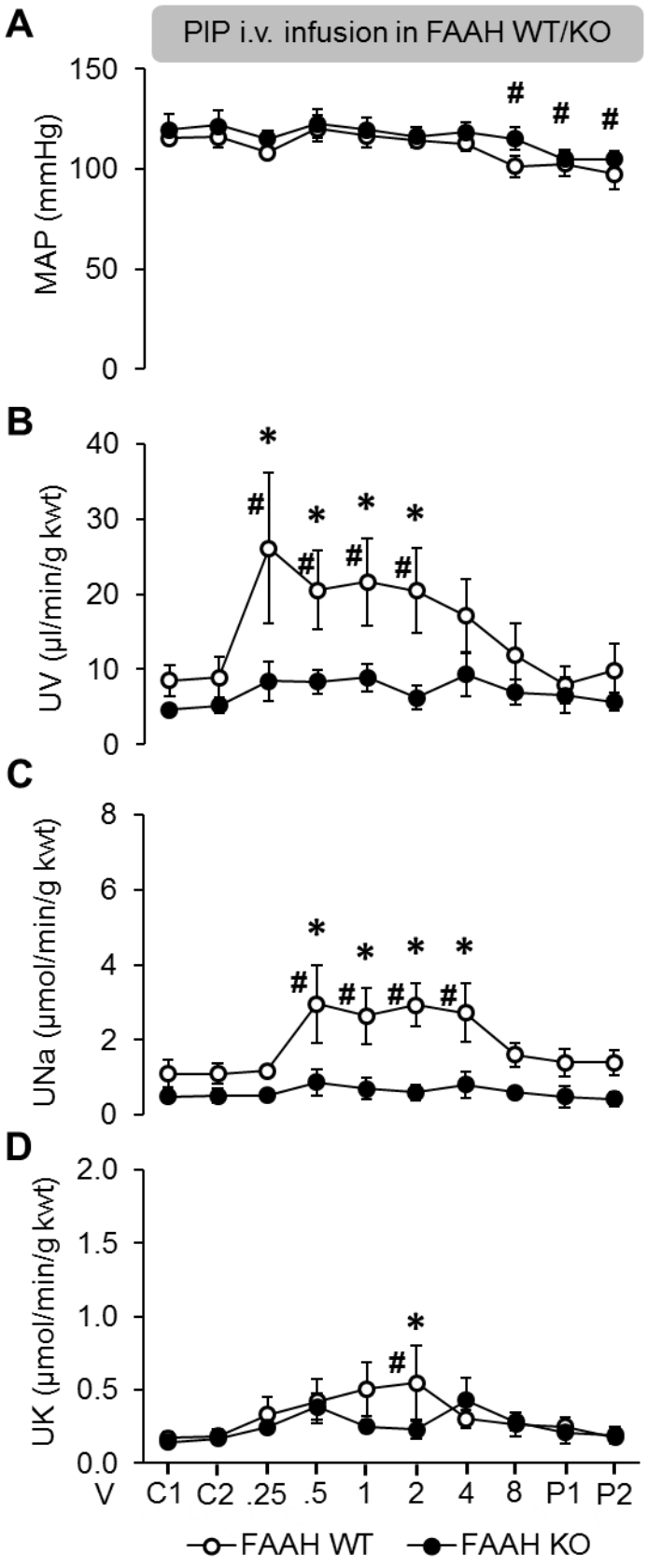
A
PIP i.v. infusion in FAAH WT/KO
MAP (mmHg)
150
100
50
0
B
UV (µl/min/g kwt)
40
30
20
10
0
C
UNa (µmol/min/g kwt)
8
6
4
2
0
D
UK (µmol/min/g kwt)
2.0
1.5
1.0
0.5
0.0
V C1 C2 .25 .5 1 2 4 8 P1 P2
FAAH WT
FAAH KO

Fig. 15 Comparison of the effects of intravenous (i.v.) infusion of the PIP fraction on blood pressure and urinary excretion endpoints in FAAH wildtype and FAAH knockout mice. MAP, mean arterial pressure; UV, urine formation rate; U_{Na}, urinary sodium excretion rate; U_K, urinary potassium excretion rate. C1 and C2 indicate pretreatment control infusion periods with vehicle alone; 0.25 – 8 AU indicate the PIP dose in area units per 10 min infusion; P1 and P2 indicate 10-min post-treatment control infusion periods. * indicates a significant difference in treatment with PIP of FAAH WT versus FAAH KO mice ($p<0.05$, one-way ANOVA with Tuckey's post-hoc tests for A, B, and C; and Fisher's LSD test for D); # indicates significant effect of treatment with PIP versus baseline ($p<0.05$, one-way ANOVA with Dunnett's post-hoc tests A, B, and C; and Fisher's LSD test for D) (n = 6 FAAH WT and 7 FAAH KO).

3.5 Discussion:

This study characterized the diuretic, natriuretic, and vasodepressor activity of a substance produced by mouse renomedullary interstitial cells that showed responsiveness to the FAAH inhibitor, PF-3845. Testing of the HPLC-purified product on acute renal functions in anesthetized normotensive mice showed that the product possessed blood-pressure-lowering and diuretic and natriuretic activities, but that the profile of its effects differed depending on the route of administration. Its contrasting biological effects after intraperitoneal administration suggest a role for liver metabolism in determining its biologic actions. While the structure of the substance responsible for the biologic activities in the PIP fraction has not yet been identified, the finding that its concentration in MMIC culture medium increased by PF-3845 treatment and that its diuretic and natriuretic activities were attenuated in FAAH KO (Fig. 15B-C) mice suggest a relationship to anandamide or other fatty acid ethanolamides or amides. These data support the existence of a substance secreted by renomedullary interstitial cells and has the capacity to lower blood pressure by either renal or extrarenal mechanisms.

The product characterized in this study was detected in culture medium of MMICs based on its ultraviolet absorption at 205 nm and its enhancement by treatment with PF-3845. Further experiments showed that it was also present in complete culture medium but was further enhanced by incubation with MMICs and by PF-3845 treatment supporting that it is a product of MMICs. Based on its unique retention time of 13.8 min, the substance is distinct from anandamide (7.7 min) and prostaglandin E_2 (5.8 min). The decreased level of the product in indomethacin-treated cultures (Fig. 11, panels A and B) suggests that prostaglandin synthesis or metabolism by cyclooxygenase may be necessary for its formation or release.

The PIP fraction exhibited the capacity to stimulate diuresis and natriuresis, glomerular filtration, and medullary blood flow and to drop blood pressure in the surgically instrumented mouse model used in this study. However, there were notable differences depending on the route of administration. Its activity as a diuretic and natriuretic effect was evident after either systemic (intravenous) (Figs. 12A, 13B-C, and 14B) or local (intramedullary) administration (Fig. 12B) regardless of whether the dose was infused over 10 min or given as a rapid bolus. In contrast, the product was inactive as a diuretic after i.p. bolus administration (5 AU, Fig. 14B). This suggests that hepatic metabolism inactivates the diuretic activity of the product. A curious aspect of the dose response curve for the diuretic and natriuretic effects of the product after intramedullary administration was its inverse U-shape. The basis for this biphasic shape is unknown. However, it is noteworthy that cannabinoid 1 receptor (CB_1) agonists such as AM7418, AM4054, THC, and WIN55,212-2 were shown to stimulate urine production with inverse U-shaped dose response curves (Chopda et al., 2013). We also observed U-shaped diuresis dose response curves when anandamide was infused into the renal medulla together with the FAAH/MAGL dual inhibitor, isopropyl dodecylfluorophosphate (Ahmad et al., 2017a). One possible explanation for this effect is that tachyphylaxis, the rapid development of acute tolerance, is occurring.

In contrast to the diuretic and natriuretic effects, the pressure-lowering effect of the PIP fraction had a distinct dose response, occurring only after the higher doses tested ($\geq$2 AU/10 min) and during the post-treatment control phases (Figs. 12A and 12B). The pressure-lowering effect of an i.v. infusion (1 AU/10 min) had a delayed onset, reaching significance only during the post-treatment phases, and it was prolonged, lasting even through the third post-treatment period (Fig. 13A). The finding that i.p. administration of a single bolus dose of the product (5

AU) elicited a marked pressure-lowering effect of delayed onset and long duration suggests that the active substance undergoes first pass metabolism in the liver to form a vasodepressor metabolite. Given the strong stimulation of MBF, it seemed surprising that diuresis was not also stimulated under these conditions, as increased MBF is known to dissipate the salt and urea gradient of the inner medulla, interfering with the kidney's ability to concentrate the urine. On the other hand, it may be considered equally surprising that such a large drop in blood pressure was not accompanied by a proportional drop in natriuresis and diuresis, based on the pressure-natriuresis relationship. The reason for the latter may be explained by the capacity of the PIP fraction to stimulate MBF.

Our laboratory is investigating the possible relationship of the fatty acid ethanolamide system of the renal medulla to the renomedullary neutral antihypertensive lipid which Muirhead devoted his life to study. Published (Ritter et al., 2012) and unpublished data from our laboratory demonstrated that intramedullary infusion of anandamide stimulated diuresis and sodium and potassium excretion but had no effect on either MAP or MBF. Subsequently we investigated whether similar infusion of FAAH inhibitors are able to recapitulate the effects of anandamide. The former act indirectly to cause the local accumulation of anandamide by inhibiting its hydrolysis. Intramedullary infusion of IDFP, a potent albeit non-selective inhibitor of FAAH, stimulated diuresis-natriuresis and enhanced MBF, supporting that endogenous anandamide in the renal medulla can regulate renal excretory and hemodynamic functions (Ahmad et al., 2017a). Because IDFP is also a potent inhibitor of monoacylglycerol lipase, the role of increased tissue concentrations of 2-arachidonoyl glycerol in its observed effects could not be excluded. This led us to evaluate the effects of PF-3845, a much more selective inhibitor of FAAH. Interestingly, when PF-3845 was infused into the renal medulla, diuresis-natriuresis and MBF

were stimulated, and a MAP-lowering effect was also observed (Ahmad et al., 2018). The findings reported here for the PF-3845-induced product fraction bear strong similarity to the effects observed after intramedullary PF-3845 *in vivo*. In addition, it is interesting that intramedullary PF-3845 and the PF-3845-induced product fraction share reported characteristics of medullipin, including the vasodepressor (Muirhead, 1993) and diuretic-natriuretic effects (Karlstrom et al., 1988). Muirhead proposed that the kidney medulla secretes a prohormone form of medullipin termed medullipin I that undergoes subsequent conversion by the hepatic cytochrome P450 system to medullipin II, the active vasodepressor form (Muirhead et al., 1988; Muirhead et al., 1989). The striking increase in vasodepressor activity after i.p. administration of the PF-3845-induced product fraction together with its delayed onset and long-lasting nature is reminiscent of the properties ascribed to medullipin II. Further studies are needed to better define this relationship and the basis of its dependence on hepatic metabolism.

The renal medulla, through its unique cellular anatomy, blood supply, hyperosmotic environment, and interactions of interstitial cells with renal tubules and vasa recta, has long been proposed to be critical as a long-term regulator of body fluid and sodium balance and blood pressure (Zhuo, 2000). The idea that interstitial cells secrete antihypertensive lipids appeared in the literature in the late 1960's with morphometric observations that the lipid granules of interstitial cells decrease in experimental models of hypertension (Tobian and Ishii, 1969; Pitcock et al., 1981). The nature of these lipids has been a topic of intense research. Noted for their high content of arachidonic acid in lipid granules and the presence of high constitutive COX levels, interstitial cells were demonstrated to synthesize and secrete prostaglandin E_2 in response to stimulation of receptors on their cell surface for vasopressor hormones such as angiotensin (Zusman and Keiser, 1977a). Prostaglandin E_2 is a vasodilator as well as diuretic

and natriuretic (Hashimoto, 1980). To our knowledge, medullipin is the only other major antihypertensive lipid proposed to be produced and released by medullary interstitial cells (Brooks et al., 1994; Cowley, 1994).

The finding that FAAH was expressed in MMICs (Fig. 8F) provides evidence for the presence of the proposed target of PF-3845. Another finding of interest for its possible relation to secretion of the diuretic-natriuretic and vasodepressor substance was the observed increase in lipid granules in MMICs exposed to PF-3845, as demonstrated using the neutral lipid dye, Sudan Black B (Fig. 9). Ultrastructural analyses of control and PF-3845-treated MMICs suggested that the increased neutral lipid staining in the PF-3845-treated cells was associated at least in part with increased size and number of cytoplasmic multilamellar bodies (Fig. 10). These organelles were found by us to be present in the vehicle-treated MMICs (Fig. 10, panel B arrow) and by others in cultured medullary interstitial cells (Mathews et al., 1979) as well as in renomedullary interstitial cells *in situ* (Lewis and Prentice, 1979; Bohman, 1980). They are proposed to play roles in the storage and secretion of lipids (Schmitz and Muller, 1991). Further investigation is needed to determine if multilamellar bodies are involved in the PF-3845-induced mechanism.

In summary, the current study supports blood pressure-lowering, MBF-increasing, and diuresis/natriuresis-stimulating effects of an endogenous lipid produced by MMICs and enhanced in the presence of a FAAH inhibitor. Our data indicate a possible relationship of this compound to medullipin, the renomedullary neutral antihypertensive lipid proposed by Muirhead. Structural identification of PIP is ongoing, but preliminary data suggest that it is a sterol-related substance. Further studies are underway to identify the substance and assess its responsiveness to altered renal perfusion pressure.

Chapter 4 – Diuretic and natriuretic effects of PIP are mediated via a CB1-dependent mechanism

4.1 Introduction

The kidneys are important for the long-term regulation of blood pressure due to their ability to regulate body fluids and electrolytes. Unsurprisingly, pathologies of the kidneys or their vasculature have been associated with the development of primary or secondary hypertension (Wadei and Textor, 2012). The kidneys modulate pressure natriuresis via numeral biological systems in the organism, some of which are the renin-angiotensin-aldosterone system (RAAS), the sympathetic nervous system and the endocannabinoid (eCB) system (Buckley and Johns, 2011; Wakui et al., 2015; Ahmad et al., 2017a). The endocannabinoid system has been studied abundantly in relation to gastrointestinal tract disorders, peripheral neuropathy, immunoregulation in infectious diseases, and the central nervous system (Blake et al., 2017; Hernandez-Cervantes et al., 2017; O'Hearn et al., 2017; Stopponi et al., 2017; Wasilewski et al., 2017). However, the complete role of the endocannabinoid system in the renal regulation of fluid homeostasis remain largely uncovered.

The endocannabinoid system is universally represented by: [1] several endogenous lipids, such as 2-arachidonoyl glycerol (2-AG) and anandamide (AEA); [2] cannabinoid receptors types I and II (CB1 and CB2, respectively); and accompanying enzymes that synthesize and degrade these lipids (fatty acid acyl hydrolase, FAAH, and monoacylglycerol lipase, MAGL) (Sampaio et al., 2015). Anandamide is predominantly synthetized via release from *N*-arachidonoyl phosphatidylethanolamine, mediated by *N*-arachidonoyl phosphatidylethanolamine-specific

phospholipase D, and undergoes a FAAH-mediated metabolism to arachidonic acid and ethanolamines (Munro et al., 1993). AEA elicits its activities predominantly by binding and activating CB1 receptors. In neural tissues CB1 activation has been characterized by inhibition of adenylyl cyclase, inositol phosphates formation, N-type calcium channels and gap junctional conductance (Howlett et al., 1990; Mackie and Hille, 1992; Nah et al., 1993).

Within the kidney, several lines of evidence purport the importance of AEA and its metabolizing enzyme, FAAH, as mediators of diuresis and natriuresis. In rodents, AEA has been demonstrated to decrease glomerular filtration rate and to increase renal blood flow, independent of blood pressure changes (Hryciw and McAinch, 2016). Furthermore, various research groups have shown that AEA and other synthetic agonists of the CB1 receptor induce diuresis and natriuresis and animal models of renal function (Li and Wang, 2006; Ritter et al., 2012; Paronis et al., 2013). Li and Wang found that an intramedullary infusion of the metabolically stable analogue of AEA, methanandamide, could stimulate diuresis without changing blood pressure (Li and Wang, 2006). They also showed that the AEA analogue did not affect cortical and medullary blood flow, a finding replicated by Ritter et al (Ritter et al., 2012). It is also noteworthy that the cannabinoid-induced diuresis has been found to be a CB1-receptor mediated effect in rodents that follows a bi-phasic pattern of activity (particularly in mice) (Chopda et al., 2013; Paronis et al., 2013). However, studies from our lab demonstrate that when the AEA metabolizing enzyme, FAAH is inhibited by a selective or non-selective inhibitor, PF-3845 and IDFP respectively, diuresis and natriuresis are accompanied by an elevation in medullary blood flow and a decrease in blood pressure (Ahmad et al., 2017a; Ahmad et al., 2018). These findings suggest that AEA's activity in the kidney is not enough clarify the complete diuretic and

natriuresis physiological profile of the endocannabinoid system that is involved in renal regulation.

We previously characterized the diuretic, natriuretic and pressure-lowering effects of a substance produced by mouse renomedullary interstitial cells after treatment with the FAAH inhibitor, PF-3845 (Daneva et al., 2018). After purification with HPLC, we tested the extract on acute renal function in anesthetized normotensive mice and saw that it was able to drop pressure and produce significant diuresis and natriuresis (Daneva et al., 2018). The PF-3845 induced product, PIP, showed a modality of biological activity after intraperitoneal administration in comparison to other administration routes, suggesting a role of liver metabolism for its functioning (Daneva et al., 2018). While the structure of the substance responsible for the biologic activities in the PIP fraction has not yet been identified, the finding that its concentration in MMIC culture medium increased by PF-3845 treatment and that its diuretic and natriuretic activities were attenuated in FAAH KO mice suggest a relationship to anandamide or other fatty acid ethanolamides or amides. In this study we tested if PIP binds to CB1 receptors in the kidney. Moreover, we tested if a pharmacological or a genetic ablation of CB1 receptors would remove the pressure-lowering, diuretic and natriuretic activity of PIP.

4.2 Methods

Reagents

Rimonabant (SR141716) was obtained from Cayman Chemical (Ann Arbor, Michigan, USA). HPLC purification of PF-3845-inducible MMIC product, PIP, was performed following a previously published extraction protocol from our laboratory (Daneva et al., 2018). For

radioactive ligand binding, WIN 55,212-2 mesylate and CP55,940 were purchased from Sigma-Aldrich (St. Louis, MO, USA). The [3H] SR141716A was obtained by PerkinElmer (Boston, MA, US).

Animals

Male and female C57BL/6J mice (Jackson Laboratory, Bar Harbor, ME) and male and female homozygous CB1 wildtype (CB1 WT) and knock-outs (CB1 KO) mice (2-5 months old) (from a colony established at Virginia Commonwealth University) were used in the present study (Steiner et al., 1999) The CB1 WT and KO mouse colony have been maintained by backcrossing onto a C57BL/6 background for more than 20 generations (Wise et al., 2008). The mice in this study weighed 20-35 grams and were housed 4-5 per cage in a temperature (20-22°C) and humidity (50-55%)-controlled environment with a 12 hr light/dark cycle with free access to food and water. All experiments involving animals in this study were approved by the Institutional Animal Care and Use Committee of Virginia Commonwealth University in accordance with the National Institutes of Health Guide for the Care and Use of Laboratory Animals.

HPLC purification of PF-3845-inducible MMIC product

MMICs were dissociated by trypsinization and plated in tissue culture dishes (3×10^6 cells/150 mm dish) followed by addition of vehicle (ethanol,0.1%) or vehicle containing PF-3845 (10 μM final concentration). The culture medium was extracted using Clean-Up C18 solid phase extraction columns (500 mg, United Chemical Technologies, Bristol, PA). Briefly, the SPE columns were conditioned with 3 mL of methanol followed by 3 mL of deionized water.

The samples of culture medium (25 mL) were then passed through the columns and washed, first using 3 mL of DI water followed by 3 mL of 25% methanol and 3 mL of 60% methanol. The lipids eluting with 100% methanol were collected and evaporated under nitrogen leaving ~500 µL. 50 µL was transferred to auto-sampler vials for reverse phase HPLC-UV analysis. Chromatographic separation was performed on a Grace Alltech C18 column, 100 × 4.6 mm, 5 µm (Grace, Columbia, MD) using an HP1050 quaternary pump system. The mobile phases were A: water with 0.1% TFA and B: 100% methanol at a flow rate of 0.8 mL/min. The following gradient was used: 0.0–0.5 min 50% B, 0.5-5 min linear gradient to 100% B, and 5-15 min holding at 100% B. Detection was by UV absorption at 205 nm using an HP1050 photodiode array detector.

Because the structure or structural class of the PF-3845-induced product has not been determined and the isolated quantities were too low to permit accurate mass measurement, doses or dose rates for testing its biological activities were expressed in area units under the peak (AU, milliabsorbance units x time in minutes) as determined by the ChemStation software (Agilent, Santa Clara, CA). Multiple batches of the isolated product were used for testing of biological activity. The isolated product was stable after storage at -20C for > 6 months.

Surgical Preparation for acute renal functional model

Mice were anesthetized and prepared surgically for the acute renal function testing procedure as described previously (Zou et al., 2001; Li et al., 2005). Anesthesia was induced with ketamine (Ketathesia™, Harry Schein Animal Health, Dublin, OH) (100 mg/kg, i.p.) and thiobutabarbital (Inactin™, Sigma Chemical Co., St. Louis, MO, 75 mg/kg, i.p.). The abdominal and neck areas were shaved, and the mice were placed on a thermostatically-controlled warming

table to maintain body temperature at 37°C. A tracheotomy was performed by inserting a 2 cm length of polyethylene PE-60 tubing to maintain a patent airway during surgery. After tracheotomy, a catheter prepared from heated and pulled plastic PE-10 tubing and filled with heparin sodium dissolved in saline (Fisher BioReagents, 0.005 mg/mL, 50 IU/mL) was inserted into the left carotid artery and attached to a pressure transducer connected to a data acquisition system (Windaq, DATAQ Instruments, Akron, OH). The right jugular vein was catheterized with a catheter prepared from PE-10 tubing for the infusion of 0.9% saline. The rate of intravenous infusion was 1 mL/h/100 g body wt to maintain fluid volume and hematocrit concentration throughout the experiment. For the acute renal function experiments, an incision was performed following the midline of the abdominal area. The left ureter was ligated with a surgical suture and cut on the kidney side of the ligation to allow produced urine to exit freely into the abdominal cavity. The urethra was ligated in proximity to the bladder, and the latter was catheterized with a 2.5 cm cut length of PE-50 tubing for the collection of urine at timed intervals. The right kidney was elevated on a piece of sterilized gauze and a pulled PE-10 catheter was implanted to 2.5 mm in depth vertically from the dorsal surface into the outer medulla. The catheter was immobilized to the kidney capsule using a cyanoacrylate tissue adhesive (Vetbond, 3M Animal Care Products, St. Paul, MN). All mice received a 1 hour equilibration period, during which the animals received continuous vehicle infusions: 1) intravenous infusion of filter-sterilized 0.9% NaCl at a rate of 1 mL/hr/ 100 g body weight, 2) intramedullary infusion with PBS containing (in mM) 205 NaCl, 40.5 Na_2HPO_4, and 9.5 NaH_2PO_4 (pH 7.4, 550 mOsm) at a rate of 2 μL/min to maintain the patency of interstitial infusion (Zhu et al., 2011). The urine excretion rate (UV) was measured gravimetrically, and the sodium and potassium concentrations in urine were measured using flame photometry. UV and

the urinary sodium and potassium excretion rates (U_{Na} and U_K, respectively) were factored per gram of kidney weight. At the end of each experiment, the animals were euthanized by exsanguination from the carotid artery catheter for collection of plasma. The placements of the intramedullary catheter in the outer medulla was routinely confirmed by post-mortem kidney dissection following the experiments.

Experimental Protocols for Renal function studies

After a 1-hour equilibration period and three sequential 10-min pretreatment control sample collection periods (C1-3), CB1 KO and WT mice were infused intramedullarily with PIP over two twenty-minute periods (1AU / 10 min) or they were injected with 5AU/10µL ETOH intraperitoneally, followed by three ten-minute post treatments (P1-3). All treatment periods were graphically presented. Similarly, in C57BL6J mice, after 1-hour equilibration period and three sequential 10-min pretreatment control sample collection periods (C1-3), rimonabant (3mg/kg) was injected subcutaneously approximately 30 minutes before two periods of intramedullary infusion of PIP (1AU / 10 min). The treatment was followed by three post-treatment periods of parameter collections (P1-3). To compare the effect of SR141716 alone, we treated a separate group of C57BL6J mice with Rimonabant alone (3mg/kg) and infused with VEH instead of PIP.

Medullary Blood Flow (MBF)

For the measurement of MBF, a laser Doppler flow probe (OxyFlo Pro; MNP 100XP; Oxford Optronix, Oxford, United Kingdom) was stabilized on the ventromediolateral surface of the right kidney to measure continuously the MBF (as previously reported in (Ahmad et al.,

2017a; Ahmad et al., 2018)The recording of the blood flow was measured by using a dual-channel laser-Doppler flowmeter (Transonic Systems Inc., Ithaca, NY).

Membrane preparations

Chinese hamster ovary cells stably expressing the human CB_1 or CB_2 receptor were cultured in a 50:50 mixture of Dulbecco's modified Eagle's medium and Ham F-12 supplemented with 100 U/ml penicillin, 100 μg/ml streptomycin, 0.25 mg/ml G418, and 5% fetal calf serum. Cells were harvested by replacement of the media with cold phosphate-buffered saline containing 0.4% EDTA followed by agitation. Membranes were prepared by homogenization of cells in 50 mM Tris-HCl, 3 mM $MgCl_2$, and 1 mM EGTA, pH 7.4, centrifugation at 50,000*g* for 10 min at 4°C, and resuspension in the same buffer at 1.5 mg/ml. Membranes were stored at −80°C until use (Wiley, Selley, Mahadenev, 2012). This cell line was cultured and maintained at Dr. Dana Selley's laboratory (Department of Pharmacology and Toxicology, Virginia Commonwealth University).

Radioligand Binding

Membranes were diluted with assay buffer B (50 mM Tris-HCl, pH 7.4, 3 mM $MgCl_2$, and 0.2 mM EGTA). Reactions containing membrane (20 μg of protein) were incubated with 0.5 nM [^{3}H]SR141716 (CB_1) and varying concentrations of CP-55,940 or PIP in assay buffer B containing 0.5% BSA. Nonspecific binding was measured in the presence and absence of 10 μM unlabeled WIN 55,212 (CB_1). The assay was incubated for 90 min at 30°C and terminated by rapid filtration under vacuum through Whatman (Clifton, NJ) GF/B glass fiber filters that were presoaked in Tris buffer containing 5 g/liter BSA (Tris-BSA), followed by five washes with cold

Tris-BSA. Bound radioactivity was determined by liquid scintillation spectrophotometry at 45% efficiency for ^{3}H. This protocol was obtained from the Selley research group (Department of Pharmacology and Toxicology, Virginia Commonwealth University) (Wiley, Selley, Mahadenev2012). All radioligand binding experiments were conducted in the above-mentioned research laboratory.

Statistical Analysis

Data are presented as the mean ± S.E.M. For comparison between multiple groups of data, one- or two-way analysis of variance (ANOVA) was applied using Tukey or Dunnett's post-hoc test when significant differences were found. A p-value ≤ 0.05 was considered statistically significant.

4.3 Results:

Effect of PF-3845-induced fraction after rimonabant treatment in an acute renal functional model using C57BL6J mice

To characterize the effects of the PIP fraction on acute renal function, the product was isolated from the culture medium of MMICs exposed to 10µM PF-3845 for 24 hours and tested for its effects on blood pressure and urinary parameters in C57BL6J mice, pre-treated with rimonabant (a selective inverse agonist of CB1 receptors). Fig. 16 presents the effects of intramedullary infusion of 1AU/10min PIP on mean arterial pressure (MAP), urine production (UV) and % medullary blood flow (%MBF) after intraperitoneal pre-treatment with rimonabant (3mg/kg) in C57BL6J mice. As control, we used another group of C57BL6J mice that received

rimonabant treatment, followed only by vehicle infusion. We observed that neither of the two treatment groups exhibited a significant change in MAP in comparison baseline. Interestingly, when rimonabant was administered intraperitoneally, pressure fluctuated within the first 10 minutes post-administration, then returned to baseline. There was no apparent decrease of MAP after treatment with PIP. Pre-treatment with rimonabant appeared to modify the physiological response to PIP. There was not observable diuretic effect during or after the intramedullary infusion of lipid fraction. However, the medullary blood flow data showed that rimonabant alone was able to significantly stimulate MBF (~ 23 % increase from baseline) without causing diuresis. Meanwhile, medullary blood flow after pre-treatment with rimonabant and administration of PIP showed an attenuated elevation (only around 12% increase to baseline). The medullary blood flow returned to baseline within 30 minutes after PIP infusion.

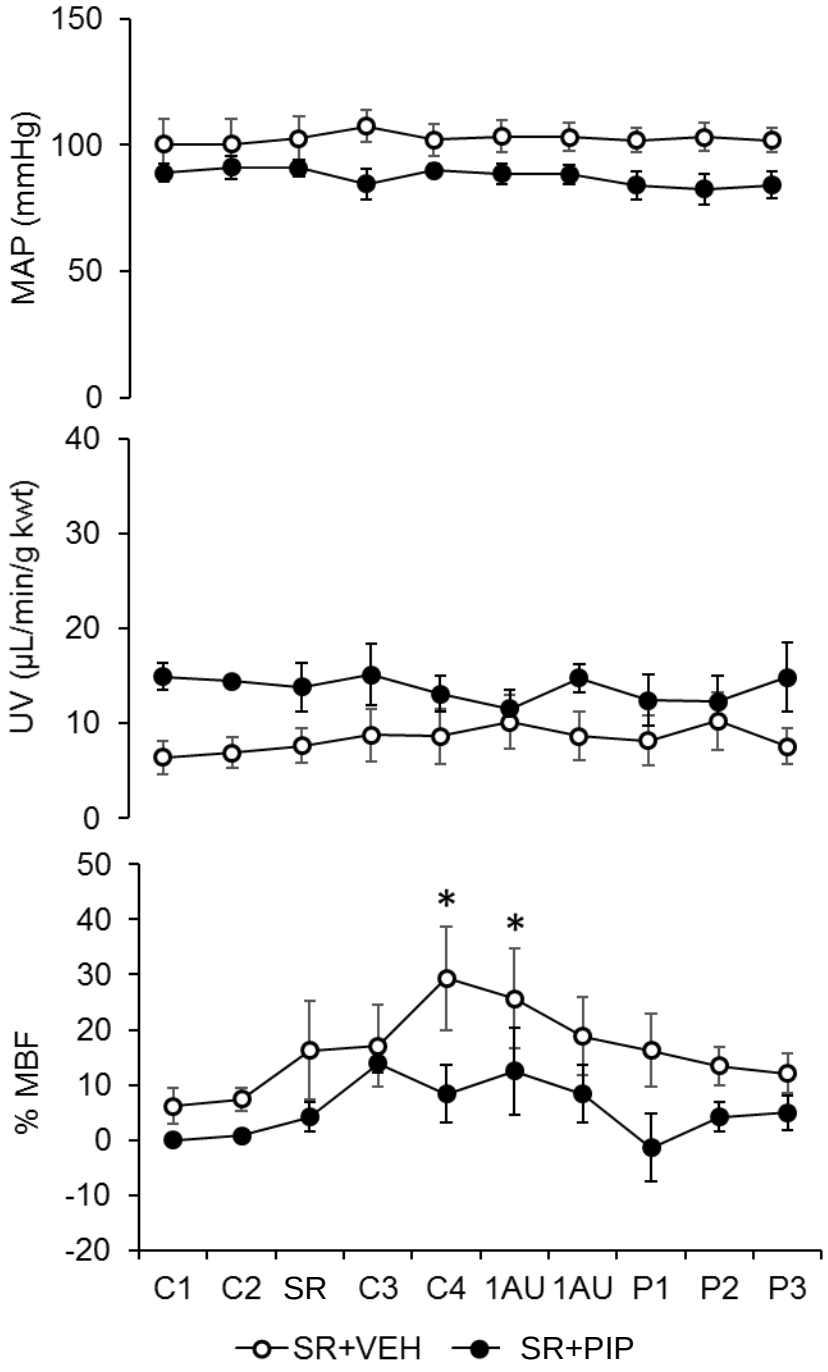

Fig. 16 Effects of an intramedullary (i.m.) infusion of PIP (1AU / 10 min) on the mean arterial pressure (MAP), urine excretion rate (UV) and medullary blood flow (MBF) in C57BL6J mice. C1-C2 indicate baseline control phases, during which the mice received intramedullary vehicle only. SR indicates that rimonabant (3mg/kg) was administered intraperitoneally at the beginning of the 10-minute period. C3-C4 are control phases to allow rimonabant to fully elicit its activity. 1AU indicates two 10-minute periods of PIP infusion. P1-P3 are post-treatment control phases. Each data point represents the mean of a 10 min period. *indicates a significant difference vs. the C1 group ($p<0.05$, one-way ANOVA with Dunnett's post-hoc tests); (n = 5 SR+VEH, n= 6 SR+PIP).

Characterization of the PF-3845-induced MMIC product in an acute renal functional animal model in CB1 WT and CB1 KO mice

The responses of MAP and urinary excretion to intramedullary infusion of the PIP fraction were also studied in CB1 WT and KO mice (Fig. 17). MAP in CB1 KO animals did not change significantly throughout the duration of the experiment. During C1 and C2, MAP ranged between 100 and 103 mm Hgs, respectively. This baseline was followed by a slightly elevated pressure during and after treatment with PIP (ranging from 103 to 106 mm Hgs). Similarly to previous findings in our lab, when WT animals received intramedullary infusion of PIP (1AU), there was a significant drop in pressure. In this experiment, MAP started dropping after the second 10 minutes infusion period (from 117 to 112 mm Hgs) and continued to drop until P3, where pressure was 95 mm Hgs (an overall drop of 25 mm Hgs from baseline). The second panel of figure 17 reveals that CB1 WT mice exhibited larger than a 3-fold increase in urine excretion during the first 10 minutes of intramedullary infusion with PIP (on average UV increased from 5 to 17 µL/min/g kwt). UV returned back to baseline after the twenty minute treatment with PIP and remained stable at approximately 6 µL/min/g kwt. Urine excretion in CB1 KO mice was not altered by infusion with the lipid fraction.

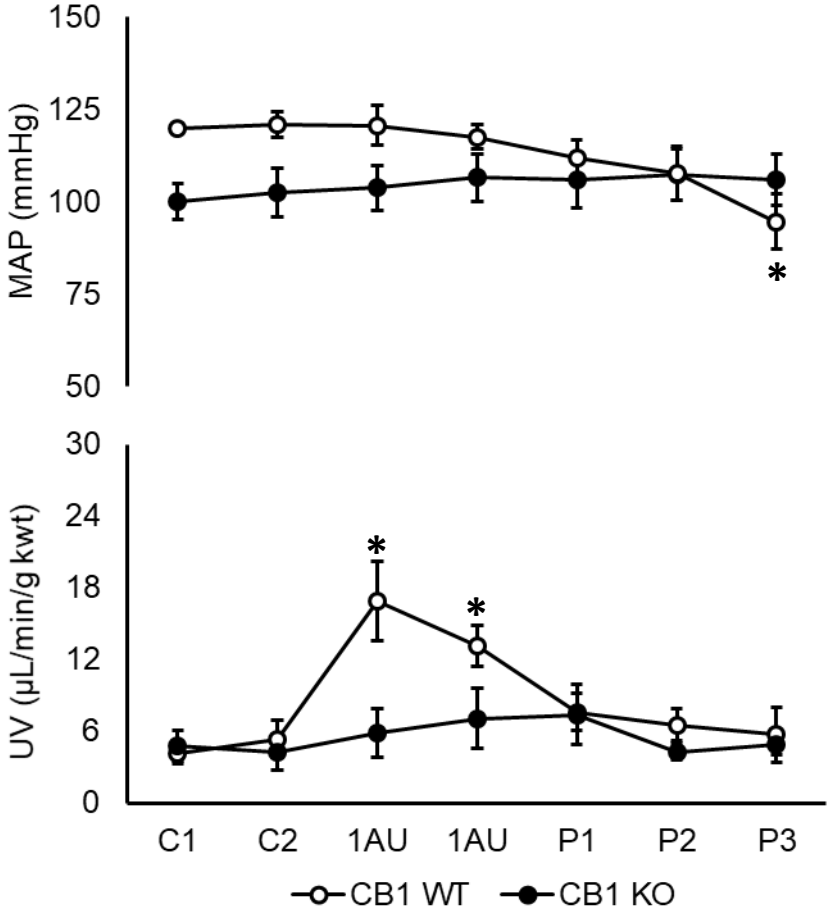

Fig. 17 Effects of an intramedullary (i.m.) infusion of PIP (1AU / 10 min) on the mean arterial pressure (MAP) and urine excretion rate (UV) in CB1 WT and CB1 KO mice. C1-C2 indicate baseline control phases, during which the mice received intramedullary vehicle only. 1AU indicates two 10-minute periods of intramedullary PIP infusion. P1-P3 are post-treatment control phases. Each data point represents the mean of a 10 min period. *indicates a significant difference vs. the C1 group ($p<0.05$, one-way ANOVA with Dunnett's post-hoc tests); (n = 5 in both groups).

To characterize the physiological activity of PIP in an acute renal functional animal model of CB1 receptor ablation, we also tested the product's ability to reduce pressure and produce diuresis in CB1 WT and KO mice after intraperitoneal injection of 5AU (see Fig. 18). The first panel reveals that when 5AUs of PIP were administered i.p. in WT mice, there was a profound decrease in MAP (from 106 at C1 to 69 mm Hgs at P4; $P< 0.0001$). This drop in pressure started immediately after PIP was injected and the decrease remained stable approximately 50 minute later (69 mm Hgs at P4). Meanwhile, in CB1 KO mice, there was no significant difference in MAP after PIP treatment (105 mm Hgs at P3 and P4) in comparison to baseline (110 mm Hgs at C1 and C2). Moreover, the i.p. injection of PIP did not produce diuresis in either group. Urine excretion in CB1 WT and KO groups ranged between 5 and 10 μL/min/g kwt. Finally, when we measured the % medullary blood flow after i.p. treatment with PIP in CB1 WT and KO mice, we discovered that in WT mice, there was a significant elevation in MBF after PIP (ranging between 56% to 61% elevation, $P<0.0001$). The medullary blood flow in CB1 WT subjects began to increase with the injection of PIP and remained elevated until the end of the experiment (56% within 10 minutes of injection and 60% at P4). MBF in CB1 KO animals was not affected by i.p. treatment with PIP.

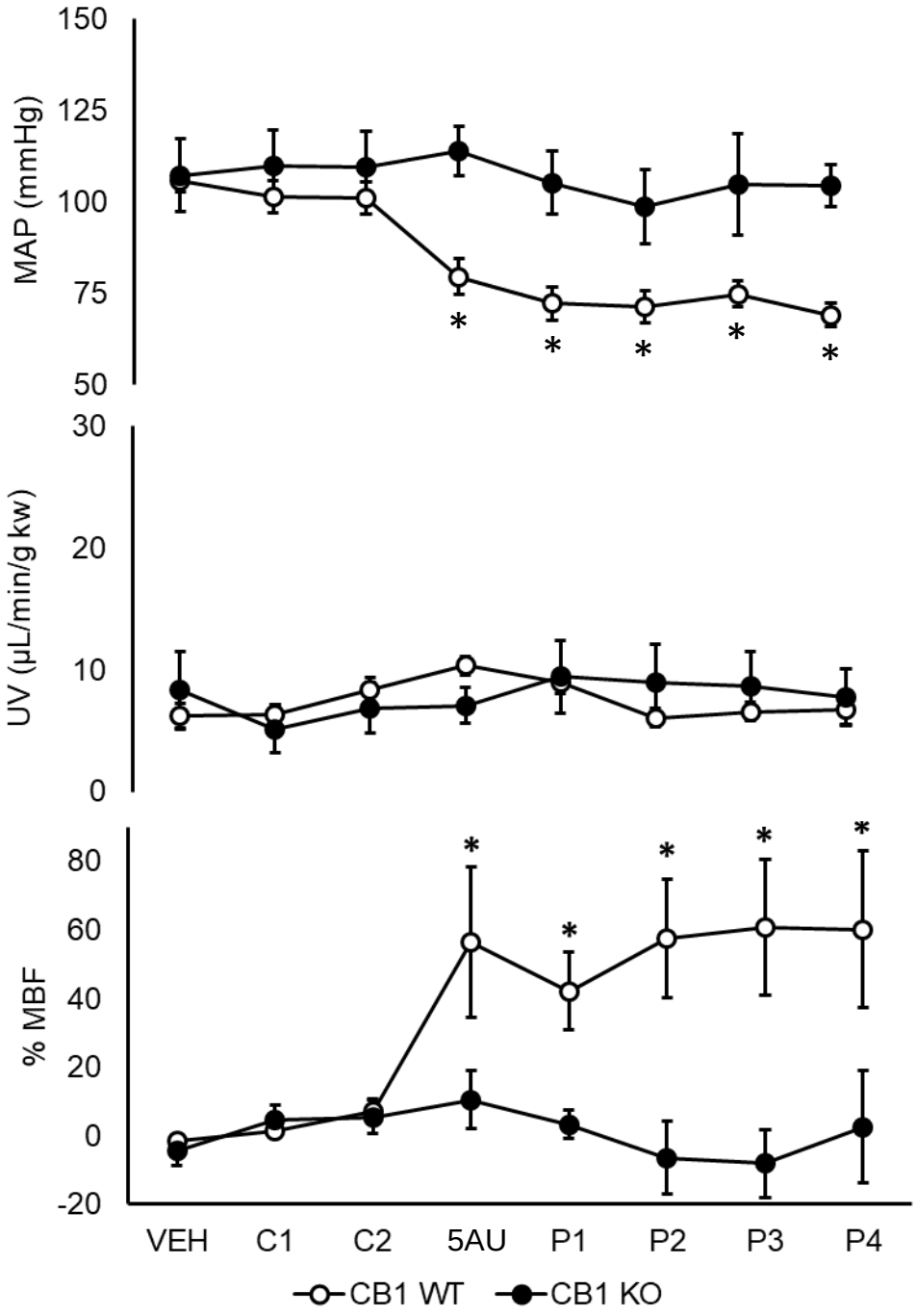

Fig. 18 Effects of an intraperitoneal (i.p.) injection of PIP (5AU) on the mean arterial pressure (MAP) and urine excretion rate (UV) in CB1 WT and CB1 KO mice. VEH indicates i.p. administration of VEH. C1-C2 indicate baseline control phases. 5AU indicates a 10-minute period, at the beginning of which the animals received a PIP i.p. injection. P1-P3 are post-treatment control phases. Each data point represents the mean of a 10 min period. *indicates a significant difference vs. the C1 group ($p<0.05$, two-way ANOVA with Dunnett's post-hoc tests); (n = 5 in both groups).

Interaction of PF-3845-induced product with cannabinoid receptors type 1 (CB1)

As shown in Fig. 19A, a known cannabinoid receptor 1 agonist, CP 55,940 successfully displaced in a concentration-dependent manner [^{3}H]-SR141716 specifically bound to CB1 receptors in human CB1-CHO cell membranes. The concentration response curve for CP 55,940 gave a K_i value of 6.17 (± 3.6). Similarly, as displayed in Fig. 19B, the PF-3845-induced product displayed an affinity for CB1 receptors in a concentration-dependent manner. However, the concentrations utilized in this study were approximate (area under the curve units), so we were unable to calculate IC50 and K_i for PIP and compare it to other known CB1 agonists. Nevertheless, the lipid fraction was able to displace approximately 80% of bound rimonabant, exhibiting competition and selectivity for binding to this cannabinoid receptor subtype.

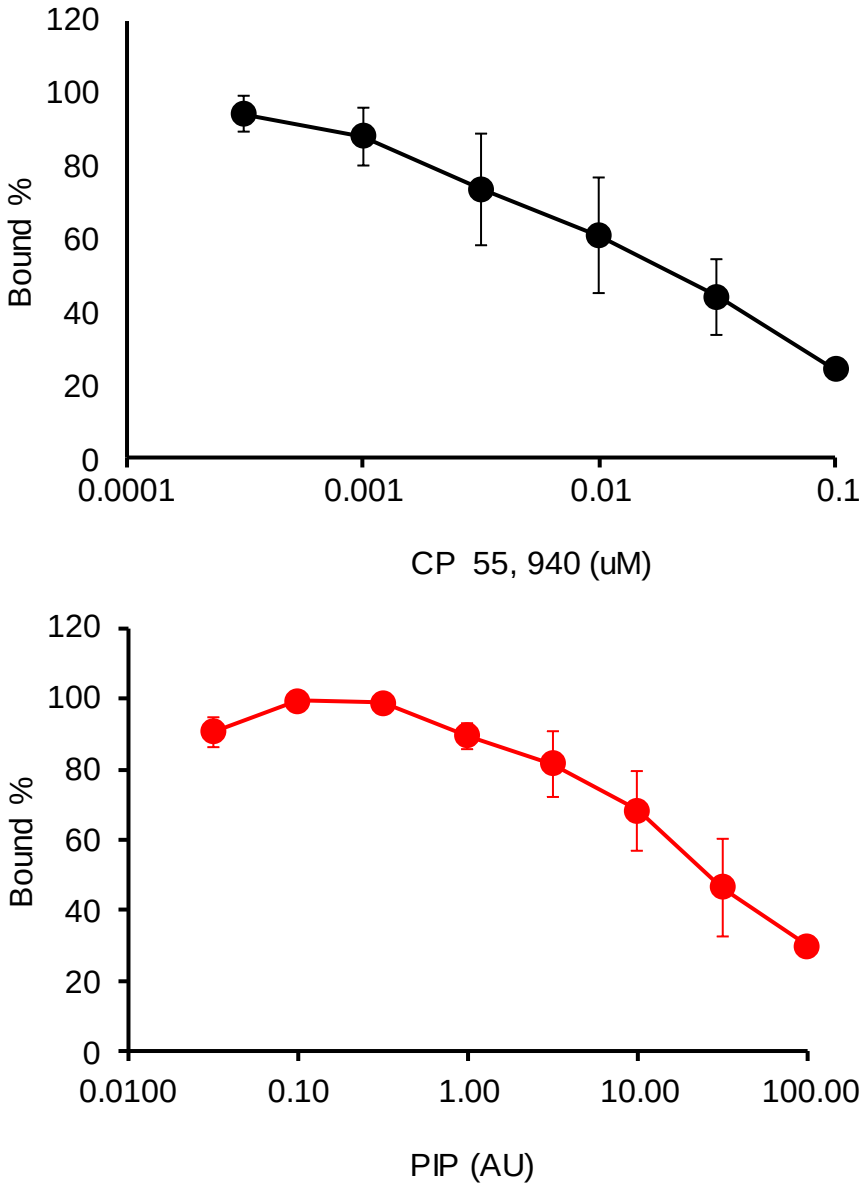

Fig. 19 Inhibition of [^{3}H] SR141716 binding to human CB1-CHO cells by (A) CP 55,940 and (B) PIP. Binding assays are carried out at 30° using as described in Methods using 0.5 nM [^{3}H] SR141716 and increasing concentrations of CP 55,940 and PIP. Data are averaged between 4 experiments in triplicate and are expressed as percentage of specific binding in the absence of competitor.

4.4 Discussion:

This study aimed to assess the mechanistic relationship between a previously described lipid fraction (Daneva et al., 2018), isolated from the medium of cultured mouse medullary interstitial cells and the endogenous cannabinoid receptor type 1. In order to do this we approached the issue in three different methodological ways: [1] *in vivo* acute renal function response to intramedullary infusion of PIP after an i.p. pre-treatment with a CB1 selective antagonist, rimonabant; [2] *in vivo* acute renal function response to intramedullary infusion or intraperitoneal injection of PIP in CB1 WT and CB1 KO mice; and [3] *in vitro* radioactive competition binding assays for CB1 receptors in human CB1-CHO cells. The HPLC-purified product, used in anesthetized, normotensive mice revealed a dependence on CB1 receptors for the mediation of its vasodepressor and diuretic properties. The marked difference in biological effects of the product, observed after intramedullary and intraperitoneal routes of administration, suggests an important role for liver metabolism as a determinant of PIP's biologic actions. Our results from the competition binding study showed that PIP is able to displace a selective CB1 antagonist [3H] SR141716-A in a concentration-dependent manner. These data support a potential role for CB1 receptors, acting both in renal and extra-renal systems to regulate blood pressure.

Intramedullary infusion of 1 AU PF-3845-induced product in C57BL6J mice, pretreated with rimonabant (a selective CB1 inverse agonist), did not show any changes in blood pressure and urine excretion. Previously, we showed that intramedullary or intravenous infusion of 1 AUs of PIP is a sufficient concentration that elicits a significantly elevated urine excretion and decreases blood pressure (Daneva et al., 2018). In the current study we showed that when

CB1 receptors are blocked with a selective antagonist (also inverse agonist) the diuretic and pressure-lowering properties of PIP are completely abolished. The concept that CB1 mediated urine excretion is involved in the regulation of blood pressure is not novel. Ahmad et al. (2018) demonstrated that inhibition of FAAH by a selective inhibitor in mice drops pressure and increases UV and U_{Na} (Ahmad et al., 2018). The group also reported that these three effects are diminished when subjects were pre-treated with rimonabant. However, publications by the same group report that intramedullary administration of AEA in anesthetized mice does not lower pressure, but only causes diuresis (Ritter et al., 2012; Ahmad et al., 2018). Thus, it has become clear that AEA may not be the only vasodepressor acting via CB1 receptors in the kidneys. Rather, it appears that another compound, possibly PIP that expresses a similar pharmacological profile (binding to CB1 receptors and metabolism by FAAH) to AEA may be responsible for the vasodepressor and diuretic activity of endocannabinoids in the renal system.

A very interesting result that we saw when we treated mice with Rimonabant (i.p.) and then with an intramedullary infusion of PIP was that rimonabant alone elicited a bigger change in medullary blood flow than when combined with PIP. Since rimonabant was able to inhibit the diuretic and vasopressor activity of PIP, when locally infused in the medulla, it was of no surprise that it prevented MBF from increasing (Fig. 16). However, rimonabant appeared to be sufficient to stimulate medullary blood flow without stimulating diuresis. Previous studies from our lab reveal that renal infusion of anandamide in rats had no effect on renal blood flow (Ritter et al., 2012). Moreover, Li & Wang demonstrated that meth-anandamide increases diuresis without accompanying natriuresis and an increase in medullary blood flow (Li and Wang, 2006). One explanation for the peculiar rimonabant-induced elevation of MBF would be that CB1 receptors are normally in a tonic state of activation. When the receptors are inhibited, all ligands

binding to them, to activate or antagonize them, become available for acting on other targets. Due to this imbalance of normal physiological activity, it is possible that a different, masked mechanism, becomes activated and increases MBF without elevating urine excretion or dropping blood pressure. This complex interaction might also explain why when PIP and rimonabant are co-administered, rimonabant's inhibitory action on MBF is impeded by PIP's enhancement of MBF through a CB1-independent pathway. Thus, it is possible that the lipid fraction's stimulation of MBF is independent of CB1 activity. Nevertheless, the endocannabinoid receptor appears to be involved in the regulation of medullary blood flood. More data is needed to elucidate its exact relation to MBF regulation.

Our findings that antagonism of the CB1 receptors blocks the vasodepressor and hemodynamic properties of the PF-3845-induced product were additionally confirmed by another in vivo assay. We utilized normotensive CB1 wildtype and knockout genetic mutant mice, which we treated with PIP - either 1AU intramedullary infusion or 5AU intraperitoneal injection in an acute renal function model. Fig. 17 (first panel) demonstrates that intramedullary treatment with a single dose of PIP in CB1 WT mice was able to drop blood pressure by the end of the experiment. This finding is in congruence with previous reports from our laboratory (Daneva et al., 2018). In addition, when CB1 WT mice were administered 5 AUs PIP, intraperitoneally, MAP dropped and remained low for the duration of the experiment. As before, this effect has previously been observed in C57BL6J mice under the same experimental conditions (Daneva et al., 2018). An intraperitoneally-induced reduction in pressure is consistent with the possibility that PIP requires fist pass metabolism in order to become a more potent vasodilator (see Fig. 18) (Daneva et al., 2018). Nevertheless, the current study demonstrated that in both acute renal function experiments, pharmacological ablation of CB1 receptors prevents

PIP from decreasing blood pressure, a finding that implicated the receptors as mediators of blood pressure regulation. While the idea that CB1 receptors control, at least partially, blood pressure via the renal system is not novel, our discovery, that an unidentified PF-3845-induced lipid requires CB1 activity to elicit vasodepression via the kidneys and possibly directly via blood vessels, presents a new perspective of how the receptors mediate pressure modulation (Deutsch and Chin, 1993; Koura et al., 2004).

Genetic blockade of CB1 receptors altered the response of urine excretion to the PF-3845-induced product when the compound was administered in the form of an intramedullary infusion. While no other group has studied PIP's diuretic mediatory pathways, there have been reports suggesting that antagonism of CB1 receptors with rimonabant, AM281 and AM251 successfully blocked cannabinoid-mediated urine excretion in animal models (Koura et al., 2004; Chopda et al., 2013). Controversially, Li and Wang claim that rimonabant could block the diuretic activity by meth-anandamide only partially, posing that TRPV1 receptors may be contributing to cannabinoid-based urine production (Li and Wang, 2006). However, in our experiments, we have generated reproducible data, arguing that PIP requires CB1 receptors in order to elicit diuresis. In support of our findings, Ahmad et al. demonstrated that inhibition of PIP's stimulatory enzyme FAAH produced diuresis, which can also be completely abolished by rimonabant (Ahmad et al., 2018).

In our genetic models for renal function, we demonstrated that intraperitoneal administration of PIP did not produce diuretic effects in CB1 WT and KO mice, but significantly elevated MBF in the former subject group. We previously demonstrated that when the lipid fraction is given as a bolus injection into the abdominal region of anesthetized C57BL6J mice, it successfully decreased blood pressure without elevating urine excretion and increased MBF

(Daneva et al., 2018). These results suggested that the changes in MBF, caused by the PF-3845-induced product, are elicited by a physiological system that is independent from the one, responsible for the observed diuretic effect after intramedullary and intravenous infusions (Daneva et al., 2018). Thus, stimulation of MBF after intraperitoneal administration may be due to actions of PIP directly on vasa recta, or other vascular beds, and not be related to tubular reabsorption modulation. While the CB1 WT data are consistent with these earlier observations, our CB1 KO data offer a new insight into the cellular mechanism of PIP's actions. Genetic blockade of the CB1 receptors completely blocked the rise in medullary blood flow. This is an interesting finding, because it implies that PIP mediates an increase in medullary blood flow via a CB1-dependent mechanistic pathway. Furthermore, it appears that this medullary blood flow stimulation does not hold a causal relationship to PIP's ability to stimulate diuresis (Daneva et al., 2018). Others have found that binding of endocannabinoids to CB1 receptors in the kidney promoted renal blood flow and glomerular filtration rate (Koura et al., 2004). It is also known that increases of renal blood flow are parallel to increases of medullary blood flow (Roman). It is possible that when PIP undergoes first pass metabolism, it becomes a stimulant for renal blood flow and medullary blood flow, but it loses its tubular diuretic abilities. However, more studies need to be conducted in order for this modality of actions to be clarified.

After we observed the in vivo dependence of the PF-3845-induced product on the cannabinoid receptors type 1 for the modulation of blood pressure, diuresis and medullary blood flow, we also examined if PIP was able to competitively bind to CB1 receptors in a well-established human CB1-CHO cell line (Paugh et al., 2006; Eldeeb et al., 2016). As shown in Fig. 19 (first panel), CP 55,940, a full agonist at CB1 and CB2 receptors, successfully displaced [^{3}H] SR141716A in CB1 expressing human CHO cells during a radioactive competition binding

assay. The concentration-response curve for CP 55,940 gave a K_i value (affinity for binding) of 6.17 µM (± 3.6) for the displacement of [3H] SR141716A. Others have found similar K_i values for CP 55,940's ability to compete for binding with rimonabant in CB1-CHO cells (Rinaldi-Carmona et al., 1998). Interestingly, we discovered that PIP also displays an affinity for binding to CB1 receptors in these cell line. Due to the unknown structure of the compound, thus molecular weight, we were unable to calculate the exact affinity (K_i) to the cannabinoid receptor. Nevertheless, we did see that PIP was able to displace approximately 80 % of rimonabant in this assay. Our finding suggests that it is possible for PIP to be mediating its vasodepressor, diuretic and MBF altering effects via a CB1-mediated pathway within and outside of the kidney. More experiments need to be conducted to determine if CB1 receptors are the sole mediator of the PF-3845-induced product's properties or other receptors, such as CB2 or TRPV1 are also involved.

In conclusion, this study focused on the elucidation of the mechanistic pathways of a PF-3845-induced product, previously characterized as a vasodepressor, diuretic and natriuretic by our group (Daneva et al., 2018). Here, we presented that global pharmacological or genetic ablation of CB1 receptors leads to diminished vasodepressor and diuretics effects of PIP, but does not prevent MBF from rising. Moreover, we observed that PIP was able to compete against [3H] SR141716A for binding to CB1 receptors in an in vitro assay using hCB1-CHO cells. Thus, we used three different methods to examine the importance of the cannabinoid type 1 receptors to the activity of PIP in the kidney. More studies need to be conducted before it can be concluded that the CB1 receptors are the main mediator of PIP's activities, but the data presented here give a glimpse into the picture.

Chapter 5 - Evidence that PIP mediates its diuretic activity via the proximal convoluted tubules of the kidney

5.1 Introduction:

The kidney is an important organ for the regulation of blood pressure through its activity on fluid volume and, therefore, water balance, electrolyte balance, acid-base balance, and excretion of uremic toxins (Tojo and Kinugasa, 2012). It is also known to excrete various hormones, such as renin, erythropoietin and activate Vitamin D_3 that assist with its primary homeostatic functions. The kidney is the principal organ that maintains the concentration and composition of extracellular fluid (ECF) by executing its excretory, metabolic and endocrine functions. Most of these functions occur in the proximal convoluted tubule (Curthoys and Moe, 2014). However, in order for the kidney to fully implement its control over fluid regulation, it requires a healthy contribution of the actions of all renal tubules, including proximal convoluted tubules (PCTs), thin descending and thick ascending loop of Henle (TDL and MTAL, respectively), distal convoluted tubules (DCTs) and collecting ducts (CDs).

Recently, members of the endocannabinoid system have been implicated as an essential component of the regulatory functioning of the renal system. The cannabinoid receptors type 1 (CB1) have been identified in human kidney as functional and widely spread in different regions of the organ (Shire et al., 1995; Barutta et al., 2010; Larrinaga et al., 2010). Some of these areas include diverse parts of the nephron: afferent and efferent arterioles, glomeruli, tubules, proximal convoluted tubules, loop of Henle, distal convoluted tubules and collecting ducts, and mesangial

cells (Koura et al., 2004; Janiak et al., 2007; Barutta et al., 2010; Jenkin et al., 2010; Larrinaga et al., 2010; Lim et al., 2010; Lim and Park, 2012; Nam et al., 2012; Tam et al., 2012; Silva et al., 2013; Jourdan et al., 2014; Sampaio et al., 2014; Lecru et al., 2015). So far, in humans, CB1 receptors have been reported to be selectively expressed in only a few tubular segments, namely, proximal convoluted tubules, distal convoluted tubules and the intercalated cells of collecting duct (Jenkin et al., 2010; Larrinaga et al., 2010; Sampaio et al., 2014; Lecru et al., 2015). The varying localization of the endocannabinoid receptors type 1 suggests that the receptors may be playing differential roles within each tubular segment in order to modulate water and sodium reabsorption.

To attest to the involvement of CB1 receptors in the regulation of tubular water reabsorption, studies have shown that CB1's primary endocannabinoid ligand, anandamide (AEA, also known as *N*-arachidonoylethanolamine) and other, exogenous cannabinoids, act in the kidney in order to produce diuresis and natriuresis in anesthetized and wake rodents (Ritter et al., 2012; Chopda et al., 2013). Moreover, anandamide and its metabolizing enzyme, fatty acid acyl hydrolase or FAAH, are enriched in the renal system, but not much is known about the localization of AEA's metabolism and activity within the kidney (Ritter et al., 2016). Regional distribution assessment of anandamide concentration in the kidney demonstrated that its concentration is higher in the renal medulla in comparison to the renal cortex (Ritter et al., 2012). High anandamide levels in the medulla could be explained due to low medullary expression of its main metabolizing enzyme, FAAH, which would allow for accumulation of the endocannabinoid in this region (Ritter et al., 2012). Experiments conducted in our lab further this idea by demonstrating an elevation in AEA after *in vivo* intramedullary treatment with a selective FAAH inhibitor, PF-3845 in mice (Ahmad et al., 2017a). The tissue-specific localization and

rising levels during treatment with the selective FAAH inhibitor suggest that anandamide may play a specific role within the kidney, and possibly in the renal medulla.

Studies focused on the tubular actions of AEA and other cannabinoids reveal a certain differentiation of activity within tubular segments of the kidney. Silva and Garcia (Silva et al., 2013) showed that in rat medullary thick ascending limb suspension, AEA inhibited sodium transport through stimulation of nitric oxide (NO) synthesis that inhibited the activity of the apical Na^+/H^+ pump and the basolateral Na^+/K^+ ATPase. Moreover, the non-selective CB1/CB2 agonist, WIN 55,212-2, and the CB1 peptide agonist, hemopressin, were demonstrated to be able to modulate the functioning of the basolateral Na^+/K^+ ATPase in proximal convoluted tubules (Sampaio et al., 2014). The study found that WIN 55,212-2 stimulated Na^+/K^+ ATPase via a PKC-dependent pathway, while hemopressin elevated the activity of cAMP and, thus, PKA (Sampaio et al., 2014). These data are consistent with reports of cannabinoids being able to modulate Na^+/K^+ ATPases in the synaptosome (Araya et al., 2007). However, it is interesting that CB1 agonists, such as WIN 55,212-2 can stimulate sodium reabsorption through stimulation of Na^+/K^+ ATPase-mediated activity, while every *in vivo* study shows that CB1 agonists produce diuresis (Paronis et al., 2013; Ritter et al., 2016; Ahmad et al., 2018). However, to this date, there is no conclusive explanation for the exact location of CB1 activity that leads to the commonly observed diuresis, natriuresis and kaliuresis after *in vivo* treatment with endo- or exo-cannabinoids.

In this study we focused on elucidating the tubular mechanism of a novel lipid product, enhanced in mouse medullary interstitial cells medium after treatment with a selective FAAH inhibitor, PF-3845 (Daneva et al., 2018). After purification with HPLC, we tested the extract on acute renal function in anesthetized normotensive mice and saw that it was able to drop pressure

and produce significant diuresis and natriuresis (Daneva et al., 2018). The PF-3845 induced product, PIP, showed a modality of biological activity after intraperitoneal administration in comparison to other administration routes, suggesting a role of liver metabolism for its functioning (Daneva et al., 2018). While the structure of the substance responsible for the biologic activities in the PIP fraction has not yet been identified, the finding that its concentration in MMIC culture medium increased by PF-3845 treatment and that its diuretic and natriuretic activities were attenuated in FAAH KO mice suggest a relationship to anandamide or other fatty acid ethanolamides or amides. Furthermore, we discovered that PIP elicits its vasodepressor and diuretic activities via a CB1-mediated mechanism (see Chapter 4). Here, we investigated the *in vivo* diuretic effects of PIP, after administration of known diuretics, amiloride, furosemide, hydrochlorothiazide and the ouabain (a less utilized diuretic compound) in order to determine the exact tubular location of the lipid fraction's water and salt reabsorption. We selected tubular targets that, according to previous findings, express CB1 receptors in the human renal tubules (Jenkin et al., 2010; Larrinaga et al., 2010; Sampaio et al., 2014; Lecru et al., 2015). While we offer some new insights into a possible target for PIP, a more thorough study should be conducted to offer a comprehensive analysis of this interaction.

5.2 Methods:

Reagents

HPLC purification of PF-3845-inducible MMIC product, PIP, was performed following a previously published extraction protocol from our laboratory (Daneva et al., 2018). Amiloride,

furosemide and hydrochlorothiazide were obtained from ApexBio, Houston, TX. Ouabain was obtained from Calbiochem-Behring, La Jolta, CA.

Animals

Male and female C57BL/6J mice (Jackson Laboratory, Bar Harbor, ME) (2-5 months old) were used in the present study. The mice in this study weighed 20-35 grams and were housed 4-5 per cage in a temperature (20-22°C) and humidity (50-55%)-controlled environment with a 12 hr light/dark cycle with free access to food and water. All experiments involving animals in this study were approved by the Institutional Animal Care and Use Committee of Virginia Commonwealth University in accordance with the National Institutes of Health Guide for the Care and Use of Laboratory Animals.

Surgical Preparation for acute renal functional model

Mice were anesthetized and prepared surgically for the acute renal function testing procedure as described previously (Zou et al., 2001; Li et al., 2005). Anesthesia was induced with ketamine (Ketathesia™, Harry Schein Animal Health, Dublin, OH) (100 mg/kg, i.p.) and thiobutabarbital (Inactin™, Sigma Chemical Co., St. Louis, MO, 75 mg/kg, i.p.). The abdominal and neck areas were shaved, and the mice were placed on a thermostatically-controlled warming table to maintain body temperature at 37°C. A tracheotomy was performed by inserting a 2 cm length of polyethylene PE-60 tubing to maintain a patent airway during surgery. After tracheotomy, a catheter prepared from heated and pulled plastic PE-10 tubing and filled with heparin sodium dissolved in saline (Fisher BioReagents, 0.005 mg/mL, 50 IU/mL) was inserted

into the left carotid artery and attached to a pressure transducer connected to a data acquisition system (Windaq, DATAQ Instruments, Akron, OH). The right jugular vein was catheterized with a catheter prepared from PE-10 tubing for the infusion of 0.9% saline. The rate of intravenous infusion was 1 mL/h/100 g body wt to maintain fluid volume and hematocrit concentration throughout the experiment. For the acute renal function experiments, an incision was performed following the midline of the abdominal area. The left ureter was ligated with a surgical suture and cut on the kidney side of the ligation to allow produced urine to exit freely into the abdominal cavity. The urethra was ligated in proximity to the bladder, and the latter was catheterized with a 2.5 cm cut length of PE-50 tubing for the collection of urine at timed intervals. The right kidney was elevated on a piece of sterilized gauze and a pulled PE-10 catheter was implanted to 2.5 mm in depth vertically from the dorsal surface into the outer medulla. The catheter was immobilized to the kidney capsule using a cyanoacrylate tissue adhesive (Vetbond, 3M Animal Care Products, St. Paul, MN). All mice received a 1 hour equilibration period, during which the animals received continuous vehicle infusions: 1) intravenous infusion of filter-sterilized 0.9% NaCl at a rate of 1 mL/hr/ 100 g body weight, 2) intramedullary infusion with PBS containing (in mM) 205 NaCl, 40.5 Na_2HPO_4, and 9.5 NaH_2PO_4 (pH 7.4, 550 mOsm) at a rate of 2 μL/min to maintain the patency of interstitial infusion (Zhu et al., 2011). The urine excretion rate (UV) was measured gravimetrically, and the sodium and potassium concentrations in urine were measured using flame photometry. UV and the urinary sodium and potassium excretion rates (U_{Na} and U_K, respectively) were factored per gram of kidney weight. At the end of each experiment, the animals were euthanized by exsanguination from the carotid artery catheter for collection of plasma. The placements of the

intramedullary catheter in the outer medulla was routinely confirmed by post-mortem kidney dissection following the experiments.

Experimental Protocols for Renal function studies

After a 1-hour equilibration period and three sequential 10-min pretreatment control sample collection periods (C1-3), all animals received a continuous intramedullary infusion with one of the following diuretics: amiloride (0.2 μg/min/g), furosemide (0.133 μg/min/g), hydrochlorothiazide (50 ng/min/g) and ouabain (6.5 ng/min/g). The concentrations of amiloride and furosemide were in congruence with reports from previous experiments (Li et al., 2012; Liu et al., 2015). Appropriate concentrations of chlorothiazide and ouabain were established by testing a dose response curve of incrementally increasing concentrations of either diuretic, until maximum in vivo diuresis was achieved (data not shown) (Doucet and Katz, 1982; Lingrel et al., 1997; Lorenz et al., 2006; Wu et al., 2015). Each diuretic was infused from this point until the end of the experiment (70 minutes altogether). After three 10-minute infusion periods with each diuretic, 1AU of PIP was co-infused for 10 minutes, followed by three 10-minute periods of diuretic drug infusion alone. The aim of the design was to establish the presence or absence of an additive effect of PIP to the diuretic activity caused by a well-established diuretic.

Medullary Blood Flow (MBF)

For the measurement of MBF, a laser Doppler flow probe (OxyFlo Pro; MNP 100XP; Oxford Optronix, Oxford, United Kingdom) was stabilized on the ventromediolateral surface of the right kidney to measure continuously the MBF (as previously reported in (Ahmad et al.,

2017a; Ahmad et al., 2018). The recording of the blood flow was measured by using a dual-channel laser-Doppler flowmeter (Transonic Systems Inc., Ithaca, NY).

Statistical Analysis

Data are presented as the mean ± S.E.M. For comparison between multiple groups of data, one- or two-way analysis of variance (ANOVA) was applied using Tukey or Dunnett's post-hoc test when significant differences were found. A p-value ≤ 0.05 was considered statistically significant.

5.3 Results:

Effect of intramedullary infusion of PF-3845-induced fraction in the presence of amiloride in an acute renal functional model using C57BL6J mice

To determine if PIP elicits its diuretic activity via collecting duct principal cells, by inhibition of the epithelial sodium channel (ENaC), we infused the ENaC inhibitor amiloride into the renal medulla of anesthetized mice in a renal function assay. This was followed by a co-administration of PIP (1AU) with amiloride (0.2 μg/min/g). As a control we also had a group of mice that received a continuous infusion of amiloride, without co-administration of PIP. Fig. 20 presents the effects on mean arterial pressure (MAP), urine excretion (UV) and medullary blood flow (% MBF) of a co-infusion of amiloride with PIP into the medulla of the kidney. An intramedullary infusion of amiloride (0.2 μg/min/g) was administered to subjects for 30 minutes (A1 to A3) before P2 (1AU) was co-administered. During this phase, amiloride did not affect MAP, which remained similar to its baseline at C1 and C2 (105 and 106 mm Hgs, respectively).

Treatment with amiloride was able to significantly elevate UV to 27 μL/min/g kwt at A2 and A3 from baseline values C1 and C2 (13 and 14 μL/min/g kwt). However, UV stabilized at approximately 27 μL/min/g kwt after the second infusion with the diuretic. When 1 AU of PIP was co-administered with amiloride as a 10-minute intramedullary infusion, PIP was able to further increase urine production. Our data showed that UV rose from 27 μL/min/g kwt to 42 and 41 μL/min/g kwt at PIP and A4 phases of the experiment. By phase A6 (or 40 minutes after PIP's initial infusion), UV was still significantly higher than UV in the mouse group not treated with PIP (at 39 mm Hgs). The percentage medullary blood flow in both subjects group increased significantly with more than 20 % elevation when compared to baseline. However, we did not see a significant difference between the control group and the PIP-treated group throughout the experiment. Neither did we observe a significant difference before and after administration of PIP. However, there was a visible pattern of an elevation in % MBF after co-infusion of amiloride and PIP. MBF increased from 19 to approximately 34.

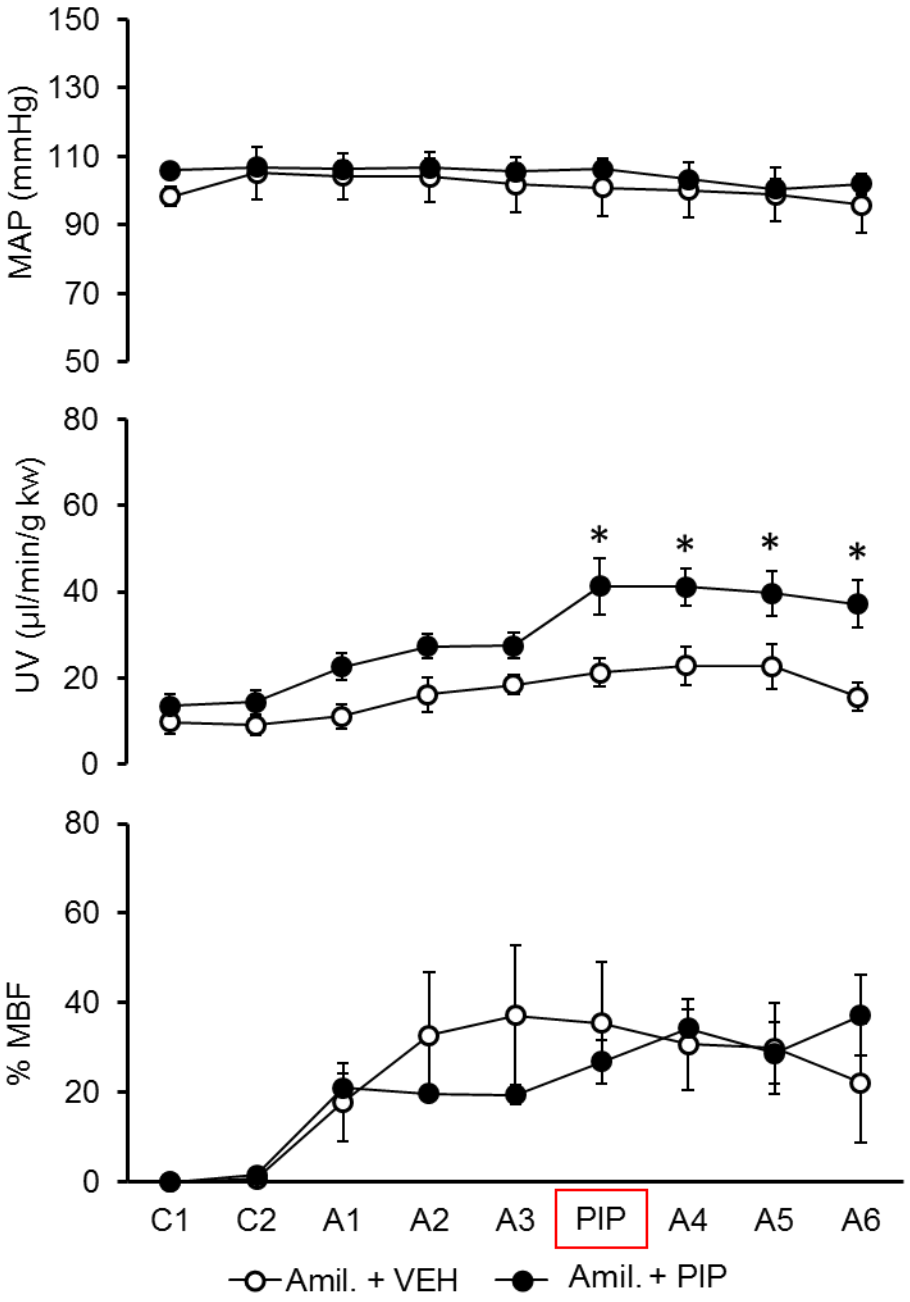

Fig. 20 The effects of an intramedullary (i.m.) co-infusion of PIP (1AU) in the presence of amiloride on the mean arterial pressure (MAP) and urine excretion rate (UV) and percentage medullary blood flow (% MBF). VEH indicates intramedullary infusion of amiloride with no PIP. C1-C2 indicate baseline control phases. A1-A6 indicate six 10-minute periods of continuous intramedullary infusion of amiloride (0.2 µg/min/g). PIP indicates a 10-minute intramedullary co-infusion of 1AU of PIP with amiloride. *indicates a significant difference of Amil. + PIP vs. the A1 period ($p<0.05$, two-way ANOVA with Dunnett's post-hoc tests); (n = 5 Amil. +VEH; n=6 Amil. + PIP).

Effect of intramedullary infusion of PF-3845-induced fraction in the presence of furosemide in an acute renal functional model using C57BL6J mice

To determine if PIP elicits its diuretic activity via the thick ascending limb of the loop of Henle, by inhibition of the $Na^+/K^+/2Cl^-$ - cotransporter (NKCC2), we infused the NKCC2 inhibitor furosemide into the renal medulla of anesthetized mice in a renal function assay. This was followed by a co-administration of PIP (1AU) with furosemide (0.133 μg/min/g). As a control we also had a group of mice that received a continuous infusion of furosemide, without co-administration of PIP. Fig. 21 presents the effects on mean arterial pressure (MAP), urine excretion (UV) and medullary blood flow (% MBF) of a co-infusion of furosemide with PIP into the medulla of the kidney. In both groups mean arterial pressure remained stable throughout the experiment. UV was elevated in both groups when furosemide (0.133 μg/min/g) was administered to the subjects with a rise of approximately 23 μL/min/g from baseline. After 1AU of PIP was co-infused with furosemide, on average UV increased with another 27 μL/min/g and remained elevated (around 34 μL/min/g) until the end of the test. Interestingly, medullary blood flow was significantly elevated (approximately 29 %) from baseline in the control group, treated only with furosemide. This result is not congruent to data, previously published by some groups (Mattson, 2003), however, other groups accommodate our finding by discovering that in human patients, furosemide improves oxygenation in the cortex and medulla by enhancing cortical and medullary blood flow (Lant, 1981; Spitalewitz et al., 1982; Vakilzadeh et al., 2015). Nevertheless, in the experimental group, treated with both diuretics, we saw no effect on medullary blood flow.

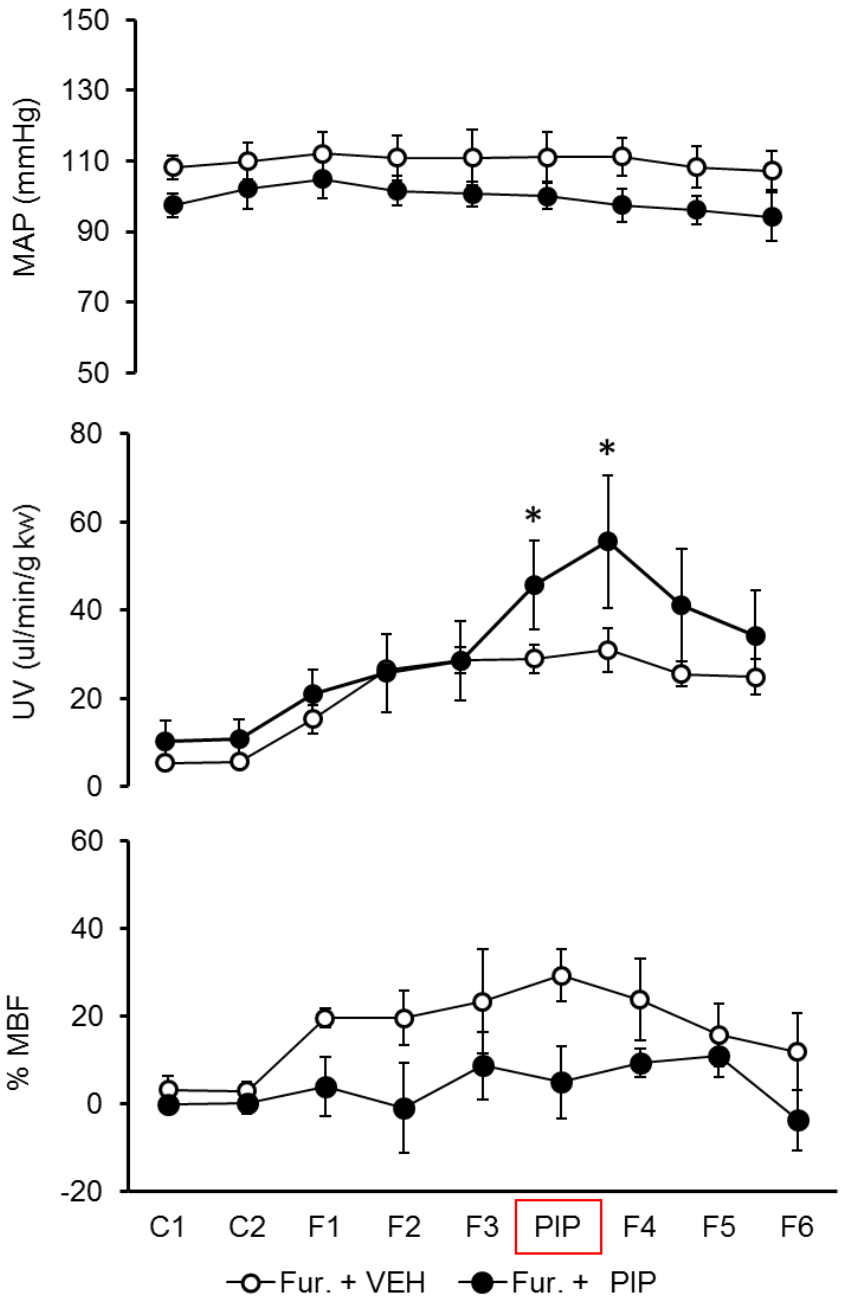

Fig. 21 The effects of an intramedullary (i.m.) co-infusion of PIP (1AU) in the presence of furosemide on the mean arterial pressure (MAP) and urine excretion rate (UV) and percentage medullary blood flow (% MBF). VEH indicates intramedullary infusion of furosemide with no PIP. C1-C2 indicate baseline control phases. F1-F6 indicate six 10-minute periods of continuous intramedullary infusion of furosemide (0.133 μg/min/g). PIP indicates a 10-minute intramedullary co-infusion of 1AU of PIP with furosemide. *indicates a significant difference of Fur. + PIP vs. the F1 period ($p<0.05$, two-way ANOVA with Dunnett's post-hoc tests); (n = 5 Fur. +VEH; n=6 Fur. + PIP).

Effect of intramedullary infusion of PF-3845-induced fraction in the presence of hydrochlorothiazide in an acute renal functional model using C57BL6J mice

To determine if PIP elicits its diuretic activity via the distal convoluted tubular cells, by inhibition of the Na^+/Cl^- - cotransporter (NCC), we infused the NCC inhibitor hydrochlorothiazide (HCT) into the renal medulla of anesthetized mice in a renal function assay. This was followed by a co-administration of PIP (1AU) with hydrochlorothiazide (50 ng/min/g). As a control we also had a group of mice that received a continuous infusion of hydrochlorothiazide, without co-administration of PIP. Fig. 22 presents the effects on mean arterial pressure (MAP), urine excretion (UV) and medullary blood flow (% MBF) of a co-infusion of hydrochlorothiazide with PIP into the medulla of the kidney. In both groups mean arterial pressure remained stable throughout the experiment. The thiazide diuretic caused a clear diuretic effect in both groups, with a moderate UV elevation of approximately 10 μL/min/g in comparison to baseline. Infusion of 1AU of PIP in the presence of thiazide caused a two-fold increase in urine excretion raising the total UV to 30 μL/min/g at H4 and H5 post-treatment phases. UV remained significantly higher to baseline and H1–H3 (hydrochlorothiazide alone) until the end of the experiment. Additionally, medullary blood flow was not affected by hydrochlorothiazide alone, with only a marginal increase of approximately 10% from C1 and C2. However, when PIP was co-administered with the thiazide diuretic, the percentage medullary blood flow was significantly elevated when compared to MBF after treatment with hydrochlorothiazide alone.

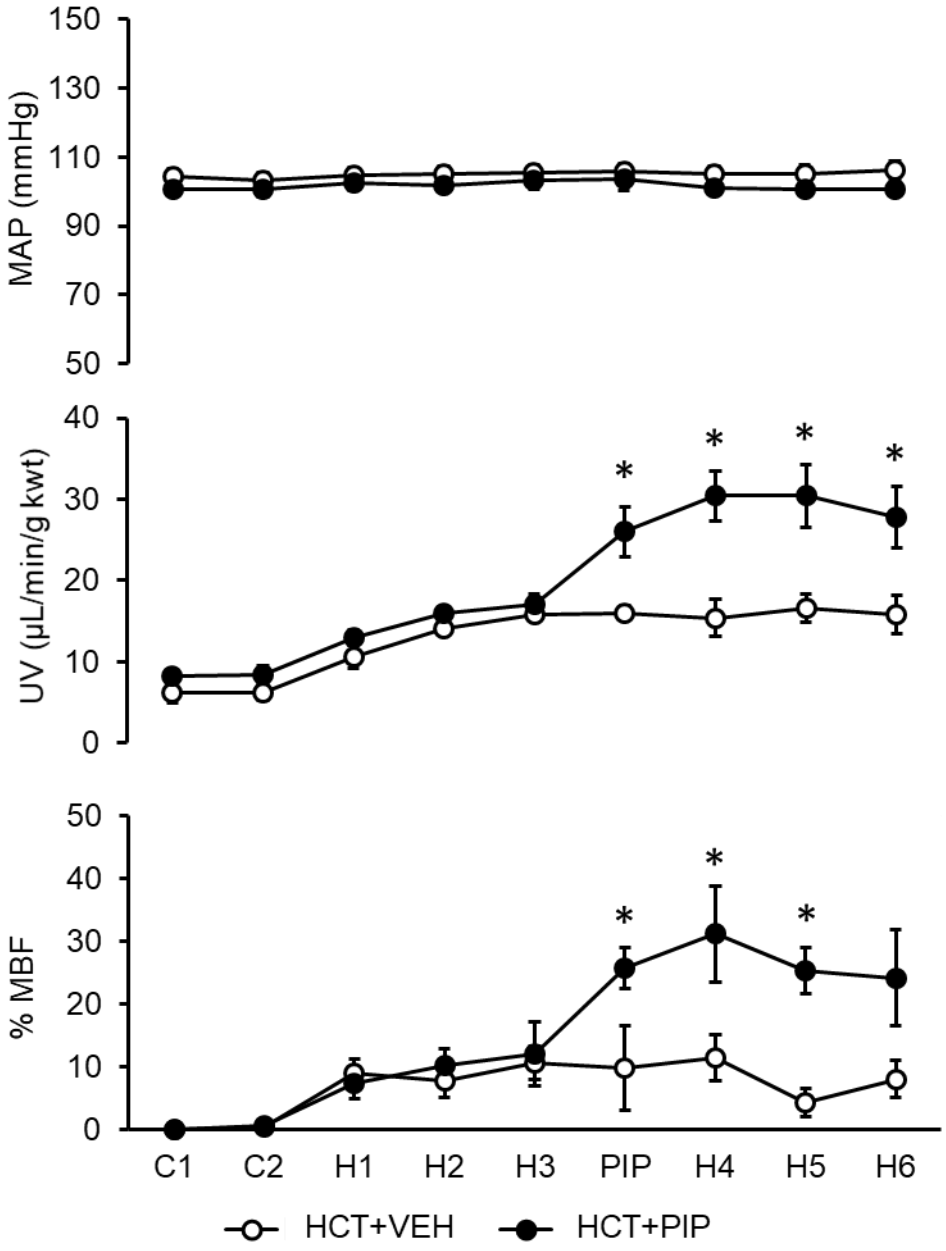

Fig. 22 The effects of an intramedullary (i.m.) co-infusion of PIP (1AU) in the presence of hydrochlorothiazide on the mean arterial pressure (MAP) and urine excretion rate (UV) and percentage medullary blood flow (% MBF). VEH indicates intramedullary infusion of hydrochlorothiazide with no PIP. C1-C2 indicate baseline control phases. F1-F6 indicate six 10-minute periods of continuous intramedullary infusion of hydrochlorothiazide (50 ng/min/g). PIP indicates a 10-minute intramedullary co-infusion of 1AU of PIP with hydrochlorothiazide. *indicates a significant difference of HCT. + PIP vs. the H1 period ($p<0.05$, two-way ANOVA with Dunnett's post-hoc tests); (n = 5 HCT+VEH; n=5 HCT+PIP).

Effect of intramedullary infusion of PF-3845-induced fraction in the presence of ouabain in an acute renal functional model using C57BL6J mice

Finally, to determine if PIP elicits its diuretic activity via the proximal convoluted tubules, by inhibition of the ouabain-sensitive Na^+/K^+ ATPase, we infused the Na^+/K^+ ATPase inhibitor ouabain into the renal medulla of anesthetized mice. This was followed by a co-administration of PIP (1AU) with ouabain (6.5 ng/min/g). As a control we also had a group of mice that received a continuous infusion of ouabain, without co-administration of PIP. Fig. 23 presents the effects on mean arterial pressure (MAP), urine excretion (UV) and medullary blood flow (% MBF) of a co-infusion of ouabain with PIP into the medulla of the kidney. In both groups mean arterial pressure remained stable throughout the experiment (showing only a slight decline from 111 to 106 mmHgs for the duration of the experiment). Ouabain caused a clear diuretic effect in both groups, with a significant UV elevation of approximately 21 μL/min/g in comparison to baseline. Infusion of 1AU of PIP in the presence of ouabain did not produce an increase in urine excretion. UV reached a peak high amount during O3 and PIP phases (41 and 43 μL/min/g, respectively), then began to decline in both groups, revealing a U-shaped curve of activity. Interestingly, % MBF after co-infusion of PIP with ouabain did not rise significantly (only a slight elevation of approximately 10 %). This differs from observations of UV and MBF effects after medullary infusion with 1AU of PIP in naïve mice.

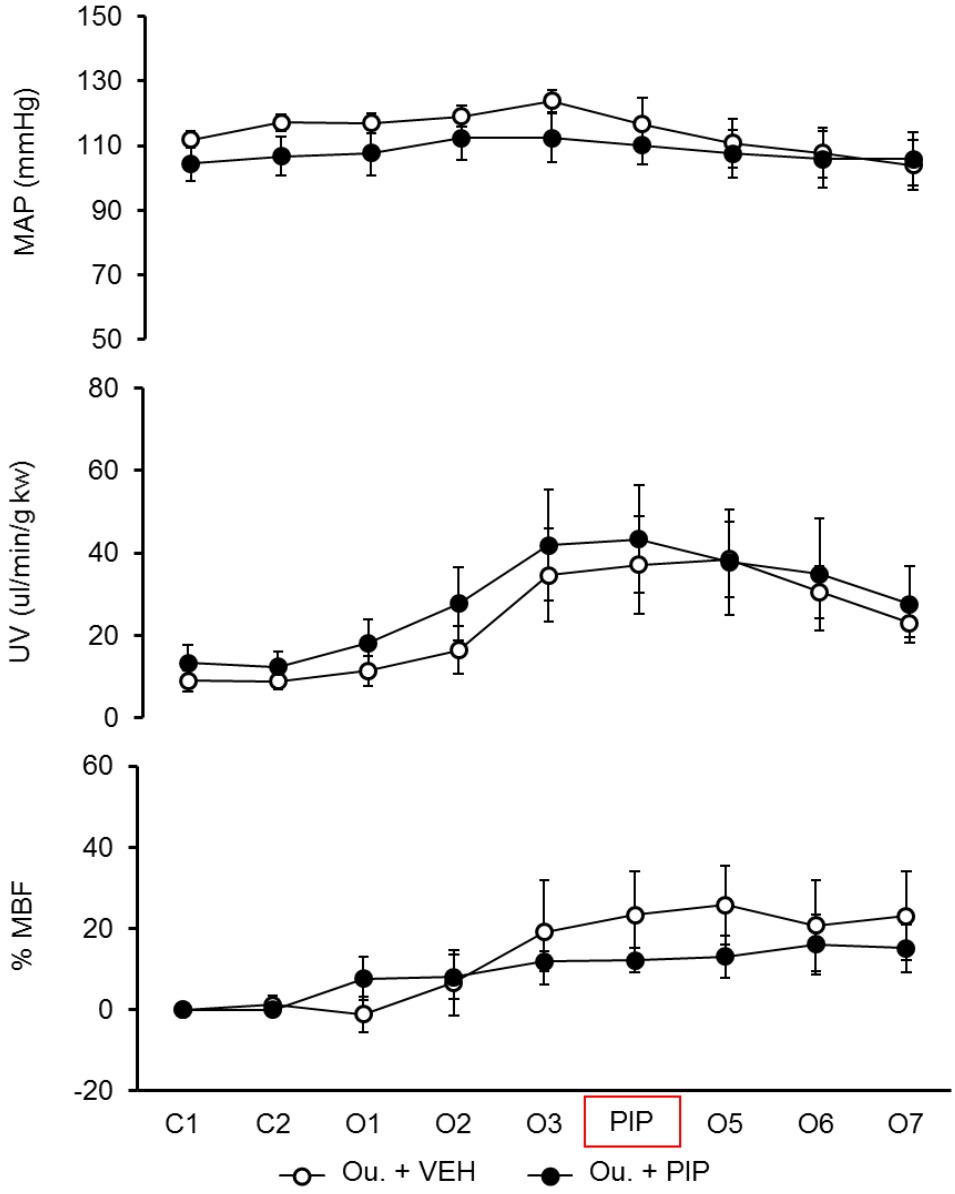

Fig. 23 The effects of an intramedullary (i.m.) co-infusion of PIP (1AU) in the presence of ouabain on the mean arterial pressure (MAP) and urine excretion rate (UV) and percentage medullary blood flow (% MBF). VEH indicates intramedullary infusion of ouabain with no PIP. C1-C2 indicate baseline control phases. O1-O6 indicate six 10-minute periods of continuous intramedullary infusion of ouabain (6.5 ng/min/g). PIP indicates a 10-minute intramedullary co-infusion with 1AU of PIP with ouabain. (n = 5 Ou. +VEH; n=5 Ou. + PIP).

5.4 Discussion:

The present study was designed to test the hypothesis that a novel lipid fraction, produced and excreted by mouse medullary interstitial cells after treatment with PF-3845 (a FAAH inhibitor), elicits its diuretic activity in the kidneys via the proximal convoluted tubules (PTs) of the nephron. We previously showed that the lipid fraction, PIP, has vasodepressor, diuretic and natriuretic activities when administered as an intramedullary or an intravenous infusion in anesthetized mice in a renal function assay (Daneva et al., 2018). Our lab has also demonstrated that both the vasodepressor and the diuretic effects are conducted through a CB1-mediated pathway (see Chapter 4). Now we show that in an *in vivo* acute renal function assay, pharmacological inhibition of the major tubular sodium reabsorption transporters revealed that inactivating the Na^+/K^+ ATPase (NKA) in the proximal convoluted tubules is the only condition for diminishing the diuretic effects of PIP. When we pre-treated mice with chemical agents that inhibited transporters in the loop of Henle, distal convoluted tubules and collecting ducts, PIP remained effective as a diuretic stimulant. This pilot study provided a novel insight into the tubule-cellular mechanism that PIP uses in order to act in the kidney. Furthermore, the experiment poses evidence for the connection between CB1 signaling and diuresis, mediated through the proximal convoluted tubules. Even though we encountered some limitations in the experiments discussed here, the study serves as a stepping stone to guide the research direction needed to be taken in order to elucidate targets of PIP's activity.

In order to localize the tubular target of PIP in the kidney, we applied a pharmacological inhibition of the major transporters, responsible for salt and water, reabsorption. As mentioned in Chapter 1.7, the primary contributor to the sodium and fluid reabsorption in the body is the proximal convoluted tubule, recycling approximately 67% of filtered water, Na^+ and Cl^- (Koeppen

and Stanton, 2013). We selected the a-typical diuretic and cardiotonic steroid, ouabain, to test if a blockade of the Na^+/K^+ ATPase on the basolateral side of the proximal convoluted tubular cells would alter the diuretic effects of an intramedullary infusion of PIP. As depicted in Figure 23 when the membrane enzyme is inhibited, the PF-3845-induced product is unable to elicit its previously observed diuretic effects (Daneva et al., 2018). Moreover, we observed that the shape of the diuretic curve after treatment with ouabain alone or ouabain and PIP follows a U-shaped pattern, consistent with our earlier findings that PIP produced a U-shaped curve of UV (Daneva et al., 2018). Furthermore, other groups have shown that exogenous cannabinoids also exhibit this particular urine excretion pattern in animal models, possibly due to tolerance development (Chopda et al., 2016).

The possibility that PIP induced diuresis via the proximal convoluted tubules becomes more realistic with the discovery that CB1 activation on proximal tubules in the nephron regulates the activity of the Na^+/K^+ ATPase via a complex signaling cascade (Sampaio et al., 2014). According to Sampaio et al., the non-selective CB1/CB2 agonist, WIN 55,212-2, and the CB1 peptide agonist, hemopressin, were demonstrated to modulate the functioning of the basolateral Na^+/K^+ ATPase in proximal convoluted tubules (Sampaio et al., 2014). The study found that WIN 55,212-2 stimulated NKA via a PKC-dependent pathway, while hemopressin elevated the activity of cAMP and, thus, PKA (Sampaio et al., 2014). Even though this report presents a contradictory role of CB1 receptors with regard to NKA, it shows that the involvement of the cannabinoid receptor in the sodium regulation can be affected differentially, depending on the ligand that binds to it. Silva and Garcia have reported that AEA was able to enhance nitric oxide production in rat MTAL cells, and the accumulated NO served as an inhibitor of both apical Na^+/H^+ pumps and the basolateral Na^+/K^+ ATPases (Silva et al., 2013). Although, Silva

and Garcia did not test the effect of NO on sodium reabsorption in PTs, other groups have made a considerable effort to elucidate this issue. Guzman et al. found that endogenous NO/iNOS stimulation by LPS and interferon-gamma decreased the catalytic activity of the ouabain-sensitive Na^+/K^+ ATPase, consistent with the inhibitory effect of NO on NKA (Guzman et al., 1995; Satoh et al., 2017). In addition to its activity on Na^+/K^+ ATPase, NO has also been reported to inhibit the Na^+/H^+ exchanger (NHE3) on the apical side of the proximal tubules (Biemesderfer et al., 1993; Azuma et al., 1996; Roczniak and Burns, 1996; Gill et al., 2002). These findings imply that there exists an intricate regulatory relationship for the reabsorption of Na^+ within the proximal convoluted tubules. It may be possible that PIP, via binding to CB1 receptors, stimulates the synthesis of NO, which inhibits the activity of NKA and/or NHE3 (see Fig. 24). The current assay's design, targeting the ouabain-sensitive NKA in PTs, was not sufficient to determine if NHE3 plays any role in the salt and water reabsorption inhibition in response to PIP treatment. Nevertheless, we demonstrated that when PT sodium transport system is impaired (pharmacologically inhibited), PIP is not able to elicit its activities.

Apart from the evidence in support of a PT-mediated diuretic effect of PIP, we tested three other well-utilized diuretics: [1] furosemide for the inhibition of $Na^+/K^+/2Cl^-$ (NKCC2) symporters on the apical membrane of the loop of Henle; [2] hydrochlorothiazide for the inhibition of the Na^+/Cl^- (NCC) symporters on the apical side of the distal convoluted tubules and [3] amiloride for the inhibition of the epithelial sodium channel (ENaC) on the apical side of collecting ducts (see Figs. 20, 21 and 22)(Koeppen and Stanton, 2013). Our data showed that the diuretic activity of intramedullary-infused PIP was not lost after inhibiting any of the above-mentioned sodium reabsorption transporters. This is an interesting finding as it suggests that the major contributors to fluids regulation in the loop of Henle, distal convoluted tubules and

collecting ducts are not even partially involved in the mediation of diuresis by PIP. In other words, none of the tubules located in proximity (within the renal medulla) to the PIP-secreting renomedullary interstitial cells are responsible for the fraction's diuretic, and possibly natriuretic, activities. Therefore, it may be argued that PIP requires diffusion through the medullary interstitium, all the way to the cortex of the kidney, in order to cause sodium and water excretion. The concept of paracrine signaling from the renal medulla to the cortex is not a novel one. Haas et al. has demonstrated that the proximal convoluted tubular reabsorption of sodium is inhibited directly by paracrine signaling originating from the renal medulla (Haas et al., 1986).

Another interesting finding that we observed in the current study was that blood pressure was not decreased by PIP in any of the four diuretic conditions. In the past, we have reported that mean arterial pressure gets reduced after both an intramedullary and intravenous infusion of PIP (Daneva et al., 2018). We have also shown that BP is dramatically affected by an intraperitoneal infusion of PIP (5AU) (Daneva et al., 2018). Furthermore, we were able to provide evidence that this vasodepressor effect depended on the presence of functional CB1 receptors in the body (see Chapter 4). The genetic and pharmacological deletion of the cannabinoid receptor completely removed both the vasodepressor and diuretic functions of the PF-3845-induced product. However, the same inhibition of vasodepressor activity was achieved by treatment with a diuretic compound, prior to infusing PIP. One implication appears to be that PIP does not drop pressure as a result of urine loss, since there was a considerable urine loss due to tubular excretion in all four experimental groups. It is possible that introduction of two separate diuretics in this model triggers a protective physiological signal for the body to maintain pressure. In our previous experiments, anesthetized mice were only treated with intramedullary or intravenous infusions of PIP. Here, we have two treatments per group, which could stimulate water preservation

mechanisms such as renin-angiotensin-aldosterone-system (and arginine vasopressin) (Koeppen and Stanton, 2013). However, it is not completely clear why inhibition of tubular mechanisms of diuresis would diminish PIP's vasodepressor activity.

The medullary blood flow data in the current set of experiments appears to also bring some new insights into the actions of PIP. When ouabain was infused into the medulla of the kidney, followed by PIP, we did not see a significant elevation in % MBF. One explanation for this lack of response may be that PIP's actions on MBF are inhibited by the ouabain pre-treatment. Even though the proximal tubullar NKAs are particularly sensitive to ouabain, the NKA enzymes are universal to all cells, therefore, ouabain could act in other cells to inhibit medullary vasodilation (Cao and Pallone 2008). When we blocked NCC in the distal convoluted tubules by administration of hydrochlorothiazide (HCT), we observed a slight increase in MBF that was not significant. However, treatment with PIP, in the presence of HCT, elevated MBF to levels, previously observed by our lab (Daneva 2018). Interestingly, the control group, treated with the NKCC2 inhibitor furosemide, displayed a mild elevation in MBF, but when PIP was infused, there was no significant difference from baseline. Some scientists have argued that furosemide does not elevate MBF, however, there are published reports claiming that the diuretic has the ability to stimulate blood flow in the medulla, under appropriate conditions (Mattson 2003; Vakilzadeh & Burnier 2015; Lant 1981; Spitalewitz & Porush 1982). Subjects, treated with the ENaC inhibitor amiloride, exhibited a mild but consistent elevation of medullary blood flow. PIP did not appear to enhance any further the microcirculatory stimulation of amiloride. Possibly, this is so, because amiloride acts through the same or similar mechanism as PIP, so the novel lipid would not be able to enhance further that mechanism. However, as Fig. 20 reveals the level of MBF after PIP infusion continues to increase and remains elevated until the end of the

experiment. This response differs from the declining pattern of MBF response to continuous intramedullary infusion of amiloride alone (see Fig. 20). Thus, the lack of significant elevation of MBF after treatment of PIP may purely be a product of individual difference between mice used in this experiment. Altogether, a combination of diuretics with PIP in these experimental settings does not seem to be able to provide sufficient causal elucidation on the renal tubular segments, responsible for the MBF-stimulating properties of PIP.

There are several limitations to the current study that would need to be considered if localization of PIP's tubular activity is to be achieved in future projects. First, while ouabain was able to help us determine that the proximal convoluted tubules are involved in PIP's diuretic actions in the kidneys, using it was not the best means of exploration, because all cells have NKAs (with varying subunits). Hence, it is difficult to differentiate if inhibition of the enzyme is directly responsible for the diuretic effect, or indirectly- by diminishing the activity of NHE3. It is a known fact that NKA is the rate-limiting step for sodium and water reabsorption by the proximal convoluted tubules (Koeppen 2013). To better assess if PIP acts on NKA or NHE3, it will be worth co-administering an NHE3 inhibitor with PIP. Secondly, all our findings are based solely on an *in vivo* renal function model. Second, a molecular assay that can measure transporter expression, activity and sodium transcellular transportation would be beneficial to locate every target of activation by PIP (possibly more than one). Third, the animals we have used for this study are all normotensive and anesthetized. As described by Daneva et al., PIP is potentially induced by renomedullary interstitial cells under conditions of elevated interstitial pressure. For us to explore the full potential of PIP to produce diuresis via tubular segments, we need to include hypertensive animals. Finally, the experiments in this chapter did not include measurements of sodium and potassium in the urine, excreted before and after all treatments.

Therefore, we were not able to make assumptions about sodium excretion, which is a limitation since water and sodium excretion go together.

In this study we tried to determine the tubular location of the diuretic activity of a compound, PIP, produced and secreted by renomedullary interstitial cells after treatment with a selective inhibitor of the cannabinoid FAAH enzyme. We presented evidence that PIP acts via the proximal convoluted tubules in order to elicit its diuretic properties. Furthermore, we showed that the inhibition of the sodium reabsorption in any of the other tubular segments of the nephron could not diminish PIP's diuretic actions. More studies would be needed to determine the exact location (if only one) of activation in the renal tubules, but this study provides initial direction in the field and narrows down tubular targets of PIP.

Conclusion

The purpose of the current studies was to characterize the diuretic, natriuretic and vasodepressor activity of a substance produced by mouse renomedullary interstitial cells that showed responsiveness to the FAAH inhibitor, PF-3845. Testing of the HPLC-purified product on acute renal functions in anesthetized normotensive mice showed that the product possessed blood-pressure-lowering and diuretic and natriuretic activities, but that the profile of its effects differed depending on the route of administration. Its contrasting biological effects after intraperitoneal administration suggest a role for liver metabolism in determining its biologic actions. While the structure of the substance responsible for the biologic activities in the PIP fraction has not yet been identified, the findings that its concentration in MMIC culture medium increased by PF-3845 treatment and that its diuretic and natriuretic activities were attenuated in FAAH KO mice suggest a relationship to anandamide or other fatty acid ethanolamides or amides. These data support the existence of a substance secreted by renomedullary interstitial cells and has the capacity to lower blood pressure by either renal or extrarenal mechanisms.

We, then, furthered the biological profiling of the PF-3845-induced lipid product by examining its mechanistic dependence on the endocannabinoid type 1 receptors for the mediation of diuresis and vasodepression in the kidney. In order to do this we approached the issue in three different methodological ways: [1] *in vivo* acute renal function response to intramedullary infusion of PIP after an i.p. pre-treatment with a CB1 selective antagonist, rimonabant; [2] *in vivo* acute renal function response to intramedullary infusion or intraperitoneal injection of PIP in genetically modified CB1 WT and CB1 KO mice; and [3] *in vitro* radioactive competition binding assays for CB1 receptors in human CB1-CHO cells. We observed that the HPLC-purified product, used in anesthetized, normotensive mice revealed a tight dependence on CB1

receptors for the conduction of its vasodepressor and diuretic properties. Furthermore, the difference in biological effects of the product, observed after intramedullary versus intraperitoneal routes of administration, suggested an important role for liver metabolism as a determinant of PIP's biologic actions. Our results from competition binding study showed that PIP was able to displace a selective CB1 antagonist [3H] SR141716-A in a concentration-dependent manner. These data support a potential role for CB1 receptors, acting both in renal and extra-renal systems to regulate blood pressure.

Finally, we designed a study to test the hypothesis that PIP elicits its diuretic activity in the kidneys via proximal convoluted tubules (PTs). We demonstrated that in an *in vivo* acute renal function assay, pharmacological inhibition of the major tubular sodium reabsorption transporters revealed that inactivating the Na^+/K^+ ATPase (NKA) in the proximal convoluted tubules is the only condition for diminishing the diuretic effects of the PF-3845-stimulated lipid product. When we pre-treated mice with chemical agents that inhibited transporters in the loop of Henle, distal convoluted tubules and collecting ducts, PIP remained effective as a diuretic stimulant. This pilot study provided a novel insight into the tubule-cellular mechanism that PIP uses in order to act in the kidney.

This thesis research offers initial biological and physiological parametric analysis of a novel endogenous lipid compound, PIP, produced and excreted by renomedullary interstitial cells in mice after treatment with a selective FAAH inhibitor. Furthermore, it provides evidence that the lipid fraction elicits its hemodynamic and vasodepressor properties by binding to receptors of the endocannabinoid system. Additionally, it demonstrates that this CB1-mediated diuretic activity of PIP is predominantly localized in the proximal convoluted tubules of the kidney. While it remains unclear what ion transporters and down-stream signaling mechanisms

are involved in the functioning of the novel lipid fraction, our findings offer a potential therapeutic agent for the treatment of hypertension. Furthermore, these data offer support for the involvement of the endocannabinoid system in the renal regulation of blood pressure and fluid balance. Finally, our findings that the novel lipid binds to CB1 receptors enhance sodium and water excretion via proximal tubules unifies hypotheses from both the cannabinoid and renal fields into one comprehensive model of hemodynamic regulation of blood pressure.

List of References

Abel EL (1979) Behavioral teratology of marihuana extract in rats. *Neurobehav Toxicol* **1**:285-287.

Abrahamov A and Mechoulam R (1995) An efficient new cannabinoid antiemetic in pediatric oncology. *Life Sci* **56**:2097-2102.

Ahmad A, Daneva Z, Li G, Dempsey SK, Li N, Poklis J, Lichtman A, Li PL and Ritter JK (2017a) Stimulation of diuresis and natriuresis by renomedullary infusion of a dual inhibitor of fatty acid amide hydrolase and monoacylglycerol lipase. *Am J Physiol Renal Physiol*:ajprenal.00196.02017.

Ahmad A, Daneva Z, Li G, Dempsey SK, Li N, Poklis JL, Lichtman A, Li PL and Ritter JK (2017b) Stimulation of diuresis and natriuresis by renomedullary infusion of a dual inhibitor of fatty acid amide hydrolase and monoacylglycerol lipase. *Am J Physiol Renal Physiol* **313**:F1068-F1076.

Ahmad A, Dempsey SK, Daneva Z, Li N, Poklis JL, Li PL and Ritter JK (2018) MODULATION OF MEAN ARTERIAL PRESSURE AND DIURESIS BY RENOMEDULLARY INFUSION OF A SELECTIVE INHIBITOR OF FATTY ACID AMIDE HYDROLASE. *Am J Physiol Renal Physiol*.

Aizman O, Uhlen P, Lal M, Brismar H and Aperia A (2001) Ouabain, a steroid hormone that signals with slow calcium oscillations. *Proc Natl Acad Sci U S A* **98**:13420-13424.

Araya KA, David Pessoa Mahana C and Gonzalez LG (2007) Role of cannabinoid CB1 receptors and Gi/o protein activation in the modulation of synaptosomal Na+,K+-ATPase activity by WIN55,212-2 and delta(9)-THC. *Eur J Pharmacol* **572**:32-39.

Arystarkhova E and Sweadner KJ (1997) Tissue-specific expression of the Na,K-ATPase beta3 subunit. The presence of beta3 in lung and liver addresses the problem of the missing subunit. *J Biol Chem* **272**:22405-22408.

Atwood BK, Wager-Miller J, Haskins C, Straiker A and Mackie K (2012) Functional selectivity in CB(2) cannabinoid receptor signaling and regulation: implications for the therapeutic potential of CB(2) ligands. *Mol Pharmacol* **81**:250-263.

Avila J, Alvarez de la Rosa D, Gonzalez-Martinez LM, Lecuona E and Martin-Vasallo P (1998) Structure and expression of the human Na,K-ATPase beta 2-subunit gene. *Gene* **208**:221-227.

Azuma KK, Balkovetz DF, Magyar CE, Lescale-Matys L, Zhang Y, Chambrey R, Warnock DG and McDonough AA (1996) Renal Na+/H+ exchanger isoforms and their regulation by thyroid hormone. *Am J Physiol* **270**:C585-592.

Bailey MA, Giebisch G, Abbiati T, Aronson PS, Gawenis LR, Shull GE and Wang T (2004) NHE2-mediated bicarbonate reabsorption in the distal tubule of NHE3 null mice. *J Physiol* **561**:765-775.

Barutta F, Corbelli A, Mastrocola R, Gambino R, Di Marzo V, Pinach S, Rastaldi MP, Perin PC and Gruden G (2010) Cannabinoid receptor 1 blockade ameliorates albuminuria in experimental diabetic nephropathy. *Diabetes* **59**:1046-1054.

Barutta F, Piscitelli F, Pinach S, Bruno G, Gambino R, Rastaldi MP, Salvidio G, Di Marzo V, Cavallo Perin P and Gruden G (2011) Protective role of cannabinoid receptor type 2 in a mouse model of diabetic nephropathy. *Diabetes* **60**:2386-2396.

Batkai S, Rajesh M, Mukhopadhyay P, Hasko G, Liaudet L, Cravatt BF, Csiszar A, Ungvari Z and Pacher P (2007) Decreased age-related cardiac dysfunction, myocardial nitrative stress, inflammatory gene expression, and apoptosis in mice lacking fatty acid amide hydrolase. *Am J Physiol Heart Circ Physiol* **293**:H909-918.

Benito C, Tolón RM, Castillo AI, Ruiz-Valdepeñas L, Martínez-Orgado JA, Fernández-Sánchez FJ, Vázquez C, Cravatt BF and Romero J (2012) β-Amyloid exacerbates inflammation in astrocytes lacking fatty acid amide hydrolase through a mechanism involving PPAR-α, PPAR-γ and TRPV1, but not CB_1 or CB_2 receptors. *Br J Pharmacol* **166**:1474-1489.

Berger A, Crozier G, Bisogno T, Cavaliere P, Innis S and Di Marzo V (2001) Anandamide and diet: inclusion of dietary arachidonate and docosahexaenoate leads to increased brain levels of the corresponding N-acylethanolamines in piglets. *Proc Natl Acad Sci U S A* **98**:6402-6406.

Bermudez-Silva FJ, Viveros MP, McPartland JM and Rodriguez de Fonseca F (2010) The endocannabinoid system, eating behavior and energy homeostasis: the end or a new beginning? *Pharmacol Biochem Behav* **95**:375-382.

Bertorello AM, Aperia A, Walaas SI, Nairn AC and Greengard P (1991) Phosphorylation of the catalytic subunit of Na+,K(+)-ATPase inhibits the activity of the enzyme. *Proc Natl Acad Sci U S A* **88**:11359-11362.

Biemesderfer D, Pizzonia J, Abu-Alfa A, Exner M, Reilly R, Igarashi P and Aronson PS (1993) NHE3: a Na+/H+ exchanger isoform of renal brush border. *Am J Physiol* **265**:F736-742.

Blake A, Wan BA, Malek L, DeAngelis C, Diaz P, Lao N, Chow E and O'Hearn S (2017) A selective review of medical cannabis in cancer pain management. *Ann Palliat Med* **6**:S215-s222.

Blanco G and Mercer RW (1998) Isozymes of the Na-K-ATPase: heterogeneity in structure, diversity in function. *Am J Physiol* **275**:F633-650.

Blankman JL, Simon GM and Cravatt BF (2007) A comprehensive profile of brain enzymes that hydrolyze the endocannabinoid 2-arachidonoylglycerol. *Chem Biol* **14**:1347-1356.

Bohman SO (1980) The ultrastructure of the renal medulla and the interstitial cells, in *The renal papilla and hypertension* (Mandal AK and Bohman SO eds) pp 7-28, Plenum, New York.

Bohman SO and Jensen PK (1976) Morphometric studies on the lipid droplets of the interstitial cells of the renal medulla in different states of diuresis. *J Ultrastruct Res* **55**:182-192.

Bouaboula M, Poinot-Chazel C, Marchand J, Canat X, Bourrie B, Rinaldi-Carmona M, Calandra B, Le Fur G and Casellas P (1996) Signaling pathway associated with stimulation of CB2 peripheral cannabinoid receptor. Involvement of both mitogen-activated protein kinase and induction of Krox-24 expression. *Eur J Biochem* **237**:704-711.

Boulpaep EL and Sackin H (1979) Equivalent electrical circuit analysis and rheogenic pumps in epithelia. *Fed Proc* **38**:2030-2036.

Brooks B, Byers LW, Muirhead EE, Muirhead M, Pitcock JA, Maddipati KR and Maxey KM (1994) Purification of class I medullipins from the venous effluent of isolated normal kidneys perfused under high pressure with saline. *Blood Press* **3**:407-417.

Buckley MM and Johns EJ (2011) Impact of L-NAME on the cardiopulmonary reflex in cardiac hypertrophy. *Am J Physiol Regul Integr Comp Physiol* **301**:R1549-1556.

Burnstock G, Evans LC and Bailey MA (2014) Purinergic signalling in the kidney in health and disease. *Purinergic Signal* **10**:71-101.
Cantiello HF (1995a) Actin filaments stimulate the Na(+)-K(+)-ATPase. *Am J Physiol* **269**:F637-643.
Cantiello HF (1995b) Role of the actin cytoskeleton on epithelial Na+ channel regulation. *Kidney Int* **48**:970-984.
Cantiello HF (1997) Changes in actin filament organization regulate Na+,K(+)-ATPase activity. Role of actin phosphorylation. *Ann N Y Acad Sci* **834**:559-561.
Cantley LC (2002) The phosphoinositide 3-kinase pathway. *Science* **296**:1655-1657.
Cervenka L, Simova M, Maly J and Heller J (2000) [Role of the kidney in long-term regulation of blood pressure and the development of hypertension]. *Cesk Fysiol* **49**:116-133.
Chopda GR, Parge V, Thakur GA, Gatley SJ, Makriyannis A and Paronis CA (2016) Tolerance to the Diuretic Effects of Cannabinoids and Cross-Tolerance to a kappa-Opioid Agonist in THC-Treated Mice. *J Pharmacol Exp Ther* **358**:334-341.
Chopda GR, Vemuri VK, Sharma R, Thakur GA, Makriyannis A and Paronis CA (2013) Diuretic effects of cannabinoid agonists in mice. *Eur J Pharmacol* **721**:64-69.
Cornelius F and Mahmmoud YA (2003) Functional modulation of the sodium pump: the regulatory proteins "Fixit". *News Physiol Sci* **18**:119-124.
Cowley AW, Jr. (1994) Franz Volhard Lecture. Evolution of the medullipin concept of blood pressure control: a tribute to Eric Muirhead. *J Hypertens Suppl* **12**:S25-34.
Cowley AW, Jr. and Roman RJ (1996) The role of the kidney in hypertension. *Jama* **275**:1581-1589.
Cravatt BF, Demarest K, Patricelli MP, Bracey MH, Giang DK, Martin BR and Lichtman AH (2001) Supersensitivity to anandamide and enhanced endogenous cannabinoid signaling in mice lacking fatty acid amide hydrolase. *Proc Natl Acad Sci U S A* **98**:9371-9376.
Cravatt BF, Giang DK, Mayfield SP, Boger DL, Lerner RA and Gilula NB (1996) Molecular characterization of an enzyme that degrades neuromodulatory fatty-acid amides. *Nature* **384**:83-87.
Curthoys NP and Moe OW (2014) Proximal tubule function and response to acidosis. *Clin J Am Soc Nephrol* **9**:1627-1638.
Daneva Z, Dempsey SK, Ahmad A, Li N, Li PL and Ritter J (2018) Diuretic, natriuretic, and vasodepressor activity of a lipid fraction enhanced in medium of cultured mouse medullary interstitial cells by a selective FAAH inhibitor. *J Pharmacol Exp Ther*.
Dautzenberg M, Keilhoff G and Just A (2011) Modulation of the myogenic response in renal blood flow autoregulation by NO depends on endothelial nitric oxide synthase (eNOS), but not neuronal or inducible NOS. *J Physiol* **589**:4731-4744.
Dehmel B, Mervaala E, Lippoldt A, Gross V, Bohlender J, Ganten D and Luft FC (1998) Pressure-natriuresis and -diuresis in transgenic rats harboring both human renin and human angiotensinogen genes. *J Am Soc Nephrol* **9**:2212-2222.
Deutsch DG and Chin SA (1993) Enzymatic synthesis and degradation of anandamide, a cannabinoid receptor agonist. *Biochem Pharmacol* **46**:791-796.
Deutsch DG, Goligorsky MS, Schmid PC, Krebsbach RJ, Schmid HH, Das SK, Dey SK, Arreaza G, Thorup C, Stefano G and Moore LC (1997) Production and physiological actions of anandamide in the vasculature of the rat kidney. *J Clin Invest* **100**:1538-1546.

Devane WA, Hanus L, Breuer A, Pertwee RG, Stevenson LA, Griffin G, Gibson D, Mandelbaum A, Etinger A and Mechoulam R (1992) Isolation and structure of a brain constituent that binds to the cannabinoid receptor. *Science* **258**:1946-1949.

DiBona GF, Kaloyanides GJ and Bastron RD (1973) Effect of increased perfusion pressure on proximal tubular reabsorption in the isolated kidney. *Proc Soc Exp Biol Med* **143**:830-834.

Dinh TP, Freund TF and Piomelli D (2002) A role for monoglyceride lipase in 2-arachidonoylglycerol inactivation. *Chem Phys Lipids* **121**:149-158.

DiPatrizio NV and Piomelli D (2012) The thrifty lipids: endocannabinoids and the neural control of energy conservation. *Trends Neurosci* **35**:403-411.

Doucet A and Katz AI (1982) High-affinity Ca-Mg-ATPase along the rabbit nephron. *Am J Physiol* **242**:F346-352.

Dresser TP, Lynch RE, Schneider EG and Knox FG (1971) Effect of increases in blood pressure on pressure and reabsorption in the proximal tubule. *Am J Physiol* **220**:444-447.

drugpolicy.org/legalization-status-report (2018) From prohibition to progress: a status report on marijuana legalization, in, Drug Policy Alliance.

Dunn MJ, Staley RS and Harrison M (1976) Characterization of prostaglandin production in tissue culture of rat renal medullary cells. *Prostaglandins* **12**:37-49.

Dunn RB, Kudrath W, Passo SS and Wilson LB (2011) Kaplan USMLE Step 1 Physiology Lecture Notes, in pp 209-223.

Efendiev R, Bertorello AM, Pressley TA, Rousselot M, Feraille E and Pedemonte CH (2000) Simultaneous phosphorylation of Ser11 and Ser18 in the alpha-subunit promotes the recruitment of Na(+),K(+)-ATPase molecules to the plasma membrane. *Biochemistry* **39**:9884-9892.

Efendiev R, Budu CE, Cinelli AR, Bertorello AM and Pedemonte CH (2003) Intracellular Na+ regulates dopamine and angiotensin II receptors availability at the plasma membrane and their cellular responses in renal epithelia. *J Biol Chem* **278**:28719-28726.

Ehrhart J, Obregon D, Mori T, Hou H, Sun N, Bai Y, Klein T, Fernandez F, Tan J and Shytle RD (2005) Stimulation of cannabinoid receptor 2 (CB2) suppresses microglial activation. *J Neuroinflammation* **2**:29.

Eitle E, Hiranyachattada S, Wang H and Harris PJ (1998) Inhibition of proximal tubular fluid absorption by nitric oxide and atrial natriuretic peptide in rat kidney. *Am J Physiol* **274**:C1075-1080.

Eldeeb K, Leone-Kabler S and Howlett AC (2016) CB1 cannabinoid receptor-mediated increases in cyclic AMP accumulation are correlated with reduced Gi/o function. *J Basic Clin Physiol Pharmacol* **27**:311-322.

Elphick MR and Egertova M (2005) The phylogenetic distribution and evolutionary origins of endocannabinoid signalling. *Handb Exp Pharmacol*:283-297.

Evans FJ (1991) Cannabinoids: the separation of central from peripheral effects on a structural basis. *Planta Med* **57**:S60-67.

Ewart HS and Klip A (1995) Hormonal regulation of the Na(+)-K(+)-ATPase: mechanisms underlying rapid and sustained changes in pump activity. *Am J Physiol* **269**:C295-311.

Feraille E and Doucet A (2001) Sodium-potassium-adenosinetriphosphatase-dependent sodium transport in the kidney: hormonal control. *Physiol Rev* **81**:345-418.

Folch J, Lees M and Sloane Stanley GH (1957) A simple method for the isolation and purification of total lipides from animal tissues. *J Biol Chem* **226**:497-509.

Folkow B (2007) Incretory renal functions--Tigerstedt, renin and its neglected antagonist medullipin. *Acta Physiol (Oxf)* **190**:99-102.
Freund TF, Katona I and Piomelli D (2003) Role of endogenous cannabinoids in synaptic signaling. *Physiol Rev* **83**:1017-1066.
Fryar CD, Chen TC and Li X (2012) Prevalence of uncontrolled risk factors for cardiovascular disease: United States, 1999-2010. *NCHS Data Brief*:1-8.
G G, SO A, S B, SP N, R C, L O, D O-H, J L, B M, J H-W, J T, K P, JL B, BF C, A M and G K (2010) - Inhibitor of fatty acid amide hydrolase normalizes cardiovascular function in. *Chem Biol* **17**:1256-1266.
Garcia-Estan J and Roman RJ (1989) Role of renal interstitial hydrostatic pressure in the pressure diuresis response. *Am J Physiol* **256**:F63-70.
Garty H and Palmer LG (1997) Epithelial sodium channels: function, structure, and regulation. *Physiol Rev* **77**:359-396.
Garvin JL, Herrera M and Ortiz PA (2011) Regulation of renal NaCl transport by nitric oxide, endothelin, and ATP: clinical implications. *Annu Rev Physiol* **73**:359-376.
Geering K (2006) FXYD proteins: new regulators of Na-K-ATPase. *Am J Physiol Renal Physiol* **290**:F241-250.
Geering K (2008) Functional roles of Na,K-ATPase subunits. *Curr Opin Nephrol Hypertens* **17**:526-532.
Geering K, Beguin P, Garty H, Karlish S, Fuzesi M, Horisberger JD and Crambert G (2003) FXYD proteins: new tissue- and isoform-specific regulators of Na,K-ATPase. *Ann N Y Acad Sci* **986**:388-394.
Ghosh S, Kinsey SG, Liu QS, Hruba L, McMahon LR, Grim TW, Merritt CR, Wise LE, Abdullah RA, Selley DE, Sim-Selley LJ, Cravatt BF and Lichtman AH (2015) Full Fatty Acid Amide Hydrolase Inhibition Combined with Partial Monoacylglycerol Lipase Inhibition: Augmented and Sustained Antinociceptive Effects with Reduced Cannabimimetic Side Effects in Mice. *J Pharmacol Exp Ther* **354**:111-120.
Giang DK and Cravatt BF (1997) Molecular characterization of human and mouse fatty acid amide hydrolases. *Proc Natl Acad Sci U S A* **94**:2238-2242.
Gill RK, Saksena S, Syed IA, Tyagi S, Alrefai WA, Malakooti J, Ramaswamy K and Dudeja PK (2002) Regulation of NHE3 by nitric oxide in Caco-2 cells. *Am J Physiol Gastrointest Liver Physiol* **283**:G747-756.
Glodny B and Pauli GF (2006) The vasodepressor function of the kidney: prostaglandin E2 is not the principal vasodepressor lipid of the renal medulla. *Acta Physiol (Oxf)* **187**:419-430.
Gomes P and Soares-da-Silva P (2002) Role of cAMP-PKA-PLC signaling cascade on dopamine-induced PKC-mediated inhibition of renal Na(+)-K(+)-ATPase activity. *Am J Physiol Renal Physiol* **282**:F1084-1096.
Gothberg G, Lundin S and Folkow B (1982) Acute vasodepressor effect in normotensive rats following extracorporal perfusion of the declipped kidney of two-kidney, one clip hypertensive rats. *Hypertension* **4**:101-105.
Granger JP and Alexander BT (2000) Abnormal pressure-natriuresis in hypertension: role of nitric oxide. *Acta Physiol Scand* **168**:161-168.
Granger JP, Alexander BT and Llinas M (2002) Mechanisms of pressure natriuresis. *Curr Hypertens Rep* **4**:152-159.
Granger JP, Haas JA, Pawlowska D and Knox FG (1988) Effect of direct increases in renal interstitial hydrostatic pressure on sodium excretion. *Am J Physiol* **254**:F527-532.

Granger JP and Scott JW (1988) Effects of renal artery pressure on interstitial pressure and Na excretion during renal vasodilation. *Am J Physiol* **255**:F828-833.
Grinspoon L and Bakalar J (1997) *Marijuana - the forbidden medicine*. Yale University Press, New Haven and London.
Grollman A, Muirhead EE and Vanatta J (1949) Role of the kidney in pathogenesis of hypertension as determined by a study of the effects of bilateral nephrectomy and other experimental procedures on the blood pressure of the dog. *Am J Physiol* **157**:21-30.
Guzman M (2003) Cannabinoids: potential anticancer agents. *Nat Rev Cancer* **3**:745-755.
Guzman NJ, Fang MZ, Tang SS, Ingelfinger JR and Garg LC (1995) Autocrine inhibition of Na+/K(+)-ATPase by nitric oxide in mouse proximal tubule epithelial cells. *J Clin Invest* **95**:2083-2088.
Gyombolai P, Pap D, Turu G, Catt KJ, Bagdy G and Hunyady L (2012) Regulation of endocannabinoid release by G proteins: a paracrine mechanism of G protein-coupled receptor action. *Mol Cell Endocrinol* **353**:29-36.
Haas JA, Granger JP and Knox FG (1986) Effect of renal perfusion pressure on sodium reabsorption from proximal tubules of superficial and deep nephrons. *Am J Physiol* **250**:F425-429.
Haas JA, Hammond TG, Granger JP, Blaine EH and Knox FG (1984) Mechanism of natriuresis during intrarenal infusion of prostaglandins. *Am J Physiol* **247**:F475-479.
Hall JE (2003) The kidney, hypertension, and obesity. *Hypertension* **41**:625-633.
Hall JE, Guyton AC, Coleman TG, Mizelle HL and Woods LL (1986) Regulation of arterial pressure: role of pressure natriuresis and diuresis. *Fed Proc* **45**:2897-2903.
Haller VL, Cichewicz DL and Welch SP (2006) Non-cannabinoid CB1, non-cannabinoid CB2 antinociceptive effects of several novel compounds in the PPQ stretch test in mice. *Eur J Pharmacol* **546**:60-68.
Hamlyn JM, Blaustein MP, Bova S, DuCharme DW, Harris DW, Mandel F, Mathews WR and Ludens JH (1991) Identification and characterization of a ouabain-like compound from human plasma. *Proc Natl Acad Sci U S A* **88**:6259-6263.
Hamlyn JM and Manunta P (2011) Endogenous ouabain: a link between sodium intake and hypertension. *Curr Hypertens Rep* **13**:14-20.
Han S, Thatte J, Buzard DJ and Jones RM (2013) Therapeutic utility of cannabinoid receptor type 2 (CB(2)) selective agonists. *J Med Chem* **56**:8224-8256.
Hanukoglu I and Hanukoglu A (2016) Epithelial sodium channel (ENaC) family: Phylogeny, structure-function, tissue distribution, and associated inherited diseases. *Gene* **579**:95-132.
Hartupee DA, Burnett JC, Jr., Mertz JI and Knox FG (1982) Acetylcholine-induced vasodilation without natriuresis during control of interstitial pressure. *Am J Physiol* **243**:F325-329.
Hashimoto T (1980) Effects of prostaglandin E2, I2 and F2 alpha on systemic and renal hemodynamics, renal function and renin secretion in anesthetized dogs. *Jpn J Pharmacol* **30**:173-186.
He W, Xie Q, Wang Y, Chen J, Zhao M, Davis LS, Breyer MD, Gu G and Hao CM (2013) Generation of a tenascin-C-CreER2 knockin mouse line for conditional DNA recombination in renal medullary interstitial cells. *PLoS One* **8**:e79839.
Hernandez-Cervantes R, Mendez-Diaz M, Prospero-Garcia O and Morales-Montor J (2017) Immunoregulatory Role of Cannabinoids during Infectious Disease. *Neuroimmunomodulation* **24**:183-199.

Herrera B, Carracedo A, Diez-Zaera M, Guzman M and Velasco G (2005) p38 MAPK is involved in CB2 receptor-induced apoptosis of human leukaemia cells. *FEBS Lett* **579**:5084-5088.
Hoagland KM, Maier KG, Moreno C, Yu M and Roman RJ (2001) Cytochrome P450 metabolites of arachidonic acid: novel regulators of renal function. *Nephrol Dial Transplant* **16**:2283-2285.
Howlett AC (2002) The cannabinoid receptors. *Prostaglandins Other Lipid Mediat* **68-69**:619-631.
Howlett AC (2005) Cannabinoid receptor signaling. *Handb Exp Pharmacol*:53-79.
Howlett AC, Bidaut-Russell M, Devane WA, Melvin LS, Johnson MR and Herkenham M (1990) The cannabinoid receptor: biochemical, anatomical and behavioral characterization. *Trends Neurosci* **13**:420-423.
Hryciw DH and McAinch AJ (2016) Cannabinoid receptors in the kidney. *Curr Opin Nephrol Hypertens* **25**:459-464.
Ishac EJ, Jiang L, Lake KD, Varga K, Abood ME and Kunos G (1996) Inhibition of exocytotic noradrenaline release by presynaptic cannabinoid CB1 receptors on peripheral sympathetic nerves. *Br J Pharmacol* **118**:2023-2028.
Ivy JR and Bailey MA (2014) Pressure natriuresis and the renal control of arterial blood pressure. *J Physiol* **592**:3955-3967.
Izzo AA and Camilleri M (2008) Emerging role of cannabinoids in gastrointestinal and liver diseases: basic and clinical aspects. *Gut* **57**:1140-1155.
Jaitovich A and Bertorello AM (2010) Salt, Na+,K+-ATPase and hypertension. *Life Sci* **86**:73-78.
Janiak P, Poirier B, Bidouard JP, Cadrouvele C, Pierre F, Gouraud L, Barbosa I, Dedio J, Maffrand JP, Le Fur G, O'Connor S and Herbert JM (2007) Blockade of cannabinoid CB1 receptors improves renal function, metabolic profile, and increased survival of obese Zucker rats. *Kidney Int* **72**:1345-1357.
Jenkin KA, McAinch AJ, Briffa JF, Zhang Y, Kelly DJ, Pollock CA, Poronnik P and Hryciw DH (2013) Cannabinoid receptor 2 expression in human proximal tubule cells is regulated by albumin independent of ERK1/2 signaling. *Cell Physiol Biochem* **32**:1309-1319.
Jenkin KA, McAinch AJ, Grinfeld E and Hryciw DH (2010) Role for cannabinoid receptors in human proximal tubular hypertrophy. *Cell Physiol Biochem* **26**:879-886.
Johnson JM, Lemberger L, Novotny M, Forney RB, Dalton WS and Maskarinec MP (1984) Pharmacological activity of the basic fraction of marihuana whole smoke condensate alone and in combination with delta-9-tetrahydrocannabinol in mice. *Toxicol Appl Pharmacol* **72**:440-448.
Johnson M, Devane W, Howlett A, Melvin L and Milne G (1988) Structural studies leading to the discovery of a cannabinoid binding site. *NIDA Res Monogr* **90**:129-135.
Jourdan T, Szanda G, Rosenberg AZ, Tam J, Earley BJ, Godlewski G, Cinar R, Liu Z, Liu J, Ju C, Pacher P and Kunos G (2014) Overactive cannabinoid 1 receptor in podocytes drives type 2 diabetic nephropathy. *Proc Natl Acad Sci U S A* **111**:E5420-5428.
Julien B, Grenard P, Teixeira-Clerc F, Van Nhieu JT, Li L, Karsak M, Zimmer A, Mallat A and Lotersztajn S (2005) Antifibrogenic role of the cannabinoid receptor CB2 in the liver. *Gastroenterology* **128**:742-755.
Kaplan JH (2002) Biochemistry of Na,K-ATPase. *Annu Rev Biochem* **71**:511-535.

Karlsson M, Contreras JA, Hellman U, Tornqvist H and Holm C (1997) cDNA cloning, tissue distribution, and identification of the catalytic triad of monoglyceride lipase. Evolutionary relationship to esterases, lysophospholipases, and haloperoxidases. *J Biol Chem* **272**:27218-27223.

Karlsson M, Reue K, Xia YR, Lusis AJ, Langin D, Tornqvist H and Holm C (2001) Exon-intron organization and chromosomal localization of the mouse monoglyceride lipase gene. *Gene* **272**:11-18.

Karlstrom G, Arnman V, Bergstrom G, Bohman SO, Rudenstam J and Gothberg G (1990) Do angiotensin converting enzyme inhibitors lower blood pressure in the rat partly via the humorally mediated antihypertensive system of the renal medulla? *J Hypertens* **8**:501-513.

Karlstrom G, Arnman V, Folkow B and Gothberg G (1988) Activation of the humoral antihypertensive system of the kidney increases diuresis. *Hypertension* **11**:597-601.

Katayama K, Ueda N, Kurahashi Y, Suzuki H, Yamamoto S and Kato I (1997) Distribution of anandamide amidohydrolase in rat tissues with special reference to small intestine. *Biochim Biophys Acta* **1347**:212-218.

Khraibi AA and Knox FG (1988) Renal interstitial hydrostatic pressure during pressure natriuresis in hypertension. *Am J Physiol* **255**:R756-759.

Kim J, Kim WY, Han KH, Knepper MA, Nielsen S and Madsen KM (1999) Developmental expression of aquaporin 1 in the rat renal vasculature. *Am J Physiol* **276**:F498-509.

Kim K, Moore DH, Makriyannis A and Abood ME (2006) AM1241, a cannabinoid CB2 receptor selective compound, delays disease progression in a mouse model of amyotrophic lateral sclerosis. *Eur J Pharmacol* **542**:100-105.

Kinoshita Y and Knox FG (1990) Response of superficial proximal convoluted tubule to decreased and increased renal perfusion pressure. In vivo microperfusion study in rats. *Circ Res* **66**:1184-1189.

Koeppen BM and Stanton BA (2013) *Renal Physiology*. Elsevier, Philadelphia, PA.

Kondo S, Kondo H, Nakane S, Kodaka T, Tokumura A, Waku K and Sugiura T (1998) 2-Arachidonoylglycerol, an endogenous cannabinoid receptor agonist: identification as one of the major species of monoacylglycerols in various rat tissues, and evidence for its generation through CA2+-dependent and -independent mechanisms. *FEBS Lett* **429**:152-156.

Koura Y, Ichihara A, Tada Y, Kaneshiro Y, Okada H, Temm CJ, Hayashi M and Saruta T (2004) Anandamide decreases glomerular filtration rate through predominant vasodilation of efferent arterioles in rat kidneys. *J Am Soc Nephrol* **15**:1488-1494.

Lake KD, Compton DR, Varga K, Martin BR and Kunos G (1997a) Cannabinoid-induced hypotension and bradycardia in rats mediated by CB1-like cannabinoid receptors. *J Pharmacol Exp Ther* **281**:1030-1037.

Lake KD, Martin BR, Kunos G and Varga K (1997b) Cardiovascular effects of anandamide in anesthetized and conscious normotensive and hypertensive rats. *Hypertension* **29**:1204-1210.

Lam PM, McDonald J and Lambert DG (2005) Characterization and comparison of recombinant human and rat TRPV1 receptors: effects of exo- and endocannabinoids. *Br J Anaesth* **94**:649-656.

Lant AF (1981) Modern diuretics and the kidney. *J Clin Pathol* **34**:1267-1275.

Laragh JH and Brenner BM (1990) *Hypertension: pathophysiology, diagnosis, and management*. Raven Press, New York.
Larrinaga G, Varona A, Pérez I, Sanz B, Ugalde A, Cándenas ML, Pinto FM, Gil J and López JI (2010) Expression of cannabinoid receptors in human kidney. *Histol Histopathol* **25**:1133-1138.
Larsson C and Anggard E (1973) Regional differences in the formation and metabolism of prostaglandins in the rabbit kidney. *Eur J Pharmacol* **21**:30-36.
Le Boisselier R, Alexandre J, Lelong-Boulouard V and Debruyne D (2017) Focus on cannabinoids and synthetic cannabinoids. *Clin Pharmacol Ther* **101**:220-229.
Lecru L, Desterke C, Grassin-Delyle S, Chatziantoniou C, Vandermeersch S, Devocelle A, Vernochet A, Ivanovski N, Ledent C, Ferlicot S, Dalia M, Said M, Beaudreuil S, Charpentier B, Vazquez A, Giron-Michel J, Azzarone B, Durrbach A and Francois H (2015) Cannabinoid receptor 1 is a major mediator of renal fibrosis. *Kidney Int* **88**:72-84.
Leleu-Chavain N, Body-Malapel M, Spencer J, Chavatte P, Desreumaux P and Millet R (2012) Recent advances in the development of selective CB(2) agonists as promising anti-inflammatory agents. *Curr Med Chem* **19**:3457-3474.
Lemley KV and Kriz W (1991) Anatomy of the renal interstitium. *Kidney Int* **39**:370-381.
Leung D, Saghatelian A, Simon GM and Cravatt BF (2006) Inactivation of N-acyl phosphatidylethanolamine phospholipase D reveals multiple mechanisms for the biosynthesis of endocannabinoids. *Biochemistry* **45**:4720-4726.
Lewis DJ and Prentice DE (1979) Ultrastructure of rhesus monkey renomedullary interstitial cells. *Lab Anim* **13**:75-79.
Leyssac PP (1964) THE EFFECT OF PARTIAL CLAMPING OF THE RENAL ARTERY ON PRESSURES IN THE PROXIMAL AND DISTAL TUBULES AND PERITUBULAR CAPILLARIES OF THE RAT KIDNEY. *Acta Physiol Scand* **62**:449-456.
Li J and Wang DH (2006) Differential mechanisms mediating depressor and diuretic effects of anandamide. *J Hypertens* **24**:2271-2276.
Li N, Yi F, Sundy CM, Chen L, Hilliker ML, Donley DK, Muldoon DB and Li PL (2007) Expression and actions of HIF prolyl-4-hydroxylase in the rat kidneys. *Am J Physiol Renal Physiol* **292**:F207-216.
Li N, Zhang G, Yi FX, Zou AP and Li PL (2005) Activation of NAD(P)H oxidase by outward movements of H+ ions in renal medullary thick ascending limb of Henle. *Am J Physiol Renal Physiol* **289**:F1048-1056.
Li Y, Ganta S and Fong P (2012) Endogenous surface expression of DeltaF508-CFTR mediates cAMP-stimulated Cl(-) current in CFTR(DeltaF508/DeltaF508) pig thyroid epithelial cells. *Exp Physiol* **97**:115-124.
Liang M, Cai T, Tian J, Qu W and Xie ZJ (2006) Functional characterization of Src-interacting Na/K-ATPase using RNA interference assay. *J Biol Chem* **281**:19709-19719.
Liang M, Tian J, Liu L, Pierre S, Liu J, Shapiro J and Xie ZJ (2007) Identification of a pool of non-pumping Na/K-ATPase. *J Biol Chem* **282**:10585-10593.
Lim JC, Lim SK, Han HJ and Park SH (2010) Cannabinoid receptor 1 mediates palmitic acid-induced apoptosis via endoplasmic reticulum stress in human renal proximal tubular cells. *J Cell Physiol* **225**:654-663.
Lim SK and Park SH (2012) The high glucose-induced stimulation of B1R and B2R expression via CB(1)R activation is involved in rat podocyte apoptosis. *Life Sci* **91**:895-906.

Lingrel JB, Arguello JM, Van Huysse J and Kuntzweiler TA (1997) Cation and cardiac glycoside binding sites of the Na,K-ATPase. *Ann N Y Acad Sci* **834**:194-206.
Liu H, Zhou D, Garcia ML, Kohler MG, Shen X, Williams DS, Klimas MT, Hargreaves RJ and Kaczorowski GJ (2015) Characteristic time courses of cortical and medullary sodium signals measured by noninvasive (23) Na-MRI in rat kidney induced by furosemide. *J Magn Reson Imaging* **41**:1622-1628.
Liu J, Wang L, Harvey-White J, Huang BX, Kim HY, Luquet S, Palmiter RD, Krystal G, Rai R, Mahadevan A, Razdan RK and Kunos G (2008) Multiple pathways involved in the biosynthesis of anandamide. *Neuropharmacology* **54**:1-7.
Long JZ, LaCava M, Jin X and Cravatt BF (2011) An anatomical and temporal portrait of physiological substrates for fatty acid amide hydrolase. *J Lipid Res* **52**:337-344.
Lorenz JN, Dostanic-Larson I, Shull GE and Lingrel JB (2006) Ouabain inhibits tubuloglomerular feedback in mutant mice with ouabain-sensitive alpha1 Na,K-ATPase. *J Am Soc Nephrol* **17**:2457-2463.
Ludanyi A, Hu SS, Yamazaki M, Tanimura A, Piomelli D, Watanabe M, Kano M, Sakimura K, Magloczky Z, Mackie K, Freund TF and Katona I (2011) Complementary synaptic distribution of enzymes responsible for synthesis and inactivation of the endocannabinoid 2-arachidonoylglycerol in the human hippocampus. *Neuroscience* **174**:50-63.
Maccarrone M, Bab I, Biro T, Cabral GA, Dey SK, Di Marzo V, Konje JC, Kunos G, Mechoulam R, Pacher P, Sharkey KA and Zimmer A (2015) Endocannabinoid signaling at the periphery: 50 years after THC. *Trends Pharmacol Sci* **36**:277-296.
Mach F, Montecucco F and Steffens S (2008) Cannabinoid receptors in acute and chronic complications of atherosclerosis. *Br J Pharmacol* **153**:290-298.
Mach F and Steffens S (2008) The role of the endocannabinoid system in atherosclerosis. *J Neuroendocrinol* **20 Suppl 1**:53-57.
Mackie K (2006) Cannabinoid receptors as therapeutic targets. *Annu Rev Pharmacol Toxicol* **46**:101-122.
Mackie K and Hille B (1992) Cannabinoids inhibit N-type calcium channels in neuroblastoma-glioma cells. *Proc Natl Acad Sci U S A* **89**:3825-3829.
Madsen KM, Verlander JW and Tisher CC (1988) Relationship between structure and function in distal tubule and collecting duct. *J Electron Microsc Tech* **9**:187-208.
Majid DS and Navar LG (2001) Nitric oxide in the control of renal hemodynamics and excretory function. *Am J Hypertens* **14**:74s-82s.
Majid DS, Said KE and Omoro SA (1999) Responses to acute changes in arterial pressure on renal medullary nitric oxide activity in dogs. *Hypertension* **34**:832-836.
Mallat A and Lotersztajn S (2008) Endocannabinoids and liver disease. I. Endocannabinoids and their receptors in the liver. *Am J Physiol Gastrointest Liver Physiol* **294**:G9-g12.
Manger WE, Van Praag D, Weiss DJ, Hart CJ, Hulse M, Rock TW and Farber SJ (1976) Effect of transplanting renomedullary tissue into spontaneously hypertensive rats (SHR). *Federal Proceedings*:556.
Manthorpe T (1973) The effect on renal hypertension of subcutaneous isotransplantation of renal medulla from normal or hypertensive rats. Including studies on spontaneous variations in blood pressure in normal and hypertensive rats. *Acta Pathol Microbiol Scand A* **81**:725-733.
Marchand GR, Ott CE, Lang FC, Greger RF and Knox FG (1977) Effect of secretin on renal blood flow, interstitial pressure, and sodium excretion. *Am J Physiol* **232**:F147-151.

Massa F, Marsicano G, Hermann H, Cannich A, Monory K, Cravatt BF, Ferri GL, Sibaev A, Storr M and Lutz B (2004) The endogenous cannabinoid system protects against colonic inflammation. *J Clin Invest* **113**:1202-1209.

Mathews J, DuCharme DW and McCandlis M (1979) Morphology of cultured renomedullary interstitial cells. *Micron* **10**:185.

Matsuda LA, Lolait SJ, Brownstein MJ, Young AC and Bonner TI (1990) Structure of a cannabinoid receptor and functional expression of the cloned cDNA. *Nature* **346**:561-564.

Mattson DL (2003) Importance of the renal medullary circulation in the control of sodium excretion and blood pressure. *Am J Physiol Regul Integr Comp Physiol* **284**:R13-27.

McAllister SD, Griffin G, Satin LS and Abood ME (1999) Cannabinoid receptors can activate and inhibit G protein-coupled inwardly rectifying potassium channels in a xenopus oocyte expression system. *J Pharmacol Exp Ther* **291**:618-626.

McDonough AA (2010) Mechanisms of proximal tubule sodium transport regulation that link extracellular fluid volume and blood pressure. *Am J Physiol Regul Integr Comp Physiol* **298**:R851-861.

McKinney MK and Cravatt BF (2005) Structure and function of fatty acid amide hydrolase. *Annu Rev Biochem* **74**:411-432.

Mechoulam R, Ben-Shabat S, Hanus L, Ligumsky M, Kaminski NE, Schatz AR, Gopher A, Almog S, Martin BR, Compton DR and et al. (1995) Identification of an endogenous 2-monoglyceride, present in canine gut, that binds to cannabinoid receptors. *Biochem Pharmacol* **50**:83-90.

Mechoulam R and Feigenbaum JJ (1987) Towards cannabinoid drugs. *Prog Med Chem* **24**:159-207.

Mechoulam R, Hanus LO, Pertwee R and Howlett AC (2014) Early phytocannabinoid chemistry to endocannabinoids and beyond, in *Nat Rev Neurosci* pp 757-764, England.

Moeckel GW, Zhang L, Fogo AB, Hao CM, Pozzi A and Breyer MD (2003) COX2 activity promotes organic osmolyte accumulation and adaptation of renal medullary interstitial cells to hypertonic stress. *J Biol Chem* **278**:19352-19357.

Molina-Holgado E, Vela JM, Arevalo-Martin A, Almazan G, Molina-Holgado F, Borrell J and Guaza C (2002) Cannabinoids promote oligodendrocyte progenitor survival: involvement of cannabinoid receptors and phosphatidylinositol-3 kinase/Akt signaling. *J Neurosci* **22**:9742-9753.

Mozaffarian D, Benjamin EJ, Go AS, Arnett DK, Blaha MJ, Cushman M, de Ferranti S, Despres JP, Fullerton HJ, Howard VJ, Huffman MD, Judd SE, Kissela BM, Lackland DT, Lichtman JH, Lisabeth LD, Liu S, Mackey RH, Matchar DB, McGuire DK, Mohler ER, 3rd, Moy CS, Muntner P, Mussolino ME, Nasir K, Neumar RW, Nichol G, Palaniappan L, Pandey DK, Reeves MJ, Rodriguez CJ, Sorlie PD, Stein J, Towfighi A, Turan TN, Virani SS, Willey JZ, Woo D, Yeh RW and Turner MB (2015) Heart disease and stroke statistics--2015 update: a report from the American Heart Association. *Circulation* **131**:e29-322.

Muirhead EE (1991) The medullipin system of blood pressure control. *Am J Hypertens* **4**:556s-568s.

Muirhead EE (1993) Renal vasodepressor mechanisms: the medullipin system. *J Hypertens Suppl* **11**:S53-58.

Muirhead EE, Brooks B, Byers LW, Pitcock JA and Brown PS (1988) Conversion of medullipin I by the liver. *Trans Assoc Am Physicians* **101**:226-234.
Muirhead EE, Brooks B, Pitcock JA and Stephenson P (1972a) Renomedullary antihypertensive function in accelerated (malignant) hypertension. Observations on renomedullary interstitial cells. *J Clin Invest* **51**:181-190.
Muirhead EE, Brooks B, Pitcock JA, Stephenson P and Brosius WL (1972b) Role of the renal medulla in the sodium-sensitive component of renoprival hypertension. *Lab Invest* **27**:192-198.
Muirhead EE, Brown GB, Germain GS and Leach BE (1970) The renal medulla as an antihypertensive organ. *J Lab Clin Med* **76**:641-651.
Muirhead EE, Byers LW, Capdevila J, Brooks B, Pitcock JA and Brown PS (1989) The renal antihypertensive endocrine function: its relation to cytochrome P-450. *J Hypertens* **7**:361-369.
Muirhead EE, Germain G, Leach BE, Pitcock JA, Stephenson P, Brooks B, Brosius WL, Daniels EG and Hinman JW (1972c) Production of renomedullary prostaglandins by renomedullary interstitial cells grown in tissue culture. *Circ Res* **31**:Suppl 2:161-172.
Muirhead EE, Germain GS, Armstrong FB, Brooks B, Leach BE, Byers LW, Pitcock JA and Brown P (1974) Renomedullary endocrine system: its antihypertensive action. *Trans Assoc Am Physicians* **87**:288-297.
Muirhead EE, Germain GS, Leach BE, Brooks B and Stephenson P (1973) Renomedullary interstitial cells (RIC), prostaglandins (PG) and the antihypertensive function of the kidney. *Prostaglandins* **3**:581-594.
Muirhead EE, Rightsel WA, Pitcock JA and Inagami T (1990) Isolation and culture of juxtaglomerular and renomedullary interstitial cells. *Methods Enzymol* **191**:152-167.
Muirhead EE, Stirman JA and Jones F (1960) Renal autoexplantation and protection against renoprival hypertensive cardiovascular disease and hemolysis. *J Clin Invest* **39**:266-281.
Mukhopadhyay P, Pan H, Rajesh M, Bátkai S, Patel V, Harvey-White J, Mukhopadhyay B, Haskó G, Gao B, Mackie K and Pacher P (2010) CB1 cannabinoid receptors promote oxidative/nitrosative stress, inflammation and cell death in a murine nephropathy model. *Br J Pharmacol* **160**:657-668.
Mummalaneni S, Qian J, Phan TH, Rhyu MR, Heck GL, DeSimone JA and Lyall V (2014) Effect of ENaC modulators on rat neural responses to NaCl. *PLoS One* **9**:e98049.
Munro S, Thomas KL and Abu-Shaar M (1993) Molecular characterization of a peripheral receptor for cannabinoids. *Nature* **365**:61-65.
Murataeva N, Straiker A and Mackie K (2014) Parsing the players: 2-arachidonoylglycerol synthesis and degradation in the CNS. *Br J Pharmacol* **171**:1379-1391.
Nah SY, Saya D and Vogel Z (1993) Cannabinoids inhibit agonist-stimulated formation of inositol phosphates in rat hippocampal cultures. *Eur J Pharmacol* **246**:19-24.
Nakamura T, Alberola AM, Salazar FJ, Saito Y, Kurashina T, Granger JP and Nagai R (1998) Effects of renal perfusion pressure on renal interstitial hydrostatic pressure and Na+ excretion: role of endothelium-derived nitric oxide. *Nephron* **78**:104-111.
Nam DH, Lee MH, Kim JE, Song HK, Kang YS, Lee JE, Kim HW, Cha JJ, Hyun YY, Kim SH, Han SY, Han KH, Han JY and Cha DR (2012) Blockade of cannabinoid receptor 1 improves insulin resistance, lipid metabolism, and diabetic nephropathy in db/db mice. *Endocrinology* **153**:1387-1396.
Noyes R, Jr. and Baram DA (1974) Cannabis analgesia. *Compr Psychiatry* **15**:531-535.

Noyes R, Jr., Brunk SF, Baram DA and Canter A (1975) Analgesic effect of delta-9-tetrahydrocannabinol. *J Clin Pharmacol* **15**:139-143.
Nwankwo T, Yoon SS, Burt V and Gu Q (2013) Hypertension among adults in the United States: National Health and Nutrition Examination Survey, 2011-2012. *NCHS Data Brief*:1-8.
O'Connor PM and Cowley AW, Jr. (2010) Modulation of pressure-natriuresis by renal medullary reactive oxygen species and nitric oxide. *Curr Hypertens Rep* **12**:86-92.
O'Hearn S, Diaz P, Wan BA, DeAngelis C, Lao N, Malek L, Chow E and Blake A (2017) Modulating the endocannabinoid pathway as treatment for peripheral neuropathic pain: a selected review of preclinical studies. *Ann Palliat Med* **6**:S209-s214.
O'Sullivan SE (2015) Endocannabinoids and the Cardiovascular System in Health and Disease. *Handb Exp Pharmacol* **231**:393-422.
Ofek O, Karsak M, Leclerc N, Fogel M, Frenkel B, Wright K, Tam J, Attar-Namdar M, Kram V, Shohami E, Mechoulam R, Zimmer A and Bab I (2006) Peripheral cannabinoid receptor, CB2, regulates bone mass. *Proc Natl Acad Sci U S A* **103**:696-701.
Onaivi ES, Ishiguro H, Gong JP, Patel S, Perchuk A, Meozzi PA, Myers L, Mora Z, Tagliaferro P, Gardner E, Brusco A, Akinshola BE, Liu QR, Hope B, Iwasaki S, Arinami T, Teasenfitz L and Uhl GR (2006) Discovery of the presence and functional expression of cannabinoid CB2 receptors in brain. *Ann N Y Acad Sci* **1074**:514-536.
Ortiz PA and Garvin JL (2002) Role of nitric oxide in the regulation of nephron transport. *Am J Physiol Renal Physiol* **282**:F777-784.
Osei-Hyiaman D, DePetrillo M, Pacher P, Liu J, Radaeva S, Batkai S, Harvey-White J, Mackie K, Offertaler L, Wang L and Kunos G (2005) Endocannabinoid activation at hepatic CB1 receptors stimulates fatty acid synthesis and contributes to diet-induced obesity. *J Clin Invest* **115**:1298-1305.
Osvaldo L and Latta H (1966) Interstitial cells of the renal medulla. *Journal of Ultrastructure Research* **15**:589-613.
Ott CE, Navar LG and Guyton AC (1971) Pressures in static and dynamic states from capsules implanted in the kidney. *Am J Physiol* **221**:394-400.
Pacher P, Bátkai S and Kunos G (2004) Haemodynamic profile and responsiveness to anandamide of TRPV1 receptor knock-out mice. *J Physiol* **558**:647-657.
Pacher P and Hasko G (2008) Endocannabinoids and cannabinoid receptors in ischaemia-reperfusion injury and preconditioning. *Br J Pharmacol* **153**:252-262.
Pacher P and Kunos G (2013) Modulating the endocannabinoid system in human health and disease--successes and failures. *Febs j* **280**:1918-1943.
Palar K and Sturm R (2009) Potential societal savings from reduced sodium consumption in the U.S. adult population. *Am J Health Promot* **24**:49-57.
Palmer SL, Thakur GA and Makriyannis A (2002) Cannabinergic ligands. *Chem Phys Lipids* **121**:3-19.
Panlilio LV, Justinova Z and Goldberg SR (2013) Inhibition of FAAH and activation of PPAR: new approaches to the treatment of cognitive dysfunction and drug addiction. *Pharmacol Ther* **138**:84-102.
Park F, Potukuchi PK, Moradi H and Kovesdy CP (2017) Cannabinoids and the kidney: effects in health and disease. *Am J Physiol Renal Physiol* **313**:F1124-f1132.
Paronis CA, Thakur GA, Bajaj S, Nikas SP, Vemuri VK, Makriyannis A and Bergman J (2013) Diuretic effects of cannabinoids. *J Pharmacol Exp Ther* **344**:8-14.

Patricelli MP and Cravatt BF (1999) Fatty acid amide hydrolase competitively degrades bioactive amides and esters through a nonconventional catalytic mechanism. *Biochemistry* **38**:14125-14130.
Paugh SW, Cassidy MP, He H, Milstien S, Sim-Selley LJ, Spiegel S and Selley DE (2006) Sphingosine and its analog, the immunosuppressant 2-amino-2-(2-[4-octylphenyl]ethyl)-1,3-propanediol, interact with the CB1 cannabinoid receptor. *Mol Pharmacol* **70**:41-50.
Paul M, Poyan Mehr A and Kreutz R (2006) Physiology of local renin-angiotensin systems. *Physiol Rev* **86**:747-803.
Pearce D, Soundararajan R, Trimpert C, Kashlan OB, Deen PM and Kohan DE (2015) Collecting duct principal cell transport processes and their regulation. *Clin J Am Soc Nephrol* **10**:135-146.
Pertwee RG (1997) Pharmacology of cannabinoid CB1 and CB2 receptors. *Pharmacol Ther* **74**:129-180.
Pertwee RG (2007) Cannabinoids and multiple sclerosis. *Mol Neurobiol* **36**:45-59.
Pertwee RG (2010) Receptors and channels targeted by synthetic cannabinoid receptor agonists and antagonists. *Curr Med Chem* **17**:1360-1381.
Pertwee RG (2012) Targeting the endocannabinoid system with cannabinoid receptor agonists: pharmacological strategies and therapeutic possibilities. *Philos Trans R Soc Lond B Biol Sci* **367**:3353-3363.
Phillips E, Wang T, Husten C, Corey C, Apelberg B, Jamal A, Homa D and King B (2017) Tobacco product use among adults - United States, 2015, in *MMWR Morb Mortal Wkly Rep* pp 1209-1215.
Piomelli D (2003) The molecular logic of endocannabinoid signalling. *Nat Rev Neurosci* **4**:873-884.
Pitcock JA, Brown PS, Byers W, Brooks B and Muirhead EE (1981) Degranulation of renomedullary interstitial cells during reversal of hypertension. *Hypertension* **3**:Ii-75-80.
Quintas LE, Pierre SV, Liu L, Bai Y, Liu X and Xie ZJ (2010) Alterations of Na+/K+-ATPase function in caveolin-1 knockout cardiac fibroblasts. *J Mol Cell Cardiol* **49**:525-531.
Randall MD, Kendall DA and O'Sullivan S (2004) The complexities of the cardiovascular actions of cannabinoids. *Br J Pharmacol* **142**:20-26.
Raven PB and Chapleau MW (2014) Blood pressure regulation XI: overview and future research directions. *Eur J Appl Physiol* **114**:579-586.
Rinaldi-Carmona M, Barth F, Heaulme M, Shire D, Calandra B, Congy C, Martinez S, Maruani J, Neliat G, Caput D and et al. (1994) SR141716A, a potent and selective antagonist of the brain cannabinoid receptor. *FEBS Lett* **350**:240-244.
Rinaldi-Carmona M, Barth F, Millan J, Derocq JM, Casellas P, Congy C, Oustric D, Sarran M, Bouaboula M, Calandra B, Portier M, Shire D, Breliere JC and Le Fur GL (1998) SR 144528, the first potent and selective antagonist of the CB2 cannabinoid receptor. *J Pharmacol Exp Ther* **284**:644-650.
Ritter JK, Li C, Xia M, Poklis JL, Lichtman AH, Abdullah RA, Dewey WL and Li PL (2012) Production and actions of the anandamide metabolite prostamide E2 in the renal medulla. *J Pharmacol Exp Ther* **342**:770-779.
Ritter JK, Li G, Xia M and Boini K (2016) Anandamide and its metabolites: what are their roles in the kidney? *Front Biosci (Schol Ed)* **8**:264-277.
Roczniak A and Burns KD (1996) Nitric oxide stimulates guanylate cyclase and regulates sodium transport in rabbit proximal tubule. *Am J Physiol* **270**:F106-115.

Rodriguez de Fonseca F, Del Arco I, Bermudez-Silva FJ, Bilbao A, Cippitelli A and Navarro M (2005) The endocannabinoid system: physiology and pharmacology. *Alcohol Alcohol* **40**:2-14.
Roman RJ (1988) Pressure-diuresis in volume-expanded rats. Tubular reabsorption in superficial and deep nephrons. *Hypertension* **12**:177-183.
Roman RJ and Cowley AW, Jr. (1985) Characterization of a new model for the study of pressure-natriuresis in the rat. *Am J Physiol* **248**:F190-198.
Roman RJ, Cowley AW, Jr., Garcia-Estan J and Lombard JH (1988) Pressure-diuresis in volume-expanded rats. Cortical and medullary hemodynamics. *Hypertension* **12**:168-176.
Roman RJ and Kaldunski ML (1988) Renal cortical and papillary blood flow in spontaneously hypertensive rats. *Hypertension* **11**:657-663.
Roy A, Al-bataineh MM and Pastor-Soler NM (2015) Collecting duct intercalated cell function and regulation. *Clin J Am Soc Nephrol* **10**:305-324.
Sagredo O, Pazos MR, Valdeolivas S and Fernandez-Ruiz J (2012) Cannabinoids: novel medicines for the treatment of Huntington's disease. *Recent Pat CNS Drug Discov* **7**:41-48.
Salaga M, Storr M and Fichna J (2014) Cross-talk between serotonin and cannabinoid signaling in the gut, new insights and future perspectives. *Pain* **155**:2204-2205.
Sallan SE, Zinberg NE and Frei E, 3rd (1975) Antiemetic effect of delta-9-tetrahydrocannabinol in patients receiving cancer chemotherapy. *N Engl J Med* **293**:795-797.
Sampaio LS, Taveira da Silva R, Lima D, Sampaio CL, Iannotti FA, Mazzarella E, Di Marzo V, Vieyra A, Reis RA and Einicker-Lamas M (2014) The Endocannabinoid System in Renal Cell: Regulation of Na+ Transport by CB1 Receptors Through Distinct Cell Signaling Pathways. *Br J Pharmacol*.
Sampaio LS, Taveira Da Silva R, Lima D, Sampaio CL, Iannotti FA, Mazzarella E, Di Marzo V, Vieyra A, Reis RA and Einicker-Lamas M (2015) The endocannabinoid system in renal cells: regulation of Na(+) transport by CB1 receptors through distinct cell signalling pathways. *Br J Pharmacol* **172**:4615-4625.
Satoh N, Nakamura M, Suzuki A, Tsukada H, Horita S, Suzuki M, Moriya K and Seki G (2017) Effects of Nitric Oxide on Renal Proximal Tubular Na(+) Transport. *Biomed Res Int* **2017**:6871081.
Savinainen JR, Saario SM and Laitinen JT (2012) The serine hydrolases MAGL, ABHD6 and ABHD12 as guardians of 2-arachidonoylglycerol signalling through cannabinoid receptors. *Acta Physiol (Oxf)* **204**:267-276.
Schafer JA (1990) Transepithelial osmolality differences, hydraulic conductivities, and volume absorption in the proximal tubule. *Annu Rev Physiol* **52**:709-726.
Schmitz G and Muller G (1991) Structure and function of lamellar bodies, lipid-protein complexes involved in storage and secretion of cellular lipids. *J Lipid Res* **32**:1539-1570.
Schneider JP, Pedersen L, Muhlfeld C and Ochs M (2015) Staining histological lung sections with Sudan Black B or Sudan III for automated identification of alveolar epithelial type II cells. *Acta Histochem* **117**:675-680.
Selkurt EE, Hall PW and Spencer MP (1949) Response of renal blood flow and clearance to graded partial obstruction of the renal vein. *Am J Physiol* **157**:40-46.
Shipley RE and Study RS (1951) Changes in renal blood flow, extraction of inulin, glomerular filtration rate, tissue pressure and urine flow with acute alterations of renal artery blood pressure. *Am J Physiol* **167**:676-688.

Shire D, Carillon C, Kaghad M, Calandra B, Rinaldi-Carmona M, Le Fur G, Caput D and Ferrara P (1995) An amino-terminal variant of the central cannabinoid receptor resulting from alternative splicing. *J Biol Chem* **270**:3726-3731.

Shoemaker JL, Seely KA, Reed RL, Crow JP and Prather PL (2007) The CB2 cannabinoid agonist AM-1241 prolongs survival in a transgenic mouse model of amyotrophic lateral sclerosis when initiated at symptom onset. *J Neurochem* **101**:87-98.

Shyjan AW, Gottardi C and Levenson R (1990) The Na,K-ATPase beta 2 subunit is expressed in rat brain and copurifies with Na,K-ATPase activity. *J Biol Chem* **265**:5166-5169.

Silva E and Soares-da-Silva P (2012) New insights into the regulation of Na+,K+-ATPase by ouabain. *Int Rev Cell Mol Biol* **294**:99-132.

Silva GB, Atchison DK, Juncos LI and García NH (2013) Anandamide inhibits transport-related oxygen consumption in the loop of Henle by activating CB1 receptors. *Am J Physiol Renal Physiol* **304**:F376-381.

Simcocks AC, O'Keefe L, Jenkin KA, Mathai ML, Hryciw DH and McAinch AJ (2014) A potential role for GPR55 in the regulation of energy homeostasis. *Drug Discov Today* **19**:1145-1151.

Simon GM and Cravatt BF (2006) Endocannabinoid biosynthesis proceeding through glycerophospho-N-acyl ethanolamine and a role for alpha/beta-hydrolase 4 in this pathway. *J Biol Chem* **281**:26465-26472.

Sofia RD, Knobloch LC, Harakal JJ and Erikson DJ (1977) Comparative diuretic activity of delta9-tetrahydrocannabinol, cannabidiol, cannabinol and hydrochlorothiazide in the rat. *Arch Int Pharmacodyn Ther* **225**:77-87.

Solez K, D'Agostini RJ, Buono RA, Vernon N, Wang AL, Finer PM and Heptinstall RH (1976) The renal medulla and mechanisms of hypertension in the spontaneously hypertensive rat. *Am J Pathol* **85**:555-568.

Spitalewitz S, Chou SY, Faubert PF and Porush JG (1982) Effects of diuretics on inner medullary hemodynamics in the dog. *Circ Res* **51**:703-710.

Steiner H, Bonner TI, Zimmer AM, Kitai ST and Zimmer A (1999) Altered gene expression in striatal projection neurons in CB1 cannabinoid receptor knockout mice. *Proc Natl Acad Sci U S A* **96**:5786-5790.

Stella N, Schweitzer P and Piomelli D (1997) A second endogenous cannabinoid that modulates long-term potentiation. *Nature* **388**:773-778.

Stopponi S, Fotio Y, Domi A, Borruto AM, Natividad L, Roberto M, Ciccocioppo R and Cannella N (2017) Inhibition of fatty acid amide hydrolase in the central amygdala alleviates co-morbid expression of innate anxiety and excessive alcohol intake. *Addict Biol*.

Sugiura T and Waku K (2000) 2-Arachidonoylglycerol and the cannabinoid receptors. *Chem Phys Lipids* **108**:89-106.

Susic D, Sparks JC and Machado EA (1976) Salt-induced hypertension in rats with hereditary hydronephrosis: the effect of renomedullary transplantation. *J Lab Clin Med* **87**:232-239.

Tam J (2016) The emerging role of the endocannabinoid system in the pathogenesis and treatment of kidney diseases. *J Basic Clin Physiol Pharmacol* **27**:267-276.

Tam J, Cinar R, Liu J, Godlewski G, Wesley D, Jourdan T, Szanda G, Mukhopadhyay B, Chedester L, Liow JS, Innis RB, Cheng K, Rice KC, Deschamps JR, Chorvat RJ, McElroy JF and Kunos G (2012) Peripheral cannabinoid-1 receptor inverse agonism reduces obesity by reversing leptin resistance. *Cell Metab* **16**:167-179.

Tam J, Ofek O, Fride E, Ledent C, Gabet Y, Muller R, Zimmer A, Mackie K, Mechoulam R, Shohami E and Bab I (2006) Involvement of neuronal cannabinoid receptor CB1 in regulation of bone mass and bone remodeling. *Mol Pharmacol* **70**:786-792.

Tamargo J, Segura J and Ruilope LM (2014) Diuretics in the treatment of hypertension. Part 2: loop diuretics and potassium-sparing agents. *Expert Opin Pharmacother* **15**:605-621.

Tian J, Li X, Liang M, Liu L, Xie JX, Ye Q, Kometiani P, Tillekeratne M, Jin R and Xie Z (2009) Changes in sodium pump expression dictate the effects of ouabain on cell growth. *J Biol Chem* **284**:14921-14929.

Tobian L and Ishii M (1969) Interstitial cell granules and solutes in renal papilla in post-Goldblatt hypertension. *Am J Physiol* **217**:1699-1702.

Tobian L, Jr. and Azar S (1971) Antihypertensive and other functions of the renal papilla. *Trans Assoc Am Physicians* **84**:281-288.

Tojo A and Kinugasa S (2012) Mechanisms of glomerular albumin filtration and tubular reabsorption. *Int J Nephrol* **2012**:481520.

Urayama O, Shutt H and Sweadner KJ (1989) Identification of three isozyme proteins of the catalytic subunit of the Na,K-ATPase in rat brain. *J Biol Chem* **264**:8271-8280.

Vagin O, Sachs G and Tokhtaeva E (2007) The roles of the Na,K-ATPase beta 1 subunit in pump sorting and epithelial integrity. *J Bioenerg Biomembr* **39**:367-372.

Vakilzadeh N, Muller ME, Forni V, Milani B, Hoffman L, Piskunowicz M, Maillard M, Zweiacker C, Pruijm M and Burnier M (2015) Comparative Effect of a Renin Inhibitor and a Thiazide Diuretic on Renal Tissue Oxygenation in Hypertensive Patients. *Kidney Blood Press Res* **40**:542-554.

Van Sickle MD, Duncan M, Kingsley PJ, Mouihate A, Urbani P, Mackie K, Stella N, Makriyannis A, Piomelli D, Davison JS, Marnett LJ, Di Marzo V, Pittman QJ, Patel KD and Sharkey KA (2005) Identification and functional characterization of brainstem cannabinoid CB2 receptors. *Science* **310**:329-332.

Varga K, Lake K, Martin BR and Kunos G (1995) Novel antagonist implicates the CB1 cannabinoid receptor in the hypotensive action of anandamide. *Eur J Pharmacol* **278**:279-283.

Varga K, Lake KD, Huangfu D, Guyenet PG and Kunos G (1996) Mechanism of the hypotensive action of anandamide in anesthetized rats. *Hypertension* **28**:682-686.

Wadei HM and Textor SC (2012) The role of the kidney in regulating arterial blood pressure. *Nat Rev Nephrol* **8**:602-609.

Wakui N, Takeda Y, Nishinakagawa S, Ueki N, Otsuka T, Oba N, Hashimoto H, Kamiyama N, Sumino Y and Kojima T (2015) Effect of obstructive jaundice on hepatic hemodynamics: use of Sonazoid-enhanced ultrasonography in a prospective study of the blood flow balance between the hepatic portal vein and hepatic artery. *J Med Ultrason (2001)* **42**:513-520.

Wang T (1997) Nitric oxide regulates HCO3- and Na+ transport by a cGMP-mediated mechanism in the kidney proximal tubule. *Am J Physiol* **272**:F242-248.

Wang Z, Tang L, Zhu Q, Yi F, Zhang F, Li PL and Li N (2011) Hypoxia-inducible factor-1alpha contributes to the profibrotic action of angiotensin II in renal medullary interstitial cells. *Kidney Int* **79**:300-310.

Wasilewski A, Misicka A, Sacharczuk M and Fichna J (2017) Modulation of the endocannabinoid system by the fatty acid amide hydrolase, monoacylglycerol and

diacylglycerol lipase inhibitors as an attractive target for secretory diarrhoea therapy. *J Physiol Pharmacol* **68**:591-596.
Whiting PF, Wolff RF, Deshpande S, Di Nisio M, Duffy S, Hernandez AV, Keurentjes JC, Lang S, Misso K, Ryder S, Schmidlkofer S, Westwood M and Kleijnen J (2015) Cannabinoids for Medical Use: A Systematic Review and Meta-analysis. *Jama* **313**:2456-2473.
Wilcox CS, Sterzel RB, Dunckel PT, Mohrmann M and Perfetto M (1984) Renal interstitial pressure and sodium excretion during hilar lymphatic ligation. *Am J Physiol* **247**:F344-351.
Wise LE, Cannavacciulo R, Cravatt BF, Martin BF and Lichtman AH (2008) Evaluation of fatty acid amides in the carrageenan-induced paw edema model. *Neuropharmacology* **54**:181-188.
Woo AL, James PF and Lingrel JB (2000) Sperm motility is dependent on a unique isoform of the Na,K-ATPase. *J Biol Chem* **275**:20693-20699.
Wright KL, Duncan M and Sharkey KA (2008) Cannabinoid CB2 receptors in the gastrointestinal tract: a regulatory system in states of inflammation. *Br J Pharmacol* **153**:263-270.
Wu XC, Johns EJ and Richards NT (1999) Relationship between erythropoietin and nitric oxide in the contraction of rat renal arcuate arteries and human umbilical vein endothelial cells. *Clin Sci (Lond)* **97**:413-419.
Wu Y, Baum M, Huang CL and Rodan AR (2015) Two inwardly rectifying potassium channels, Irk1 and Irk2, play redundant roles in Drosophila renal tubule function. *Am J Physiol Regul Integr Comp Physiol* **309**:R747-756.
Xie C and Wang DH (2009) Ablation of transient receptor potential vanilloid 1 abolishes endothelin-induced increases in afferent renal nerve activity: mechanisms and functional significance. *Hypertension* **54**:1298-1305.
Xie Z (2003) Molecular mechanisms of Na/K-ATPase-mediated signal transduction. *Ann N Y Acad Sci* **986**:497-503.
Zahler R, Brines M, Kashgarian M, Benz EJ, Jr. and Gilmore-Hebert M (1992) The cardiac conduction system in the rat expresses the alpha 2 and alpha 3 isoforms of the Na+,K(+)-ATPase. *Proc Natl Acad Sci U S A* **89**:99-103.
Zhang J, Lee MY, Cavalli M, Chen L, Berra-Romani R, Balke CW, Bianchi G, Ferrari P, Hamlyn JM, Iwamoto T, Lingrel JB, Matteson DR, Wier WG and Blaustein MP (2005) Sodium pump alpha2 subunits control myogenic tone and blood pressure in mice. *J Physiol* **569**:243-256.
Zhu Q, Xia M, Wang Z, Li PL and Li N (2011) A novel lipid natriuretic factor in the renal medulla: sphingosine-1-phosphate. *Am J Physiol Renal Physiol* **301**:F35-41.
Zhuo JL (2000) Renomedullary interstitial cells: a target for endocrine and paracrine actions of vasoactive peptides in the renal medulla. *Clin Exp Pharmacol Physiol* **27**:465-473.
Zou AP, Yang ZZ, Li PL and Cowley AJ (2001) Oxygen-dependent expression of hypoxia-inducible factor-1alpha in renal medullary cells of rats. *Physiol Genomics* **6**:159-168.
Zusman RM and Keiser HR (1977a) Prostaglandin biosynthesis by rabbit renomedullary interstitial cells in tissue culture. Stimulation by angiotensin II, bradykinin, and arginine vasopressin. *J Clin Invest* **60**:215-223.
Zusman RM and Keiser HR (1977b) Prostaglandin E2 biosynthesis by rabbit renomedullary interstitial cells in tissue culture. Mechanism of stimulation by angiotensin II, bradykinin, and arginine vasopressin. *J Biol Chem* **252**:2069-2071.

Curriculum Vitae of Zdravka Daneva

Ph.D. Candidate, Virginia Commonwealth University School of Medicine, VA

Personal Information

Date of Birth	10/25/1989
Country of Origin	Bulgaria
Citizenship	Bulgarian
Country of Residence	USA
Current Job/Position	Ph.D. Candidate, Virginia Commonwealth University, VA, USA
Current Address	2912 Calcutt Drive; Midlothian 23113, VA, USA
Phone Number	+1 (804) 245 7927
E-mail:	ava.daneva@gmail.com
	zpdaneva@mymail.vcu.edu

Education

Ph.D. Pharmacology and Toxicology **2013-2018 (expected graduation in December)**

- Department of Pharmacology and Toxicology, Virginia Commonwealth University School of Medicine, VA, USA
- Courses: Biochemistry (Cell. and Mol. Biology); Cellular and Molecular Neuroscience, Systems Neuroscience, Basic Concepts for Pharmacology and Toxicology, Principles of Pharmacology, Scientific Integrity, Statistical Methods I
- GPA: 3.150 of 4
- Total Graduate level credits: 162

MA (SocSci) Psychology/Management (Joint Honors) **2009-2013**

- Department of Psychology; School of Business, University of Glasgow, Scotland, UK
- Courses (Psychology): Social Psychology, Individual Differences, Statistics I & II, Occupational Psychology, Perception and Visual Cognition, Physiology, Human Development, Concepts and Historical Issues, Professional Skills.
- Courses (Management): Organizational Behavior, Management Research Methods, Operations Management, Public Sector Management, Project Management, Marketing, Accounting Management, Cases in Operations Management, Innovation and Participation at Work.
- GPA: 2:1 Honors Degree.

Professional Skills

Animal Care

- Maintenance and breeding

Molecular and Biochemical techniques

- Aseptic maintenance and expansion of cell lines, routine analysis of cell culture samples, cell-culture parameters (cell growth rate, cell density, viability, etc.), growing cell lines on trans-membranes and glass slips for cellular signaling assays using fluorescence microscopy
- PCR and RT-PCR
- ELIZA
- Cellular Na- and Ca- signaling fluorescence assays (using SBFI and FURA-1 dies) of renal tubular cells
- Radioligand binding: [^{35}S] GTPγS binding, selective antagonist [3H]SR141716A and selective agonist [3H] WIN 55212-2 / [3H]CP55,940 binding to CB1 receptors
- HPLC extraction and purification of lipids
- TLC extraction, purification and quantification of lipids

Physiological techniques

- Animal handling, injections (i.p., i.v.), dissections (for organ and blood collection)
- Proficient in non-invasive blood pressure measurement by tail-cuff methods (CODA ADInstruments) in mice
- Expert in renal functional *in vivo* studies in small rodents (carotid artery, jugular vein, bladder and kidney medulla catheterization; unilateral ureter ligation)

- Expert in *in vivo* measurement of medullary blood flow (Laser Doppler flow meter and probe), renal blood flow (Transonic ultrasonic flowmeter), GFR measurement using MediBeacon (non-invasive, transdermal GFR sensor using FITC-Sinistrin)
- Proficient in cannulation of amygdala, hippocampus and nucleus accumbens in mice and rats
- Proficient in wire myography for testing stretching of mouse aorta and mesenteric arteries
- Expert in animal dissections and isolation of renal tubular segments (glomerulus, proximal/distal convoluted tubules, collecting ducts, thick ascending loop of Henle)

Behavioral Techniques

- Basic motor and sensory function in mice and/or rats: tetrad (mice), homecage activity (rats), rotarod (mice)
- Learning and memory: Morris water maze, object recognition, fear conditioning (mice)
- Social behavior: three-chamber sociability and social novelty test (mice)
- Anxiety and depression-like behaviors in mice and/or rats: forced swim test (rats), tail suspension test (mice), elevated plus/zero maze (mice), light/dark chamber test (mice), novelty-induced hypophagia (mice), Marble-buring test (mice), Nestlet shredding test (mice)
- Reward: sucrose preference test, conditioned place preference (mice)

Statistical Analysis

- Expert in Microsoft Office (Excel, Word, PowerPoint)
- Expert in Minitab 5, Graph Prism, SPSS and Sigma Plot

Laboratory Skills and Management

- Record keeping
- Organizing drug/animal inventories
- Scheduling and handling lab inspections (Lab Safety, Radiation Safety, IACUC/DAR and DEA)
- Inventory procurement

Professional Experience/Service

- Ph.D. training at the Department of Pharmacology and Toxicology, VCU (2013-present)
- Training of graduate students and post-doctoral trainees in acute renal surgeries, aseptic surgical procedures, records keeping, animal handling, drug administration techniques, software operation (ADInstruments, DATAQ, WINDAQ), statistical analysis (2013-present)
- Judging at the annual Science Fair at the IQRA Academy, Richmond, USA (2016 and 2017)
- Pharmacology and Toxicology Research Retreat Entertainment Director (2016-2017)

Professional Training

- Oral presentation on "Болести и лечение през вековете" (transl. "Diseases and treatments throughout the ages") at the Bulgarian Academy of Sciences, Bulgaria, EU, 2017
- Oral presentation on "Drugs of Abuse" as part of the "Gypsy project", Sliven, Bulgaria 2014
- Certificate of training in "An introduction to the AALAS Transgenics Training Program", Colony Management I: Basics" (AALAS 2015)
- Certificate of training in "Pain Management in Laboratory Animals" (AALAS 2015)
- Certificate of training in "Post-Procedure Care of Mice & Rats in Research: minimizing Pain & Distress" (AALAS 2015)
- Certificate of training in "Basic Rodent Handling Techniques" (VCU 2013)
- Certificate of training in "Aseptic Techniques for Rodent Survival Surgery" (AALAS 2012)
- Certificate of training in "Mice" (AALAS 2012)
- Certificate of training in "Introduction to mice" IACUC, Virginia Commonwealth University, USA, 2013
- Summer research project at VCU Department of Pharmacology and Toxicology - Lichtman lab (2011)

Poster Presentation

- **Zdravka Daneva,** Sara Dempsey, Ashfaq Ahmad, Carl Wolf, Ningjun Li, Pin-Lan Li, and Joseph K Ritter. Diuretic and Natriuretic Activity of a Lipid Induced by Fatty Acyl Amide Hydrolase Inhibition in Cultured Mouse Medullary Interstitial Cells *Experimental biology, Chicago, April 22-26, 2017, USA*
- Joseph K Ritter, Ashfaq Ahmad, **Zdravka Daneva**, Sara Dempsey, Guangbi Li, Ningjun Li, Aron Lichtman, Justin Poklis, Pin-Lan Li. Stimulation of Diuresis and Salt Excretion by Renomedullary Infusion of a Dual Inhibitor of Fatty Acid Amide Hydrolase (FAAH) and Monoacylglycerol Lipase (MAGL). *Hypertension. 2017;70:AP468. San Francisco, September 13-16, 2017, USA.*
- Ashfaq Ahmad, Sara K. Dempsey, **Zdravka Daneva**, Justin L. Poklis, Ningjun Li, Pin Lan Li, and Joseph Ritter. Modulation of mean arterial pressure and diuresis by renomedullary infusion of selective inhibitors of fatty acid amide hydrolase. *Pharmacology, Experimental Biology, San Diego, April 20, 2018, USA*

Memberships and Titles

- Pharmacology and Toxicology Student Association at Virginia Commonwealth University (2013-present, President 2016-2017)
- American Physiological Society (2013-present)
- American Society for Pharmacology and Experimental Therapeutics (2014-present)

Publications

- **Daneva Z**, Dempsey SK, Ahmad A, Wolf C, Li N, Li PL, and Ritter JK. Diuretic, natriuretic, and vasodepressor activity of a lipid fraction enhanced in medium of cultured mouse medullary interstitial cells by a selective FAAH inhibitor. *J Pharmacol Exp Ther. 2018* (available online)
- Ahmad A, Dempsey SK, **Daneva Z**, Li N, Poklis JL, Lichtman A, Li PL, Ritter JK. Mechanism of diuretic action of anandamide in anesthetized mice with and without fatty acid amide hydrolase (**Under review** in American Journal of Physiology - Renal Physiology)
- Ahmad A, Dempsey SK, **Daneva Z**, Azam M, Li N, Li PL, Ritter JK. (2018) Role of Nitric Oxide in the Cardiovascular and Renal Systems. *Int J Mol Sci.* 3:19(9).

- Ahmad A., Dempsey SK, **Daneva Z**, Li N, Poklis JL, Li PL, Ritter JK. (2018) Modulation of mean arterial pressure and diuresis by renomedullary infusion of a selective inhibitor of fatty acid amide hydrolase. *Am J Physiol Renal Physiol* (Epub ahead of print)
- Ahmad A, **Daneva Z**, Li G, Dempsey SK, Li N, Poklis JL, Lichtman A, Li PL, Ritter JK. (2017) Stimulation of diuresis and natriuresis by renomedullary infusion of a dual inhibitor of fatty acid amide hydrolase and monoacylglycerol lipase. *Am J Physiol Renal Physiol* 1; 313(5)